Copyright Warning & Restrictions

The copyright law of the United States (Title 17, United States Code) governs the making of photocopies or other reproductions of copyrighted material.

Under certain conditions specified in the law, libraries and archives are authorized to furnish a photocopy or other reproduction. One of these specified conditions is that the photocopy or reproduction is not to be "used for any purpose other than private study, scholarship, or research." If a, user makes a request for, or later uses, a photocopy or reproduction for purposes in excess of "fair use" that user may be liable for copyright infringement,

This institution reserves the right to refuse to accept a copying order if, in its judgment, fulfillment of the order would involve violation of copyright law.

Please Note: The author retains the copyright while the New Jersey Institute of Technology reserves the right to distribute this thesis or dissertation

Printing note: If you do not wish to print this page, then select "Pages from: first page # to: last page #" on the print dialog screen

THE CONTINUOUS NON-EQUILIBRIUM PARAMETRIC PUMP: A THEORETICAL AND EXPERIMENTAL STUDY

by

J. LAWRENCE RAK

A Thesis

Presented in Partial Fulfillment of

the Requirements for the Degree

of

Doctor of Engineering Science

at

New Jersey Institute of Technology

Newark, New Jersey
1978

APPROVAL OF DISSERTATION

THE CONTINUOUS NON-EQUILIBRIUM PARAMETRIC PUMP: A THEORETICAL AND EXPERIMENTAL STUDY

by

J. Lawrence Rak

for

DEPARTMENT OF CHEMICAL ENGINEERING

NEW JERSEY INSTITUTE OF TECHNOLOGY

BY

FACULTY COMMITTEE

APPROVED: _____

_____

_____

_____

_____

Newark, New Jersey
1978

ACKNOWLEDGEMENT

This work was completed under the direction and with the advice and guidance of Dr. H. T. Chen of the Chemical Engineering Department. Grateful thanks are extended to Dr. Chen and to the Doctoral Committee for their assistance. The help of A. Rastogi in developing the computer program was invaluable. Financial support through a grant from E.I. du Pont de Nemours & Co. for the two-semester residence is gratefully acknowledged. Financial support from the Veterans Administration and tuition reimbursement from FMC Corporation, with whom I am currently employed, is also appreciated. The typing of initial drafts and the final manuscript was performed by C. Daidone, C. Benci, and P. Polts.

To my wife, Frances,

"If not for you, babe,
I couldn't even find the door;
I couldn't even see the floor.
...If not for you."

ABSTRACT

A continuous parametric pump in which the feed and product streams flow steadily both in upflow and downflow (hot and cold temperatures, respectively) is examined theoretically and experimentally. The model system is Sodium Chloride-Water-Bio Rad AG11A8 Ion Retardation Resin, a physical system characterized by relatively slow interphase mass transfer rates. For short half-cycle times, where interphase equilibrium is not approached, separation of the salt from water is found to be enhanced by longer half-cycle times, smaller reservoir displacements, and longer adsorbant columns. In most cases, separation improves with increasing number of cycles. However, steadily degrading separation is found to exist when solute loading on the cold half-cycle exceeds the regenerating capacity of the hot half-cycle upflowing fluid, a situation produced by increased lean (bottom) product withdrawal rate.

A computational method for predicting continuous non-equilibrium parametric pump performance is developed. The method is based on a set of exterior solute material balances, the equations of change for the two-phase system and a linear adsorption isotherm for the solute-solvent-adsorbant system. The method of characteristics is combined with a finite difference approximation to solve the equations of change. There is good agreement between predicted and experimental results.

TABLE OF CONTENTS

LIST OF FIGURES

LIST OF TABLES

INTRODUCTION

The field of parametric pumping has received considerable attention in recent years. This name is given to a process where the inherent ability of a particular two-phrase system to achieve separation of the components of a fluid mixture is enhanced by synchronizing an oscillating direction of interphase mass transfer with an oscillating direction of fluid flow. The result is a spatial separation of an initially homogenous fluid mixture into two mixtures, one lean and the other concentrated in solute. The direction of interphase mass transfer can be made to oscillate by periodically changing the algebraic sign of the driving force, i.e., by periodically changing the position of physical equilibrium. This coupling of two directional physical phenomena is central to the uniqueness of the parametric pumping process.

The simplest parametric pump is batch operated and will illustrate the coupling action. Suppose it is desired to remove component A from fluid mixture of A and B. A is preferentially adsorbed on solid S, which is held fixed in the column pictured in Figure 1. The column interstital space and the two piston-operated fluid reservoirs at either end of the column are filled with the fluid mixture at some initial concentration of A, y_o. Suppose that the position of interphase equilibrium is highly temperature dependent. Let the temperature of the two-phase system be made to

change periodically with time by alternately heating or cooling the system by applying some heat transfer medium of appropriate temperature to the column jacket. Then y, the concentration of A in the liquid and x, the concentration of A on the solid, will periodically adjust themselves to new values in response to the change in the thermodynamic state of the system induced by changing temperature. Usually, A will adsorb on S when the system is cooled and desorb when the system is heated.

Now, let the direction of flow of the fluid be made to change periodically with time by the piston arrangement shown in Figure 1 and let the direction of flow be sychronized with the system temperature; e.g., flow only upward when heating and only downward when cooling. Then the volume of fluid enclosed in the column interstitial space will be depleted in A by adsorption on S only when it moves downward and enriched in A by desorption from S only when it moves upward. After successive application of hot upflow and cold downflow intervals, fluid depleted in A migrates to the bottom of the column; fluid enriched in A migrates to the top. The result is a net displacement of component A to the top of the column after a number of sychronized temperature-flow cycles. Separation of the system fluid into a fraction relatively lean in A at the column bottom and a fraction relatively concentrated in A at the column top has been achieved.

In 1966, Wilhelm and his co-workers gave preliminary results on the separation of NaCl from water using a batch parametric pumping

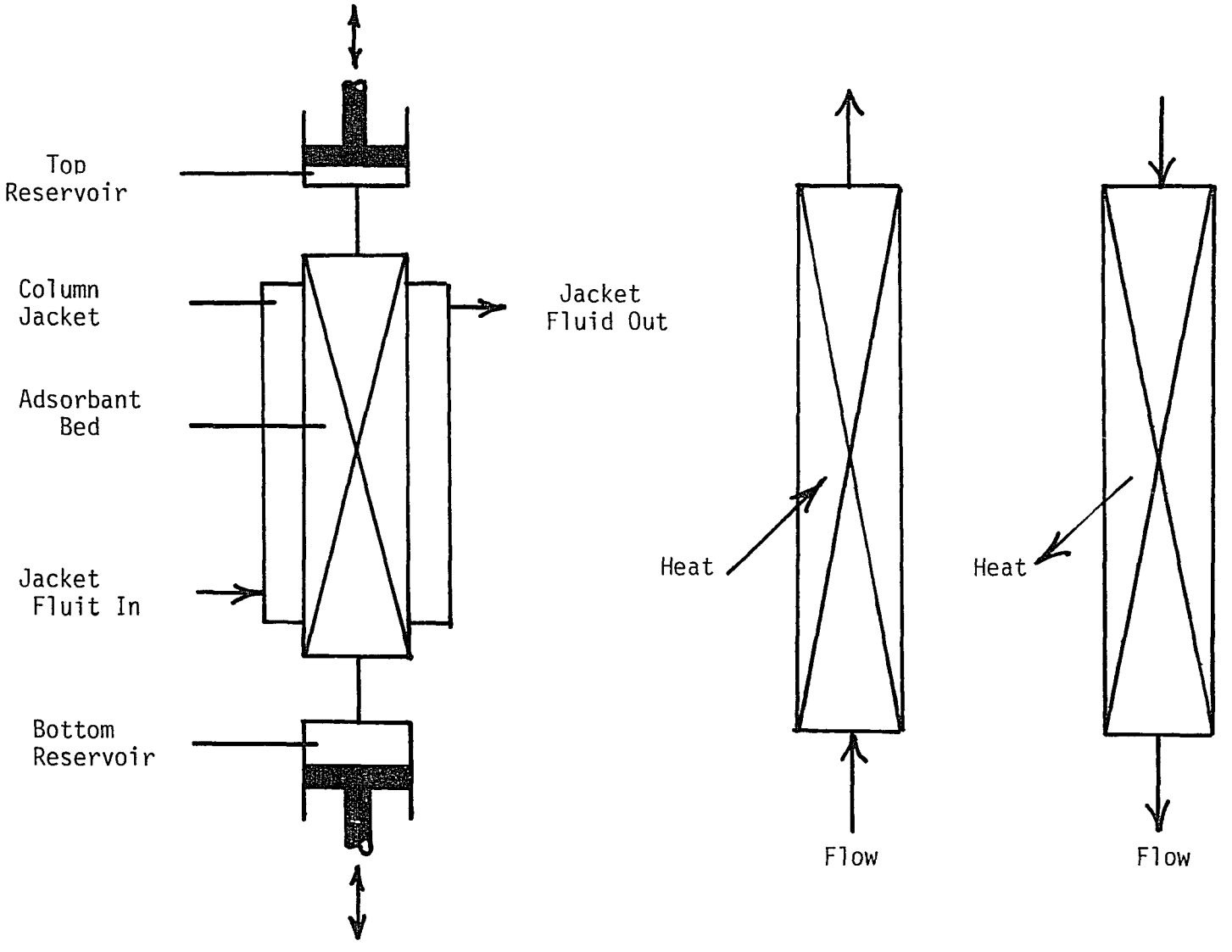

FIGURE 1 - THE BATCH PARAMETRIC PUMP

process in the recuperative mode.[32] In these initial experiments, detailed by Rice,[21] an alternating up and down fluid flow direction across a stationary bed of solid particles (IRC-45 and IR-50 Ion Exchange resins in mixed bed) was synchronized with an alternating hot and cold temperature field in the bed. In the recuperative mode,[23] the liquid influent to the bed was heated or cooled prior to contacting the adsorbant phase rather than using a jacketed column. After several cycles of operation, the homogenous fluid portion of the system was separated into a fluid lean in NaCl, which existed in a reservoir at the bottom of the bed and a fluid rich in NaCl, which existed in a reservoir at the top of the bed. Later work,[34] detailed by Rolke,[22] utilized the direct mode of operation, where temperature cycles in the adsorbant bed were induced in the entire bed contents by external heating and cooling. The experimental system was the same and the results were theoretically justified using a "tinker-toy" model derived from the equation of continuity, and equilibrium relation, and a mass-transfer expression.

In 1968, Wilhelm and Sweed[33] showed that the ability of a solid adsorbant to achieve separation of the components of a fluid mixture could be greatly enhanced by parametric pumping. Using the direct mode on a batch system, toluene was separated from n-heptane using silica gel adsorbant. Experimental results showed large separations and were analyzed by means of the STOP-GO computer algorithm.[27] In this method a numerical solution is derived from the model equations

by dividing each half-cycle (up or down flow) into a number of time increments, each treated as a small flow displacement with no interphase mass transfer followed by a period of mass transfer with no flow.

Utilization of the parametric pumping process is not limited, of course, to temperature induced liquid-solid mass transfer systems. Jenczewski and Myers[16] separated ethane and propane on activated carbon, Patrick, et.al.[17] separated SO_2 and air on silica gel; and Turncock and Kadlec[29] separated nitrogen and methane using Type 5A molecular sieves, all with temperature as the driving parameter. Shendalman and Mitchell[26] used pressure as the driving parameter to separate carbon dioxide and helium on silica gel. Sabadell and Sweed[22] used pH to separate Na+ and K+ ions in aqueous solution using a strong cation exchange resin, and Chen, et al,[12] have separated Protiens by pH parapumping using Sephaldex resin. Wankat[30] has treated parametric pumping of liquid-liquid extraction, where one fluid phase is held stationary, either by coating a liquid substrate with it, or by containing in a column and inducing the alternating flow pattern in the mobile phase by periodically inverting the column.

Nor is parametric pumping limited to single adsorbant beds, one-solute systems, or oscillating flow patterns. In cycling-zone adsorption,[19] the mobile phase flows unidirectionally but enters successive zones of alternating driving parameter values, e.g. hot and cold temperature,[11,31] or high and low pH,[3] both of which are

utilized to separate glucose and fructose in aqueous solution. Straight parametric pumping has also been used for sugar separation in aqueous media.[6] The separation of Na^+ and K^+ in aqueous media has already been mentioned.[24] In addition, toluene and analine are separated from n-heptane using silica gel adsorbant in thermal parametric pumping.[8,10]

Theoretical treatment of parametric pumping processes in systems where interphase mass transfer is rapid has largely been based on the work of Pigford, Baker, and Blum.[18] They applied a theory of operation to the batch parametric pump based on the assumption that interphase mass transfer was so rapid that local fluid-solid equilibrium existed everywhere in the bed at all times. They showed that the solute traveled through the adsorbant bed in sharply defined wave fronts whose distance of penetration into the column could be theoretically established. Aris[2] generalized the approach recognizing that the treatment of Pigford, et.al. applied to a particular case of the more general theory.

Chen and Hill[4] then extended the analysis to semi-continuous and continuous parametric pumps. In the former case, a portion of the lean and concentrated products are removed intermittently from the lower and upper reservoirs, respectively, during one or both half-cycles of operation and a feed stream of constant composition is also introduced intermittently during a portion of one or both half-cycles. In the continuous case, a fluid of composition y_o is

continuously fed into the dynamically coupled thermodynamic change-fluid flow field. Product streams are then removed continuously from the top and bottom of the column at compositions y_{TP} and y_{BP}, respectively, where $y_{TP} \geq y_o \geq y_{BP}$. Feed is introduced and products are removed at such a rate that the fluid volume contained in the system remains constant.

Chen and Hill[4] showed that there were three regions of operation for all parametric pumps. The regions are defined by the relative lengths of concentration front penetration during hot and cold half-cycles of operation and column length. Separations were found to be severely limited in two of the regions of operation and unlimited in the other, where complete removal of solute from the lean product was possible. Later work experimentally verified these findings for the semi-continuous[7] and continuous cases[5] and suggested that, for shorter half-cycle times, separation was limited in all three regions of operation because of a significant departure from equilibrium operation.[9,20] In all this work the experimental system was the same as Wilhelm and Sweed.

Attempts to theoretically treat the non-equilibrium case have all been based on reducing the model equations (partial differential equations) to linear ordinary form and solving them numerically. Sweed and Gupta[15] have developed a mixing cell algorithm and a near-quilibrium model as alternates to the STOP-GO algorithm. In the present work, the method of characteristics is combined with a

numerical solution based on Euler's method to predict parametric pump behavior for a non-equilibrium system.

Earlier, Gregory[14] investigated parametric pumping in batch and a type of semi-continuous operation. The experimental system was NaCl, H_2O, Bio Rad AG11A8 Ion Retardation Resin. Interphase mass transfer which takes place by simultaneous adsorption of Na^+ and Cl^- ions on negatively and positively charged resin sites, appeared to be relatively slow, and Gregory predicted, using the STOP-GO algorithm, and demonstrated experimentally, that separation of NaCl from water increased steadily with the number of cycles of operation to a nearly constant value for a narrow range of operating conditions.[28]

In the present work, completely continuous parametric pumping is applied to the same physical-chemical system. Whereas, in Gregory's study, no product flow or intermittent product flow obtained during certain portions of each half-cycle of operation, this work treats the case where lean and concentrated products exist from opposite ends of the adsorbant bed in a continuous manner. Using the method described above to solve the model equations it is shown that, under non-equilibrium operation the solute moves through the bed in a diffuse manner; no sharply defined wave fronts are found to exist. Limited, but steadily decreasing separations are achieved where loading of the adsorbant bed by solute during a cold half-cycle is exceeded by the capacity for removal of solute from

the bed during the next hot half-cycle, in agreement with the general trend of Gregory's results. However, when operating outside the range of Gregory's work, a limited separation of steadily decreasing magnitude is found to exist. This result is related to the situation where column loading during the cold half-cycle exceeds regenerative action during the next hot half-cycle. A gradual buildup of solute in the adsorbant bed is noted in these cases and it is found that the active variables in changing the ability of the column to purge itself of adsorbed solute is the rate of lean product withdrawal. The effects of cycle time, reservoir displacement and column height on separation are examined and comparisons with the equilibrium theory are made.

THEORY

A. Process Description

Consider a two-phase system composed of a homogeneous fluid mixture of components A,B,C,. . ., and a solid, S, which preferentially adsorbs component A. This reversible interphase mass transfer operation may be symbolized by

$$A\ (sol'n) \rightleftharpoons A\ (ads.). \tag{1}$$

If liquid A,B,C,. . . and solid S are brought into contact, either direction of (1) will prevail until equilibrium is reached, i.e., until the thermodynamic state of the system can be described by a relation of the form

$$x = f\ (\Psi_i, y_i, x_i). \tag{2}$$

Thus, given a particular system we are free to control the direction of (1) by controlling the thermodynamic state of the system through the action of the intensive system parameters, Ψ_i, in (2).

If the solid phase is held fixed in space, the fluid phase can be made to move relative to the solid phase. We are equally free to choose the direction of that motion. It is the dynamic coupling of these two phenomena, i.e., the sychronizing of interphase mass transfer with bulk fluid flow, that characterizes the parametric pump.

If the direction of (1) is found to be highly temperature dependent and the effect of other intensive thermodynamic properties is minimal, then (2) becomes

$$x = f(T,y). \qquad (3)$$

The function f is the adsorption isotherm for the system in question and it may take one of several forms, linear, Langmuir, Freudlich, etc. With each change in T, the system will seek to satisfy (3) by the action described by (1). With each change of state the appropriate direction of (1) will prevail tending toward the equilibrium described by (3).

A continuous parametric pump has been hypothesized, and studied theoretically and experimentally for equilibrium systems. It is apparent for these pumps, that the feed may be introduced at either end of the column. It is also apparent, however, that introducing feed solution at the lean end of the column would enrich a stream already depleted in A with additional solute, thereby reducing the effect of the separation. Since, in general, we desire to maximize the effect of the separation technique, we will only consider feeding the enriched end of the column. Successful operation of the parametric pump, i.e., sustained removal of lean and concentrated product streams from either end of the column is dependent on the permanence of the fluid and solid phase concentration gradients imposed on the column by the coupled mass transfer-fluid flow process.

The particular continuous parametric pump shown in Figure 2 will be considered. Feed flows to the column top at a constant rate $(\phi_T + \phi_B)$ Q, where Q is the reservoir displacement rate, equal for both top and bottom of the column, respectively. The product streams are located at the reservoirs themselves, so that during reservoir discharge product flows only from the reservoir and not from the column discharge or feed streams. We heat the column during upflow for a time period, τ, and cool it during downflow for an equal time interval so that we take a product lean in A from the column bottom and one enriched in A from the column top, as described by (4).

B. External Equations

A set of external equations for the continuous parametric pump are derived from a set of material balances made for a particular full cycle, consisting of a hot upflow half-cycle and a cold downflow half-cycle, each of duration τ. Referring to Figure 3, during the hot, upflow half-cycle, the concentration of the effluent from the column top varies with time and has the general behavior of a desorption breakthrough curve, while the concentration of the fluid entering the column bottom is constant. The effluent mixes with feed solution before a portion of the combined stream is taken off as top product. The remainder of the stream enters the top reservoir, where it is mixed with solution from the previous cold cycle that has remained in the top reservoir "dead volume." From Figure 4, during the ensuing cold half-cycle, a portion of the stream

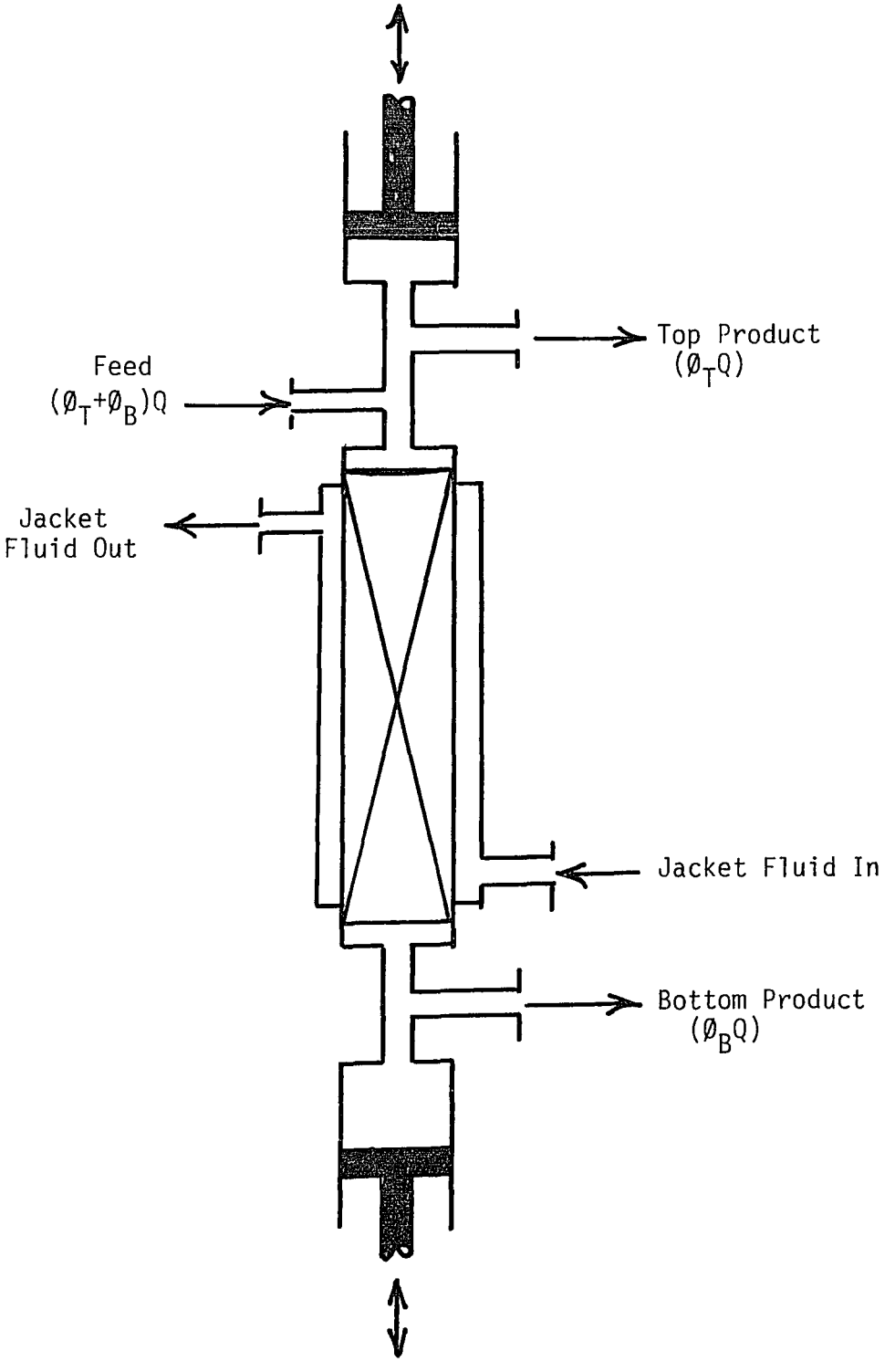

FIGURE 2 - THE CONTINUOUS TOP FEED PARAMETRIC PUMP

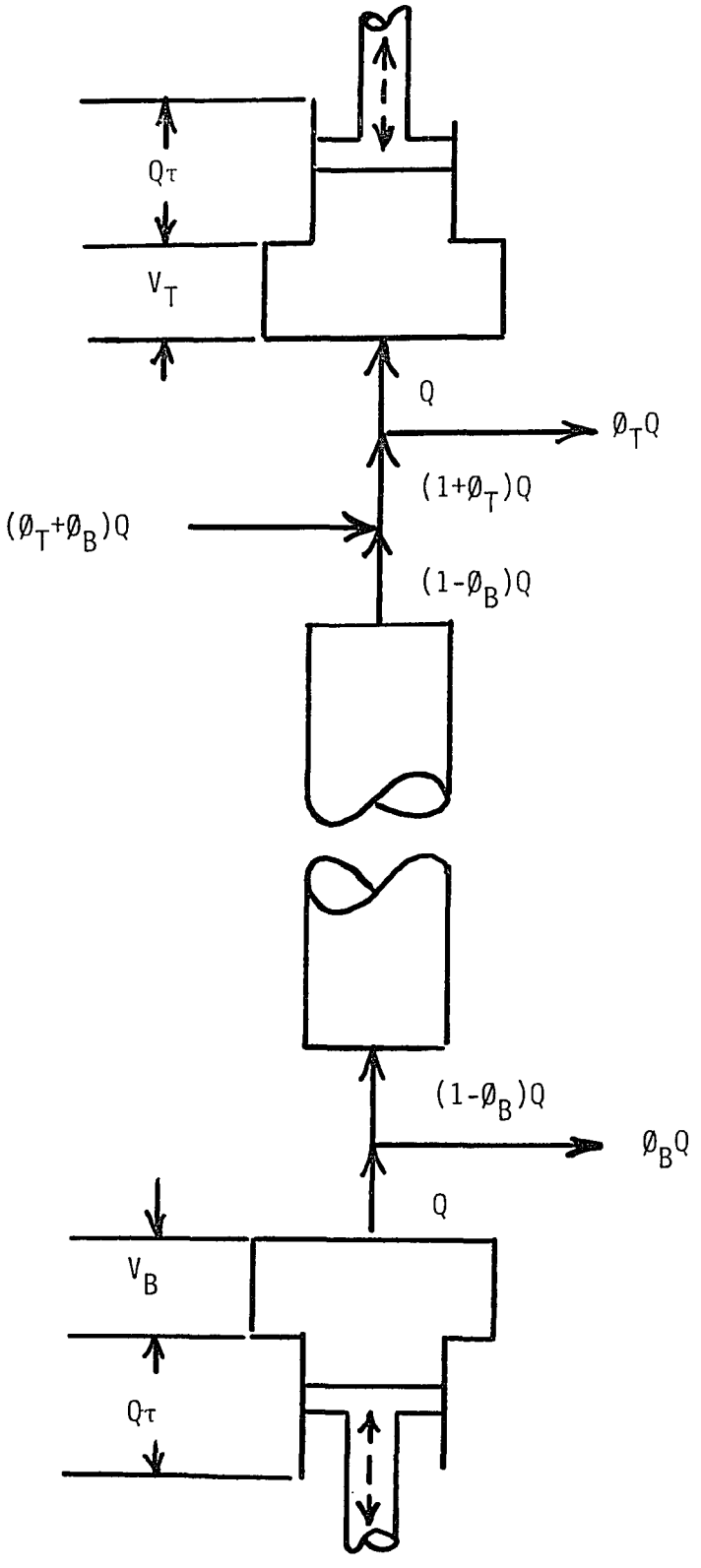

FIGURE 3 - UPFLOW HALF-CYCLE

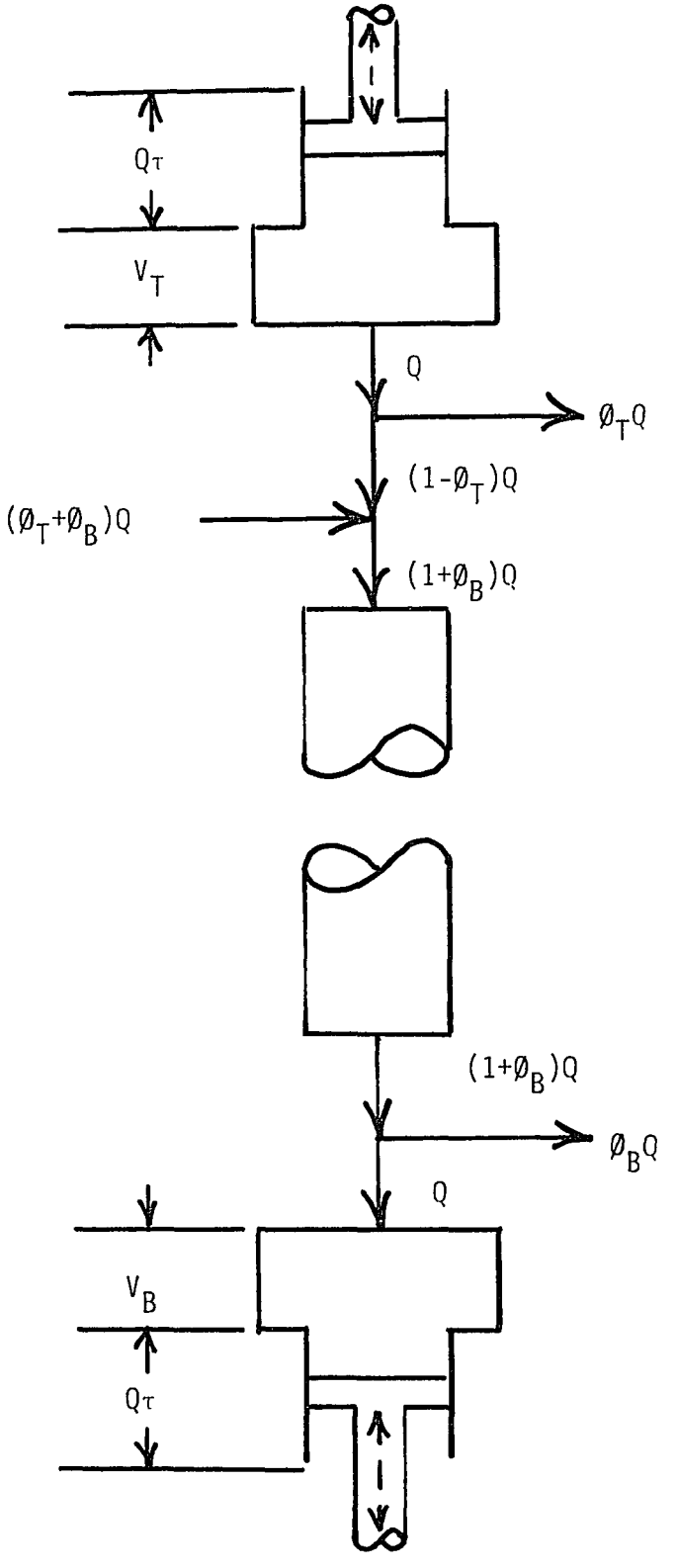

FIGURE 4 - DOWNFLOW HALF-CYCLE

leaving the top reservoir is removed as top product before the remainder mixes with feed solution to form the constant concentration influent to the column top.

Meanwhile, referring to Figure 4, during this cold half-cycle, the concentration of the effluent from the column bottom varies with time behaving much like an adsorption break-through curve. A portion of this stream is removed as bottom product and the remainder enters the bottom reservoir, where it is mixed with solution that has remained in the bottom reservoir dead volume from the previous hot half-cycle. During the ensuing hot half-cycle a portion of the effluent from the bottom reservoir is again removed as bottom product while the remainder forms the constant concentration influent to the column bottom (see Figure 3). The development which follows generates expressions for the concentration of the top and bottom cold cycle product streams and the boundary condition concentration for the column top during downflow and the column bottom during upflow.

From Figure 3, at the feed point, during the up-flow half-cycle,

$$(\phi_T + \phi_B)y_o + (1 - \phi_B)\langle y_{T1}\rangle_n = (1 + \phi_T)\langle y_{TP1}\rangle_n \tag{5}$$

and, for a successive upflow-downflow sequence, at the top reservoir,

$$Q_T\langle y_{TP1}\rangle_n + V_T\langle y_{TP2}\rangle_{n-1} = (Q_T + V_T)\langle y_{TP2}\rangle_n. \tag{6}$$

Dividing (6) through by $Q\tau$ and letting

$$C_T = \frac{V_T}{Q\tau} \tag{7}$$

we substitute the result into (5) and rearrange to obtain

$$\langle y_{TP2} \rangle_n = \left(\frac{1}{1+C_T} \right) \left[\left(\frac{1-\phi_B}{1+\phi_T} \right) \langle y_{T1} \rangle_n + \left(\frac{\phi_B+\phi_T}{1+\phi_T} \right) y_o \right] + \left(\frac{C_T}{1+C_T} \right) \langle y_{TP2} \rangle_{n-1} \tag{8}$$

where, for n=1, $\langle y_{T1} \rangle_1 = \langle y_{TP2} \rangle_o = y_o$. Equation (8) gives the cold half-cycle top product for cycles 1 through n. To obtain the column top boundary condition for the nth cold half-cycle, we make a downflow material balance at the feed point,

$$(1-\phi_T) \langle y_{TP2} \rangle_n + (\phi_T + \phi_B) y_o = (1+\phi_B) \langle y_{T2} \rangle_n \tag{9}$$

Rearranging (9), we obtain the cold half-cycle boundary condition

$$\langle y_{T2} \rangle_n = \left(\frac{1-\phi_T}{1+\phi_B} \right) \langle y_{TP2} \rangle_n + \left(\frac{\phi_T+\phi_B}{1+\phi_B} \right) y_o \tag{10}$$

From Figure 4, for the downflow cold cycle we see that

$$\langle y_{BP2} \rangle_n = \langle y_{B2} \rangle_n \tag{11}$$

and a material balance on the bottom reservoir for a successive downflow-upflow sequence gives

$$Q\tau \langle y_{BP2} \rangle_n + V_B \langle y_{BP2} \rangle_{n-1} = V_B + Q\tau \langle y_{B1} \rangle_{n+1}. \tag{12}$$

Rearranging (12), letting

$$C_B = \frac{V_B}{Q\tau} \tag{13}$$

we adjust the subscript designations to obtain the hot half-cycle boundary condition,

$$\langle y_{B1} \rangle_n = \left(\frac{1}{1+C_B}\right) \langle y_{BP2} \rangle_{n-1} + \left(\frac{C_B}{1+C_B}\right) \langle y_{BP2} \rangle_{n-2} \tag{14}$$

where, for n=1, $\langle y_{BP2} \rangle_o = \langle y_{BP2} \rangle_{-1} = y_o$.

Equations (10) and (14) are used to determine the fluid phase boundary conditions for downflow and upflow, respectively, while equations (8) and (11) are used to calculate the cold half-cycle product concentrations. The terms $\langle y_{T1} \rangle$ and $\langle y_{B2} \rangle$ in equations (8) and (11), which are also implicitly present in (10) and (14) are calculated by solution of the internal equations governing mass transfer within the adsorbant column.

C. Internal Equations

The equation of continuity for the two-phase solution-adsorbant system, neglecting axial diffusion, radial concentration gradients and variation of fluid density with concentration, is

$$\varepsilon v \frac{\partial y}{\partial z} + \varepsilon \frac{\partial y}{\partial t} + (1-\varepsilon) \rho_s \frac{\partial x}{\partial t} = 0. \tag{15}$$

For adsorption processes where liquid film resistence to mass transfer is rate controlling, the interphase transport of the adsorbed component of the fluid mixture is said to be driven by

departure of the actual liquid concentration from the equilibrium liquid concentration for the existing solid concentration. Thus,

$$\frac{\partial x}{\partial t} = \lambda\ (y-y^*). \tag{16}$$

In general, the mass transfer coefficient, λ, is a function of liquid phase physical properties, solid geometry, and liquid velocity. The principal parameters of interest in the case of parametric pumping are temperature effects on fluid properties and fluid velocity since they will be markedly different for the hot and cold temperature half-cycles. Concentration effects on fluid properties can be ignored for dilute solutions and moderate ranges of concentration.

The equation relating the existing solid concentration to an equilibrium liquid concentration is given by the adsorption isotherm for the liquid solid system at the temperature of interest. If the form of adsorption isotherm is linear,

$$y^* = \frac{x}{M} \tag{17}$$

where

$$M = M\ (T). \tag{18}$$

combining (16) and (17),

$$\frac{\partial x}{\partial t} = \lambda (y-\frac{x}{M}) \tag{19}$$

and, combining (19) and (15), and rearranging,

$$v\ \frac{\partial y}{\partial z} + \frac{\partial y}{\partial t} + \left(\frac{1-\epsilon}{\epsilon}\right) \rho_s\ \ \lambda (y-\frac{x}{M}) = 0. \tag{20}$$

Equations (19) and (20) are a set of first order linear partial differential equations in two independent and two dependent variables.

At the beginning of either a hot or cold half-cycle, the column will have imposed upon it from the previous half-cycle both a liquid and solid phase axial solute distribution, which together form a set of initial conditions. These are

$$@t = 0,\ z \geq 0,\ y = y(z), \tag{21}$$

$$@t = 0,\ z \geq 0,\ x = x(z). \tag{22}$$

For upflow the concentration of the fluid entering the column bottom is constant and the upflow boundary condition for the liquid phase is (see equation (14)).

$$@\ z = 0,\ t \geq 0,\ y = \langle y_{B1} \rangle \tag{23}$$

The solid phase concentration at the column bottom is, of course, variable, but a combination of (19) and (23) yields an implicit solid phase boundary condition,

$$\frac{\partial x}{\partial t}\bigg|_{z=o} = \lambda_1 \left(\langle y_{B1} \rangle - \frac{x}{M} \right). \tag{24}$$

For downflow the concentration of the fluid entering the column top is constant and the downflow liquid phase boundary condition for a column of height, h, is given by

$$@z = h,\ t \geq 0,\ y = \langle y_{T2} \rangle. \tag{25}$$

Considerations similar to these employed in developing the solid phase boundary condition for the upflow half-cycle lead to the implicit boundary condition

$$\left.\frac{\partial x}{\partial t}\right|_{x=h} = \lambda_2 \left(\langle y \rangle_{T2} - \frac{x}{M_2}\right). \tag{26}$$

Equations (19) and (20) can be reduced to a more manageable form by introducing a new variable, $\bar{z}$,[1,11] defined by

$$\bar{z} = \frac{z}{v} . \tag{27}$$

Then, by the chain rule, operating on (27),

$$\frac{\partial y}{\partial z} = \frac{\partial y}{\partial \bar{z}} \frac{\partial \bar{z}}{\partial z} = \frac{1}{v} \frac{\partial y}{\partial \bar{z}} . \tag{28}$$

Substituting (28) into (20) gives

$$\frac{\partial y}{\partial \bar{z}} + \frac{\partial y}{\partial t} = - \left(\frac{1-\varepsilon}{\varepsilon}\right) \rho_s \lambda (y - \frac{x}{M}) . \tag{29}$$

Now, consider two families of curves in the $\bar{z}$ -t plane, where, for one family of lines

$$\frac{\partial t}{\partial \bar{z}} = 1, \tag{30}$$

and, for the other,

$$\frac{\partial \bar{z}}{\partial t} = 0. \tag{31}$$

These lines are pictured on Figure 5. Along any direction in the $\bar{z}$-t plane,

$$\frac{dy}{d\bar{z}} = \frac{\partial y}{\partial \bar{z}} + \frac{\partial y}{\partial t} \frac{\partial t}{\partial \bar{z}} . \tag{32}$$

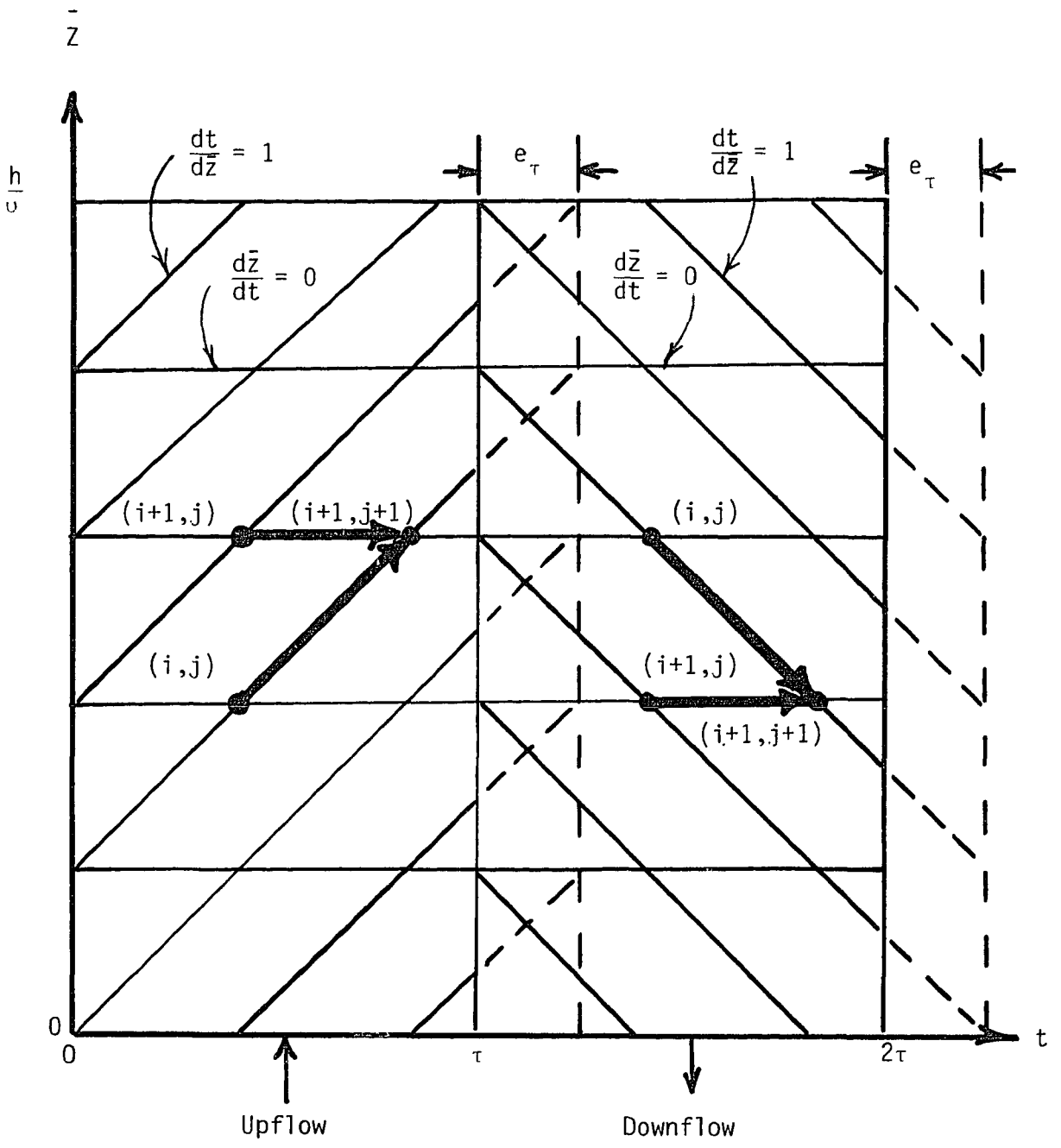

FIGURE 5 - UPFLOW AND DOWNFLOW CHARACTERISTICS

and

$$\frac{dx}{dt} = \frac{\partial x}{\partial t} + \frac{\partial x}{\partial \bar{z}} \frac{\partial \bar{z}}{\partial t} \quad . \tag{33}$$

Therefore, along characteristic lines described by (30), using (32) and (30) in (29),

$$\frac{dy}{d\bar{z}} = - \left(\frac{1-\varepsilon}{\varepsilon}\right) \rho_s \lambda \, (y - \frac{x}{M}) \tag{34}$$

and, along characteristics described by (31), using (33) and (31) in (19) gives

$$\frac{dx}{dt} = \lambda \, (y - \frac{x}{M}) \tag{35}$$

Equations (34) and (35) now form a set of ordinary differential equations which can be solved numerically to obtain x and y as functions of $\bar{z}$ and t. The boundary and initial conditions are revised to reflect the new independent variables as follows:

a.) initial conditions,

$$@t=0, \; \bar{z} > 0, \; y = y(\bar{z}) \tag{36}$$

$$@t=0, \; \bar{z} > 0, \; x = x(\bar{z}) \tag{37}$$

b.) upflow boundary conditions,

$$@ \; \bar{z}=0, \; t > 0, \; y = \langle y_{B1} \rangle \tag{38}$$

c.) downflow boundary conditions

$$\left.\frac{dx}{dt}\right|_{\bar{z}=0} = \lambda_1 \, (\langle y_{B1} \rangle - \frac{x}{M_1}) \tag{39}$$

$$@\bar{z} = h/v_2, \; t > 0, \; y = \langle y_{T2} \rangle \tag{40}$$

$$\left.\frac{dx}{dt}\right|_{\bar{z}=h/v_2} = \lambda_2 \, (\langle y_{T2} \rangle - \frac{x}{M_2}) \quad . \tag{41}$$

Euler's Method is employed to reduce the above ordinary differential equations to finite difference form. Integrating (34), we obtain

$$y(\bar{z}) = y(\bar{z}_o) - \left(\frac{1-\varepsilon}{\varepsilon}\right) \rho_s \lambda \int_{\bar{z}_o}^{\bar{z}} \frac{(y-\underline{x})}{M} d\bar{z} \tag{42}$$

and, integrating (35)

$$x(t) = x(t_o) + \lambda \int_{t_o}^{t} \frac{(y-\underline{x})}{M} dt. \tag{43}$$

We choose a suitably small finite distance interval, Δz, and use equations (27) and (30) to find that

$$\frac{\Delta z}{v} = \Delta \bar{z} = \Delta t = \delta \tag{44}$$

We approximate the integral by the trapezoidal rule and let i,j refer to points in the $\bar{z}$,t plane. Then (42) becomes (see Figure 5)

$$y_{i+1,\ j+1} = y_{i,j+1} - \left(\frac{1-\varepsilon}{\varepsilon}\right) \rho_s \lambda \frac{\delta}{2} \left[y_{i+1,j+1} - \frac{x_{i+1,\ j+1}}{M} + y_{i,j+1} - \frac{x_{i,\ j+1}}{M} \right] \tag{45}$$

and (43) is transformed into

$$x_{i+1,\ j+1} = x_{i+1,j} + \frac{\lambda\delta}{2} \left[y_{i+1,j+1} - \frac{x_{i+1,j+1}}{M} + y_{i+1,j} - \frac{x_{i+1,j}}{M} \right] \tag{46}$$

Finally, in order to solve the above equations an iterative scheme will be used. If the k+1st estimate of x and y are desired and the kth estimates of both quantities have been obtained, using a

superscript for the iteration number, our working equations become

$$y^{k+1}_{i+1,j+1} = y_{i,j+1} - \left(\frac{1-\varepsilon}{\varepsilon}\right) \rho_s \frac{\lambda\delta}{2} \left[y^{k}_{i+1,j+1} - x^{k}_{\frac{i+1,j+1}{M}} + y_{i,j+1} - \frac{x_{i,j+1}}{M} \right] \tag{47}$$

and

$$x^{k+1}_{i+1,j+1} = x_{i+1,j} + \frac{\lambda\delta}{2} \left[y^{k}_{i+1,j+1} - x^{k}_{\frac{i+1,j+1}{M}} + y_{i+1,j} - \frac{x_{i+1,j}}{M} \right] . \tag{48}$$

Starting with some realistic values for $x^{1}_{i+1,j+1}$ and $y^{1}_{i+1,j+1}$, say $x_{i+1,j}$ and $y_{i+1,j}$, the iterative scheme is carried out k+1 times, until, for some chosen error in x and y, designated e,

$$\left| \frac{x^{k+1}_{i+1,j+1} - x^{k}_{i+1,j+1}}{x^{k}_{i+1,j+1}} \right| \leq e_x \tag{49}$$

and

$$\left| \frac{y^{k+1}_{i+1,j+1} - y^{k}_{i+1,j+1}}{y^{k}_{i+1,j+1}} \right| \leq e_y \tag{50}$$

D. Applying the Model

The external equations discussed in section B are combined with the solution to the internal equations discussed in section C to predict performance of the continuous non-equilibrium parametric pump. The calculation scheme will be described in detail.

1. Initial Condition. At time zero the system is at equilibrium at the high temperature with the liquid concentration everywhere equal to the feed composition. The process is initiated by a hot upflow half-cycle to further insure establishment of the equilibrium condition. No mass transfer takes place; the system remains at equilibrium at the higher temperature and the concentration of the effluent from the column top remains constant at y_o.

2. Cold Downflow Half-Cycle. The initial axial concentration profiles for this first cold half-cycle are

$$y=y_o \tag{51}$$

$$x=\frac{y_o}{M_1} \tag{52}$$

and the liquid concentration at the column top, our downflow boundary condition, is

$$\langle y_{T2} \rangle = y_o \tag{53}$$

Starting at the column top (z=h), (41) is solved anayltically giving the solid phase concentration, x, as a function of time, to yield

$$x=M_2 \langle y_{T2} \rangle \left[1- \left(\frac{1-M_1}{M_2}\right) \exp \left(\frac{-\lambda_2 t}{M_2}\right)\right] \quad . \tag{54}$$

An appropriate time interval for application of (47) - (50) is chosen and, using (54), x is calculated at z=h for $t=\delta$, 2δ, 3δ, . . ., $m\delta$. For $t=\delta$, the liquid and solid concentrations along the

axial direction are calculated using (47) and 48) along with some first guess at x and y for k=1. Thus, at each time interval, x and y will have been determined at z=h, h-δv, h-2δv, . . ., 0 by solution of (47) - (50). After m time intervals, we have

$$m\delta \simeq \tau, \tag{55}$$

i.e., given our choice of distance parameter $\bar{z}=\delta$, a reasonable number of time intervals can bring the time, t, as close to the actual cycle time, τ, as desired. Because of our choice of characteristic equation, we are constrained by (44) in our choice of distance and/or time interval length, and will, in general, not be able to satisfy (55) exactly. However, our choice of δ prescribes the error in cycle time inherent in the calculation procedure, which is (see Figure 5),

$$e_\tau = \frac{\pm\delta}{2\tau} \quad . \tag{56}$$

Therefore, the shorter the finite difference step used in solving (47) - (50), the smaller the error in the computed half-cycle time, mδ, and the smaller the resulting error of the estimate of local concentration value at t=τ.

3. Hot Upflow Half-Cycle. Once the cold half-cycle is completed, the initial axial concentration profiles for both the liquid and solid phases are then established for the succeeding hot half-cycle. In a manner similar to that employed for the previous cold half-cycle, solution of (39) establishes the solid phase boundary

condition at the column bottom for each time interval, δ. The solution is

$$x=M_1 \langle y_{B1} \rangle_n \left[1 - \left(\frac{1-M_2}{M_1}\right) \exp\left(\frac{-\lambda_1 t}{M_1}\right)\right] . \qquad (57)$$

Successive applications of (47) - (50) are performed at succeeding axial positions from the column bottom to the column top for each time interval until (55) is approximately satisfied within the error limit given by (56). At this point the initial condition for the next cold half-cycle is established, i.e., the axial concentration profile for both solid and liquid phases at the end of a hot half-cycle are the initial conditions required by (40) for the ensuing cold half-cycle. The method is then applied for n full cycles, each consisting of a hot and cold half-cycle, in that order.

4. Product Concentration. From (8) and (11) it is apparent that estimation of the cold half-cycle product concentrations requires knowledge of the average concentration of the column effluent for each half-cycle. This average is easily computed for r finite difference time intervals for the column top by

$$\langle y_{T1} \rangle = \left(\sum_{i=1}^{r_1} y_{Ti}\right) / r_1 \qquad (58)$$

and, for the column bottom by

$$\langle y_{B2} \rangle = \left(\sum_{i=1}^{r_2} y_{Bi}\right) / r_2 \qquad (59)$$

Direct substitution of (58) and (59) into (8) and (11), respectively, give the cold half-cycle top and bottom product concentrations for each of the n cycles of operation.

5. Computer Solution. The computer program given in Appendix I was devised to carry out the calculations described in Section 4, above.[11] For reasonably short half-cycle times, distance intervals smaller than h/65 gave negligible improvement in the computed estimates for liquid and solid-phase concentrations. For half-cycle times longer than 120 minutes, the finite difference interval $\delta=h/65v$ became too large to achieve convergence of the iteration calculation due to the low value for fluid-phase velocity, v. Therefore, the number of finite-difference distance intervals was doubled to 130 to compute concentrations at 180 minute half-cycle times.

Less than ten iterations were normally required to satisfy the error criterion established by equations (49) and (50). Computer output for all the cases investigated are on file in their original form in the Chemical Engineering Department Library.

Values for the relavent physical parameters are read initially into the program, these being hot and cold temperatures, column height, reservoir displacement, half-cycle time, product withdrawal ratios for top and bottom, and feed composition. The equilibrium parameters, M in equation (17) are calculated as a function of temperature by the relationship given in equation (85). Using the

bed cross-section, solids void fraction, reservoir displacement rate and half-cycle time, fluid velocities for both half-cycles are calculated via the relations

$$v_1 = Q(1-\phi_B)/\varepsilon A \tag{60}$$

and

$$v_2 = Q(1+\phi_B)/\varepsilon A \tag{61}$$

and these velocities, in turn, are used to estimate the mass transfer coefficient via equation (64). Finally, the finite difference interval is calculated by using the given number of axial distance intervals, N, the column height and the velocity, so that

$$\delta = \frac{h}{Nv} \tag{62}$$

Since δ is identical to the time unit finite difference interval, Δt, the number of time intervals required for completion of the calculation for a given half-cycle is given by

$$R = \frac{v\tau}{h} \quad N \tag{63}$$

After choosing appropriate axial position and time intervals for generation of output, solution of the model equations proceeds in subroutine XYCALC. Upon completion of the half-cycle, the average product concentrations and boundary conditions for the next half-cycle are calculated in the main body of the program before return to XYCALC for the next series of calculations.

Experimental conditions were chosen to facilitate comparisons with the well-established equilibrium theory of operation. A summary

of that theory's development and comments relative to interpretation of equilibrium theory operation appear in Appendix II.

EXPERIMENTAL METHOD

A. The Experimental System

Sodium Chloride can be removed from its aqueous solution by attachment of the ionic species to a suitable solid phse. BioRad AG11A8 Ion Retardation Resin is one such solid. The resin is an "amphoteric ion exchange resin," which contains an equal number of positively and negatively charged sites within the resin matrix. Ionic species are attracted to sites of opposite charge (rather than exchanged for another ion of like charge) in such a way that ionic neutrality is maintained in both liquid and solid phases. The ionic species, then, diffuse through a liquid film surrounding the resin particle (slow) and then react electro-chemically with the ionic fragment of opposite charge connected to the resin matrix (rapid). The desorption reaction follows the reverse sequence. The rapid electro-chemical dissociation is followed by a relatively slow diffusion through the liquid film to the bulk of the surrounding liquid.

Uncomplicated, therefore, by counterdiffusion of exchanged ionic species, or by the presence of fluid-phase reactions involving the exchanged species (H^+ and OH^- ions, for example), the interphase mass transfer can be viewed as one where diffusion across the liquid film surrounding the solid particle is the controlling resistance and where the difference between bulk liquid concentration and the

liquid concentration corresponding to the existing local solid concentration is the driving force.

The resistance to mass transfer is a direct function of the properties of the liquid film, whose thickness and viscosity are controlled by temperature, fluid velocity and concentration within the liquid film. For moderate concentrations, this last effect can be ignored, but both temperature and velocity will be markedly different between the cold and hot parametric pumping half-cycles, and, therefore, so will resistance to mass transfer. Experimental determinations of the resistance (λ in eq (16)) were performed and empirical relations of the form

$$\lambda = \beta v^{\alpha} \tag{64}$$

were derived, where β is a function of temperature and $\alpha = 0.30$.[14] These are described in Appendix III.

Adsorption isotherms for the system Sodium Chloride-Water-BioRad AG11A8 Resin have been determined at 5°C and 55°C[14] and are linear for the range 0 - .2M NaCl in the liquid phase, that is, the isotherm is described by

$$y^* = \frac{x}{M} \tag{65}$$

where M is a function of temperature. A linear dependence of M with temperature was assumed of the form

$$M = M_o + \mu\ (273.16 + T) \tag{66}$$

and an isotherm was calculated for 70°C. The experimental and calculated isotherms are pictured on Figure 6,[14] where the specific region of interest treated in this work is marked. The linearity of the adsorption isotherms in this region is apparent.

B. Description of Apparatus

The laboratory continuous parametric pump is pictured in Figure 7. A 1.0cm x 90cm adjustable length jacketed glass column (A) was packed to a specified height with 40 - 80 mesh Bio-Rad AG11A8 Ion Retardation Resin in equilibrium at room temperature with aqueous sodium chloride solution of feed concentration. The reservoirs at either end of the column (B and C for top and bottom, respectively), which created the axial flow displacements were $50cm^3$ Becton-Dickenson Multi-Fit glass syringes driven by a Harvard Apparatus variable speed infusion-withdrawal pump (D) set for reciprocal operation. While the plunger at C ran in the forward direction, emptying C, the plunger at B withdrew, filling B, and vice versa. The reservoir displacement rate was set by adjusting the speed of the drive mechanism. The syringe plungers were lightly greased with Dow-Corning flouro-silicone stopcock grease. To insure that both reservoirs were well-mixed, small teflon-coated magnetic stirring bars were placed in the syringes and driven by water-activated magnetic stirrers (not pictured).

The synchronous temperature changes within the column were achieved by supplying the column jacket with 70°C water during upflow and 5°C water during downflow. The hot and cold water

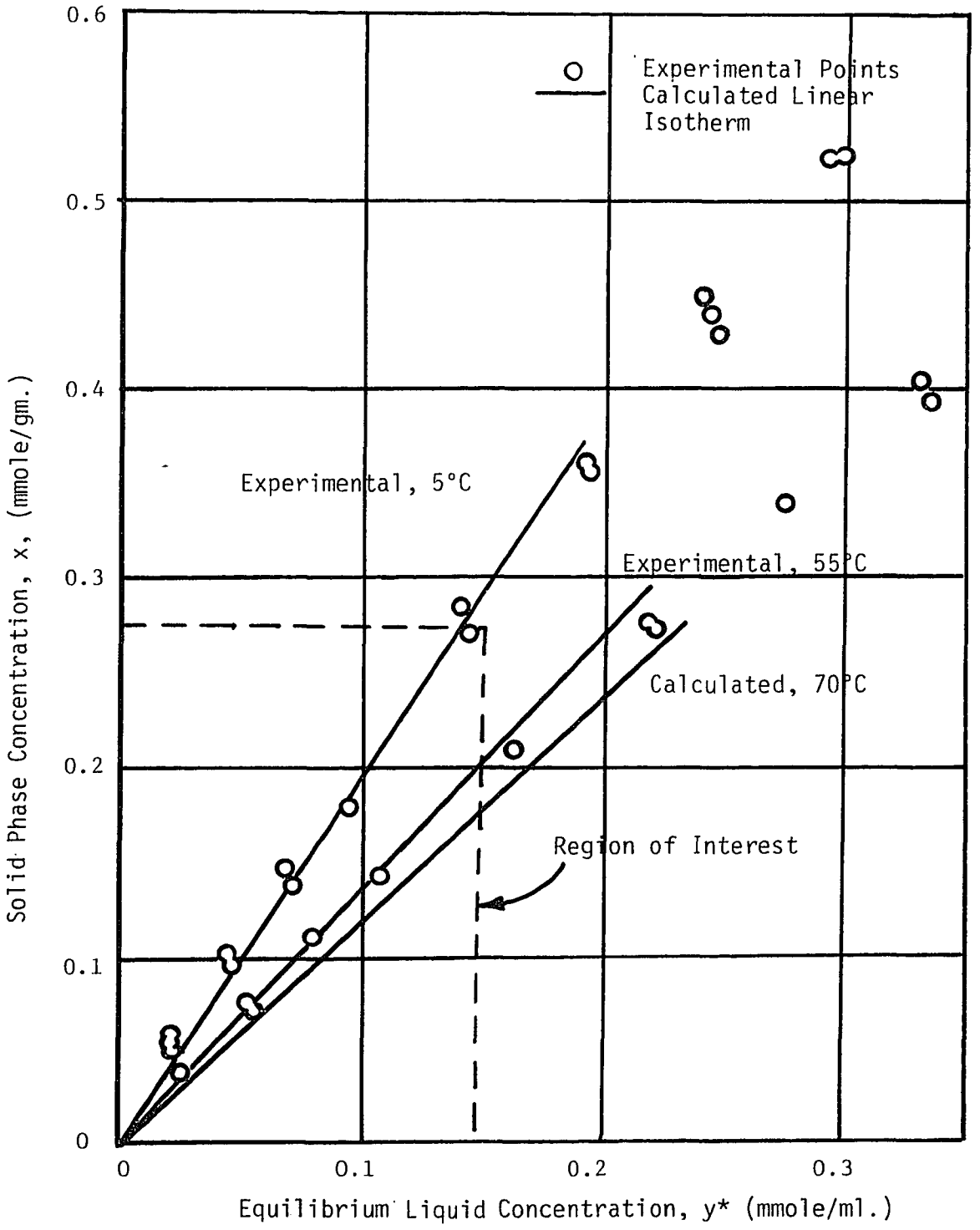

FIGURE 6 - ADSORPTION ISOTHERMS FOR THE SYSTEM SODIUM CHLORIDE - WATER - BIO RAD AG11A8 RESIN (FROM GREGORY, REFERENCE 14)

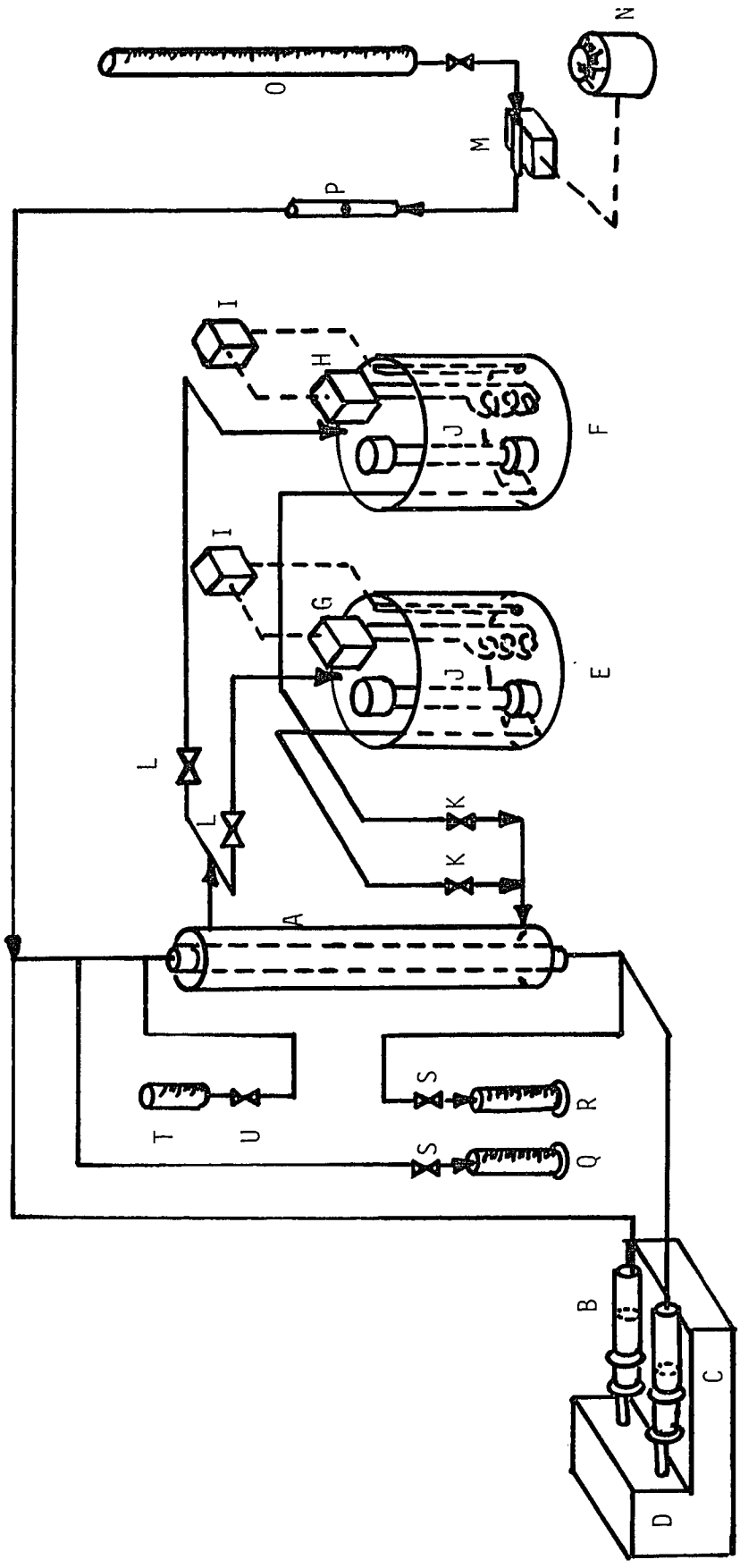

FIGURE 7 - EXPERIMENTAL CONTINUOUS PARAMETRIC PUMP

sources were constant temperature baths (E and F for hot and cold baths, respectively). The hot bath temperature was maintained by a George Ulanit Co. Heetgrid electric immersion heater (G) and the cold bath temperature by a Neslab Instruments U-Cool refrigerated cooling coil (H). Both temperatures were regulated by H B Instrument Co. Quickset temperature controllers (I). Little Giant submerged centrifugal pumps (J) circulated the water to and from the baths. Two check valves (K) at the column jacket entrance prevented the baths from mixing and stopcock valves (L) at the column jacket exit insured return of jacket fluid to the proper bath.

The fluid feed was delivered to the column top by a Chemical Apparatus Co. Vibrostaltic laboratory pump (M) whose pumping rate was regulated by a Variac motor control (N). The feed tank was a calibrated burette (O) and the feed rate was monitored by a calibrated Manostat rotamater (P). The top and bottom products exited continuously to calibrated receivers (Q and R, respectively), their flow rate being controlled by glass and teflon cappilary valves (S). Air pockets and flow disruptions due to expansion and contraction effects in the interstitial column fluid induced by rapid temperature change between half-cycles were relieved by a $10cm^3$ expansion-contraction reservoir (T) and Valve (U) at the column top. The expansion-contraction reservoir was initially filled with $2.0cm^3$ feed solution. The connecting tubing (1/32 "ID), joints and adapters were constructed of teflon and/or glass and manufactured by Rainin Instrument Corporation.

C. Experimental Procedure

Before each run fresh resin in the self-adsorbed form was equilibrated with feed solution at room temperature for 24 hours. Fresh feed solution was prepared for each run by weighing an exact amount of USP Grade NaCl into distilled water and bringing the solution to an exact volume. The concentration was checked by electrical conductivity, the conductivity apparatus having been pre-checked with a standard 0.1000M NaCl solution.

The adsorbant column was packed to specified height for each run by introducing a slurry of fresh resin in equilibrium with feed solution at room temperature to the column top. The feed tank and connecting tubing were filled with feed solution. The bottom reservoir was filled with a predetermined amount of feed solution and the top reservoir, except for its "dead volume" was empty. The "dead volume" contained feed solution. The expansion-contraction reservoir contained $2.0cm^3$ feed solution. Hot water was directed to the column jacket with the expansion-contraction reservoir valve open and, as the column contents approached thermal equilibrium with the jacket fluid, the expansion contraction reservoir rose to $5.0cm.^3$ After 2.5 minutes at 70°C, the expansion-contraction reservoir valve was closed and feed solution was delivered to the column top at the feed rate set for the particular run. Two column volumes of feed solution were delivered to the column top and removed at the bottom product take-off valve to bring the column

contents to the same initial condition for each run, i.e., resin in equilibrium with feed solution at 70°C.

Each run began with a hot upflow half-cycle, the flow pattern actuated by simultaneous filling of the top reservoir and emptying of the bottom reservoir. Top and bottom products were continuously withdrawn at a uniform rate by adjusting the top and bottom product valve positions and observing the volume in the calibrated receivers. Feed was continuously delivered to the column top, its rate being observed at the rotameter. When the required reservoir volume was displaced from column bottom to column top, the reservoir pump was shut off, the feed stopped and the product valves closed. The expansion-contraction reservoir valve was opened, the hot water pump shut off, and the cold water pump activated. The expansion-contraction reservoir volume dropped to $2.0cm^3$ in 2.5 minutes and the expansion-contraction reservoir valve was shut. Meanwhile, the feed volume, half-cycle time, and product volume were observed. Reservoir pump action was reversed and the cold downflow half-cycle was initiated. Again top and bottom products were continuously removed and feed solution continuously delivered as in the previous half-cycle. At the completion of the cold half-cycle the next hot half-cycle was begun after relieving expansion effects as before. This procedure was repeated for the desired number of full cycles.

The top and bottom products were analyzed for Sodium Chloride content by electrical conductivity at each cold half-cycle. When necessary, the sample was diluted to 8.0 cm^3 with distilled water

to fill the conductivity cell. The product concentrations in mmoles/ml were then determined by

$$\text{Product Molarity} = \frac{\text{Sample Molarity x Sample Volume}}{\text{Product Volume}}$$

DISCUSSION

A. General

Computer solution of the model equations was used to generate performance curves for continuous parametric pumps at various values of the operating parameters of interest in this study. These performance curves give the variation in solute separation, i.e., top and bottom product concentrations for the cold half-cycle, with number of cycles and were then compared with the results of experimental runs to establish the efficacy of the model equations in predicting parametric pump performance.

Once the validity of the model had been established, the internal operation of the parametric pump was investigated using the model equations. Liquid phase and solid phase concentrations were calculated as a function of axial position and time for each half-cycle, generating various concentration curves for any set of operating conditions. The concentration curves were then compared with the performance curves to explain the behavior of the parametric pump.

The major variables affecting the shape of continuous parametric pump performance curves are, in addition to temperature, not studied here, bottom product withdrawal rate (ϕ_B), column displacement per half-cycle ($Q\tau$) and column height (h). The half-cycle

duration, τ, is also of interest in analyzing the performance of non-equilibrium parametric pumps. Indeed, variation of the shape of a parametric pump performance curve with half-cycle duration is the basic indication of non-equilibrium operation, since if equilibrium operation is assured, no variation with time is possible. Therefore, this parameter will be investigated first.

B. Effect of Half-Cycle Duration, τ

It is apparent that maximum separation of solute between the lean and concentrated product streams is achieved when the adsorbant column is operated at equilibrium. Under those conditions, the maximum quantity of solute is removed from the liquid to the solid phase at the cold temperature, insuring the minimum possible solute concentration in the lean product. Similarly, under equilibrium conditions, the maximum quantity of solute is discharged from the solid to the liquid phase at the hot temperature, insuring, in turn, the maximum possible solute concentration in the enriched product. Therefore, if better separation, i.e., leaner bottom product concentrations and richer top product concentrations, are obtained with longer half-cycle times, it is apparent that equilibrium operation has not been attained at the shorter half-cycle time.

The first set of experimental runs was chosen to illustrate this point. Table 1 summarizes the experimental conditions for three runs at 24, 36, and 48 minute half-cycle duration, respectively. Column height, reservoir volume and lean product discharge rate were

TABLE 1

EXPERIMENTAL CONDITIONS FOR RUNS WITH VARIABLE CYCLE TIME

Operating Variable	Value
Hot Temperature	343° K
Cold Temperature	278° K
Reservoir Displacement	25 cm^3
Bottom Product Withdrawal Ratio	0.04
Top Product Withdrawal Ratio	0.36
Dead Volume	4.5 cm^3
Feed Composition	0.100 mole NaCl/liter
Feed Rate	0.4167 cm^3/min
Column Height	90 cm

chosen such that, if equilibrium conditions obtained, Region I operation was assured, i.e., $L_1<L_2<h$ from equations (A-15), (A-16), and (A-17).

The experimental results are presented in Table 2. From the graphical representation of the data on Figure 8, it is apparent that longer half-cycle times gave markedly better separations and that assuming non-equilibrium operation for the 24-minute half-cycle time is justified. Figure 8 also compares the separation predicted by the model equations (Table 3) with the experimental data, showing a reasonable fit to the data and indicating that the model equations, do, in fact predict the same trend as do the experimental results.

Figure 9 compares calculated bottom product concentrations at longer half-cycle times given on Table 4, illustrating the approach to equilibrium conditions. The equilibrium theory performance curve was generated using equation (44) from reference 5 and the operating parameters from Table 1. The model equations predict that, for this physical system, equilibrium operation of the parametric pump is not reasonably approached, even at a 3-hour half-cycle time. And the deviation of the curve for 24 minutes from the equilibrium theory prediction further establishes the non-equilibrium nature of operation in that time region. This half-cycle time was used for the remainder of the experiments.

TABLE 2

EXPERIMENTAL RESULTS, VARIABLE CYCLE TIME

(CONCENTRATIONS IN MOLES NaCl/LITER)

Half-Cycle Time (Minutes)	24		36		48	
No. Cycle	Top Product	Bottom Product	Top Product	Bottom Product	Top Product	Bottom Product
1	0.100	0.0935	0.100	0.0870	0.100	0.0916
2	0.106	0.0717	0.111	0.0718	0.106	0.0824
3	0.105	0.0648	0.112	0.0621	0.105	0.0695
4	0.113	0.0566	0.116	0.0611	0.113	0.0542
5	0.120	0.0521	0.114	0.0473	0.120	0.0495
6	0.124	0.0500	0.114	0.0459	0.124	0.0403
7	0.122	0.0490	0.112	0.0457	0.122	0.0424
8	0.119	0.0476	0.114	0.0430	0.119	0.0380
9	0.122	0.0453	0.111	0.0374	0.122	0.0355
10	0.125	0.0404	0.113	0.0376	0.125	0.0292
11	0.122	0.0397	0.112	0.0362	0.122	0.0269
12	0.119	0.0394	0.115	0.0317	0.119	0.0261
13	0.121	0.0386	0.112	0.0280	0.121	0.0223
14	0.121	0.0369	0.112	0.0269	0.121	0.0209
15	0.115	0.0372	0.113	0.0276	0.115	0.0211
16	0.115	0.0368	0.111	0.0272	0.115	0.0197
17	0.120	0.0370	0.112	0.0258	0.120	0.0177
18	0.117	0.0363	0.111	0.0256	0.117	0.0162
19	0.116	0.0366	0.110	0.0260	0.116	0.0165
20	0.118	0.0370	0.111	0.0262	0.118	0.0161

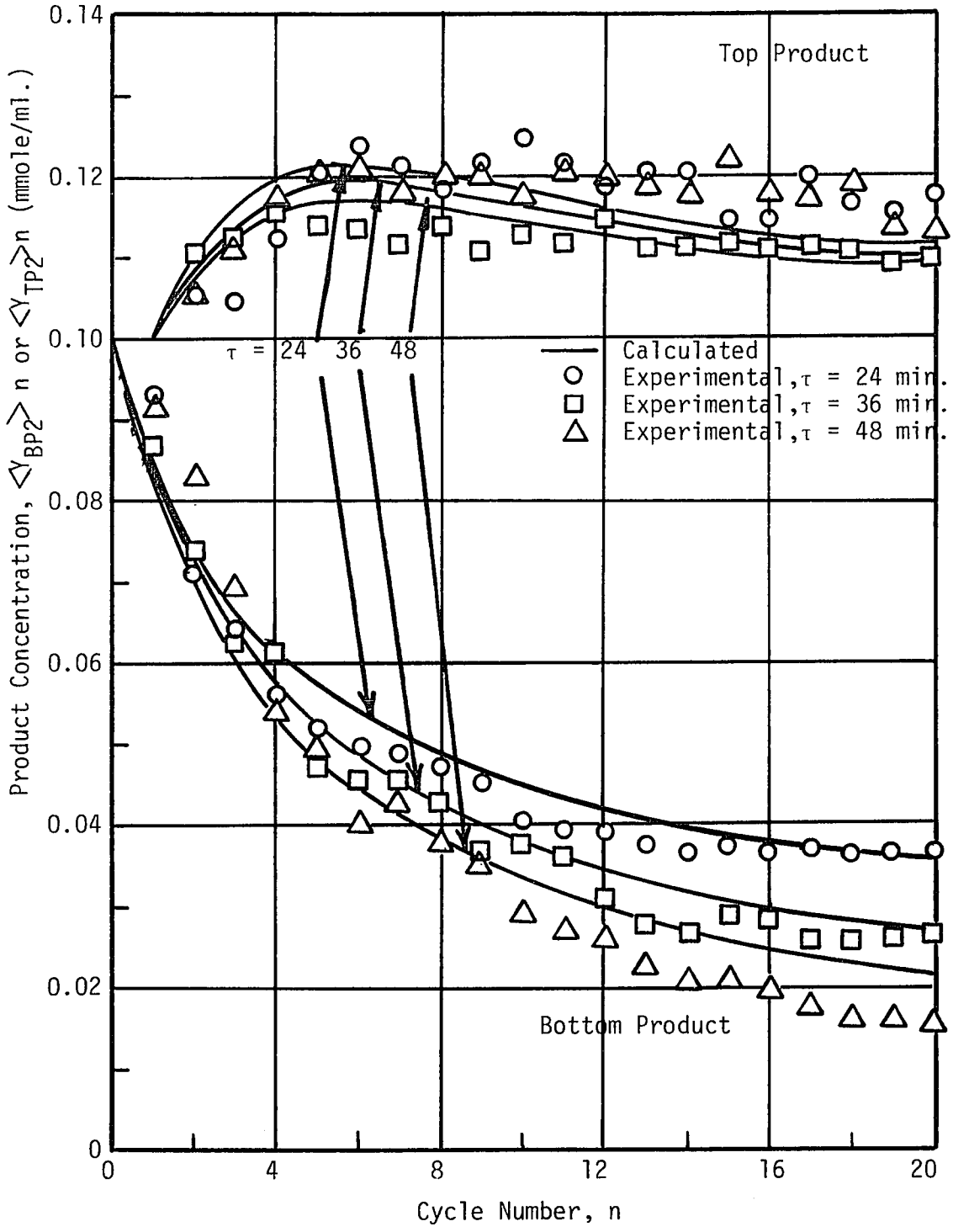

FIGURE 8 - EFFECT OF HALF-CYCLE TIME ON SEPARATION

TABLE 3

CALCULATED RESULTS, VARIABLE CYCLE TIME

(CONCENTRATIONS IN MOLES NaCl/LITER)

Half-Cycle Time (Minutes)	24		36		48	
Cycle No.	Top Product	Bottom Product	Top Product	Bottom Product	Top Product	Bottom Product
1	0.1000	0.0812	0.1000	0.0799	0.1000	0.0792
2	0.1085	0.0728	0.1096	0.0733	0.1103	0.0689
3	0.1133	0.0662	0.1150	0.0627	0.1161	0.0605
4	0.1159	0.0612	0.1181	0.0568	0.1194	0.0541
5	0.1171	0.0572	0.1195	0.0521	0.1211	0.0489
6	0.1172	0.0539	0.1198	0.0482	0.1215	0.0446
7	0.1167	0.0511	0.1195	0.0449	0.1213	0.0410
8	0.1161	0.0487	0.1187	0.0421	0.1206	0.0379
9	0.1152	0.0466	0.1178	0.0397	0.1196	0.0352
10	0.1144	0.0448	0.1168	0.0376	0.1186	0.0330
11	0.1135	0.0432	0.1159	0.0358	0.1175	0.0310
12	0.1127	0.0419	0.1150	0.0342	0.1165	0.0292
13	0.1120	0.0407	0.1141	0.0328	0.1155	0.0277
14	0.1114	0.0396	0.1133	0.0316	0.1147	0.0264
15	0.1108	0.0387	0.1126	0.0305	0.1139	0.0252
16	0.1103	0.0378	0.1120	0.0295	0.1131	0.0242
17	0.1098	0.0371	0.1114	0.0287	0.1125	0.0233
18	0.1094	0.0365	0.1109	0.0279	0.1119	0.0225
19	0.1090	0.0359	0.1104	0.0273	0.1114	0.0218
20	0.1087	0.0354	0.1100	0.0267	0.1109	0.0212

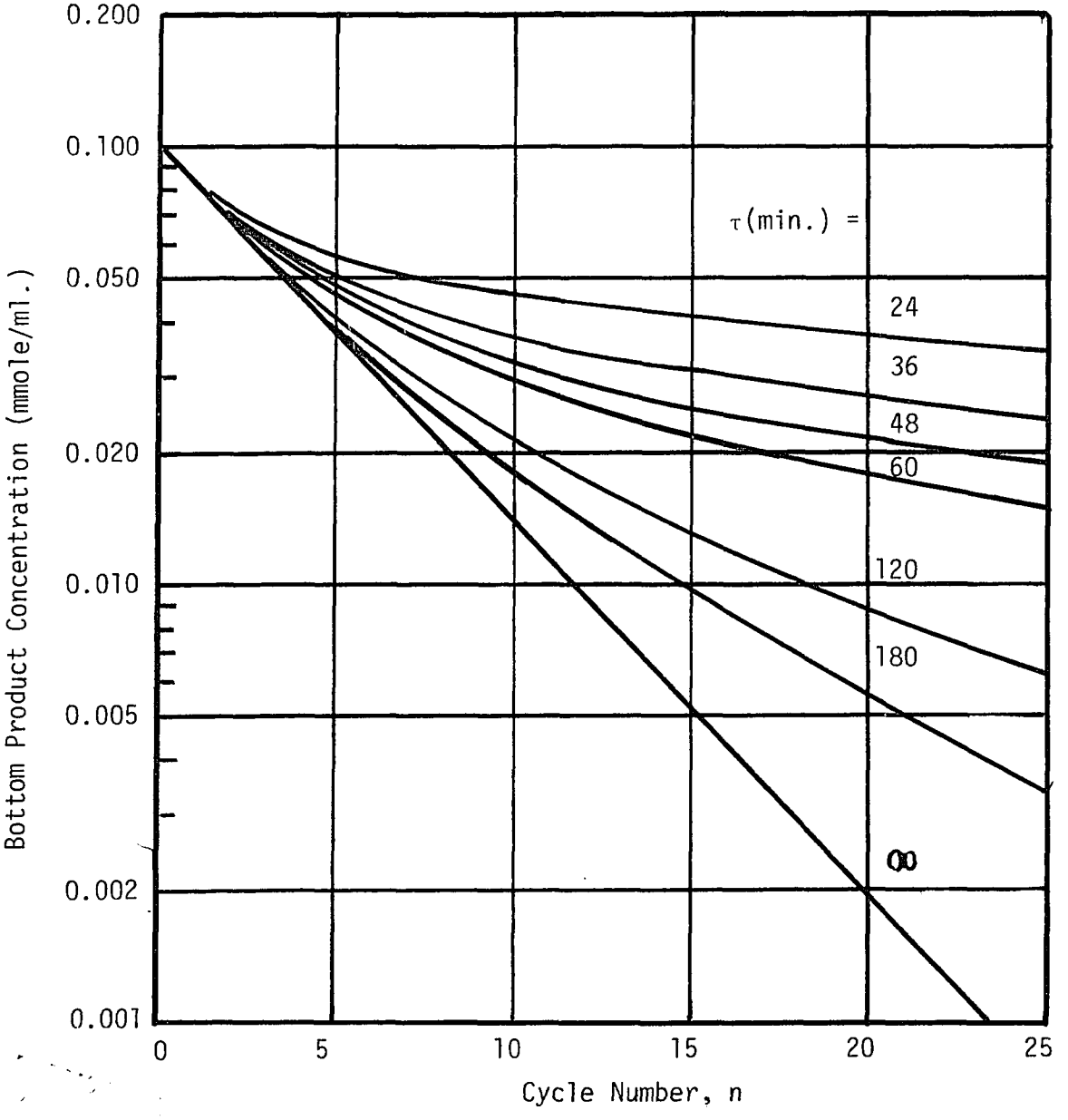

FIGURE 9 - CALCULATED EFFECT OF HALF-CYCLE TIME ON SEPARATION - h = 90 cm, Q_τ = 25 cm^3, ϕ_B = 0.04, ϕ_T = 0.36

TABLE 4

CALCULATED BOTTOM PRODUCT CONCENTRATIONS

VARIABLE CYCLE TIME

(CONCENTRATIONS IN MOLES NaCl/LITER)

Half-Cycle Time (Minutes)	24	36	48	60	120	180
Cycle No.						
1	0.0812	0.0799	0.0792	0.0788	0.0777	0.0773
2	0.0728	0.0703	0.0688	0.0678	0.0654	0.0644
3	0.0662	0.0630	0.0605	0.0540	0.0554	0.0538
4	0.0612	0.0568	0.0541	0.0522	0.0475	0.0454
5	0.0572	0.0521	0.0489	0.0466	0.0410	0.0386
10	0.0448	0.0376	0.0330	0.0297	0.0217	0.0184
15	0.0387	0.0305	0.0252	0.0216	0.0129	0.0096
20	0.0354	0.0267	0.0212	0.0173	0.0085	0.0055
25	0.0336	0.0247	0.0190	0.0151	0.0063	0.0035

C. Effect of Bottom Product Withdrawal Rate, ϕ_B

In equilibrium parametric pump operation, increasing bottom product withdrawal rate ϕ_B to the point where $\phi_B = b$ marks the transition from Region I to Region II. In Region I, bottom product concentration is independent of ϕ_B and is seen to be a monotonically decreasing function with cycle number (see Figure A-2). In Region II, however, the bottom product concentration is minimized after a number of cycles before a steadily increasing concentration characterizes the lean product concentration performance curve (Figure A-2). On Appendix II of this work, an explanation of this phenomenon is given in terms of concentration front penetration length, equilibrium operation being characterized by the movement of sharply defined wave fronts along the column's axial length. In essence, if hot half-cycle concentration front penetration is exceeded by cold half-cycle concentration front penetration, solute tends to migrate toward the lean end of the column, disrupting separation and producing the degenerating separation characterizing equilibrium Region II (Figure A-2).

There are no sharply defined wave fronts along the axis of a non-equilibrium adsorption column. Axial concentration gradients are continuous, smooth, and their shape is time-dependent as well. However, penetration theory may also apply, in a qualitative sense, to the non-equilibrium case. If, on the average, downward movement of solute along the column's axial length is greater during the cold half-cycle than upward movement of solute on the hot half-cycle,

solute will tend to migrate toward the bottom of the column, having the same disruptive effect on separation as in the Region II equilibrium case. The bottom product withdrawal rate, ϕ_B, is the principal variable affecting the relative movement of liquid along the column axis between the hot and cold half-cycles since the velocities of the cold and hot flowing fluid, respectively, are given by

$$v_1 = \frac{Q}{\varepsilon A} \quad (1-\phi_B) \tag{67}$$

and

$$v_2 = \frac{Q}{\varepsilon A} \quad (1+\phi_B) \tag{68}$$

Movement of solute is affected by the rate of interphase mass transfer as well as fluid velocity (bulk flow), but it will be shown that the bottom product withdrawal rate, ϕ_B, has the above described effect on separation.

The next series of experimental runs were designed to examine this effect. Table 5 summarizes the experimental conditions for a series of experimental runs where, for a given column height and reservoir displacement, the bottom product rate was varied across a wide range ($0.04 \leq \phi_B \leq 0.28$). The experimental results are given in Table 6 and calculated results for the same conditions are given in Table 7.

For the first group of runs, at 90 cm. column height, operating parameters were chosen such that column operation matched the requirements for equilibrium Region I and II, that is $L_1 < h$, and $L_2 < h$, if equilibrium operation could be obtained. In addition, for

TABLE 5

EXPERIMENTAL CONDITIONS FOR RUNS WITH VARIABLE BOTTOM PRODUCT WITHDRAWAL RATE (LONG COLUMN)

Operating Variable	Value
Hot Temperature	343° K
Cold Temperature	278° K
Reservoir Displacement	25 cm^3
Feed Rate Ratio ($\phi_B+\phi_T$)	0.400
Dead Volume	4.5 cm^3
Feed Composition	0.100 moles NaCl/liter
Column Height	90 cm
Half-Cycle Time	24 min.

TABLE 6

EXPERIMENTAL RESULTS, VARIABLE

BOTTOM PRODUCT RATE, LONG COLUMN

(CONCENTRATIONS IN MOLES NaCl/LITER)

Bottom Product Withdrawal Ratio	0.04		0.16		0.28	
Cycle No.	Top Product	Bottom Product	Top Product	Bottom Product	Top Product	Bottom Product
1	0.100	0.0935	0.100	0.0824	0.100	0.0908
2	0.106	0.0717	0.114	0.0752	0.119	0.0787
3	0.105	0.0648	0.115	0.0692	0.122	0.0727
4	0.113	0.0566	0.120	0.0655	0.130	0.0738
5	0.120	0.0521	0.127	0.0719	0.131	0.0718
6	0.124	0.0500	0.128	0.0724	0.133	0.0723
7	0.122	0.0490	0.123	0.0733	0.134	0.0784
8	0.119	0.0476	0.127	0.0727	0.136	0.0811
9	0.122	0.0453	0.127	0.0708	0.136	0.0816
10	0.125	0.0404	0.127	0.0721	0.136	0.0817
11	0.122	0.0397	0.127	0.0731	0.136	0.0822
12	0.119	0.0394	0.125	0.0732	0.135	0.0821
13	0.121	0.0386	0.125	0.0716	0.136	0.0823
14	0.121	0.0369	0.127	0.0703	0.133	0.0824
15	0.115	0.0372	0.125	0.0682	0.135	0.0826
16	0.115	0.0368	0.126	0.0680	0.135	0.0832
17	0.120	0.0370	0.124	0.0655	0.134	0.0848
18	0.117	0.0363	0.126	0.0645	0.137	0.0847
19	0.116	0.0366	0.126	0.0621	0.133	0.0843
20	0.118	0.0370	0.125	0.0613	0.132	0.0849

TABLE 7

CALCULATED RESULTS, VARIABLE

BOTTOM PRODUCT RATE, LONG COLUMN

(CONCENTRATIONS IN MOLES NaCl/LITER)

Bottom Product Withdrawal Ratio	0.04		0.16		0.28	
Cycle No.	Top Product	Bottom Product	Top Product	Bottom Product	Top Product	Bottom Product
1	0.1000	0.0812	0.1000	0.0810	0.1000	0.0809
2	0.1085	0.0728	0.1093	0.0744	0.1096	0.0761
3	0.1133	0.0662	0.1151	0.0740	0.1160	0.0741
4	0.1159	0.0612	0.1189	0.0675	0.1203	0.0740
5	0.1171	0.0572	0.1213	0.0660	0.1233	0.0748
6	0.1172	0.0539	0.1228	0.0651	0.1254	0.0759
7	0.1167	0.0511	0.1238	0.0645	0.1269	0.0772
8	0.1161	0.0487	0.1244	0.0642	0.1281	0.0785
9	0.1152	0.0466	0.1248	0.0640	0.1289	0.0796
10	0.1144	0.0448	0.1250	0.0639	0.1295	0.0807
11	0.1135	0.0432	0.1252	0.0638	0.1300	0.0816
12	0.1127	0.0419	0.1253	0.0638	0.1304	0.0823
13	0.1120	0.0407	0.1253	0.0638	0.1307	0.0830
14	0.1114	0.0396	0.1254	0.0638	0.1310	0.0835
15	0.1108	0.0387	0.1254	0.0638	0.1312	0.0840
16	0.1103	0.0378	0.1254	0.0638	0.1314	0.0844
17	0.1098	0.0371	0.1254	0.0638	0.1315	0.0847
18	0.1094	0.0365	0.1254	0.0638	0.1316	0.0850
19	0.1090	0.0359	0.1254	0.0638	0.1317	0.0852
20	0.1087	0.0354	0.1254	0.0638	0.1318	0.0854

these runs, fluid breakthrough from one end of the column to the other was precluded by the length of the column, i.e.,

$$\frac{Q\tau(1-\phi_B)}{\varepsilon A} < \frac{Q\tau(1+\phi_B)}{\varepsilon A} < h. \tag{69}$$

From the graphical representation of the experimental data on Figure 10, it is apparent that the same qualitative behavior exists in the non-equilibrium case. For low bottom product withdrawal rates (ϕ_B=0.04) the bottom product concentration curve has a monotonically decreasing character, matched, within reason, by the behavior predicted by the computational model. For high bottom product withdrawal rates (ϕ_B=0.28) the characteristic degenerating separation is the case both theoretically and experimentally.

Figure 11 shows calculated concentration curves for the operating conditions outlined on Table 5, where lean product concentration is plotted against number of cycles of operation at various bottom product withdrawal ratios. The calculated data are given on Table 8. The curves show a minimum in bottom product concentration first appearing at ϕ_B=0.20 at the seventh cycle of operation. No such minimum appears for ϕ_B=0.16, at least in the first twenty-five cycles of operation. These curves indicate that a gradual transition from monotonically decreasing bottom product concentration to a performance curve containing a minimum is obtained by increasing bottom product withdrawal rate. They also show, qualitatively at least, that non-equilibrium behavior is analogous to equilibrium behavior as far as lean product withdrawal ratio is concerned.

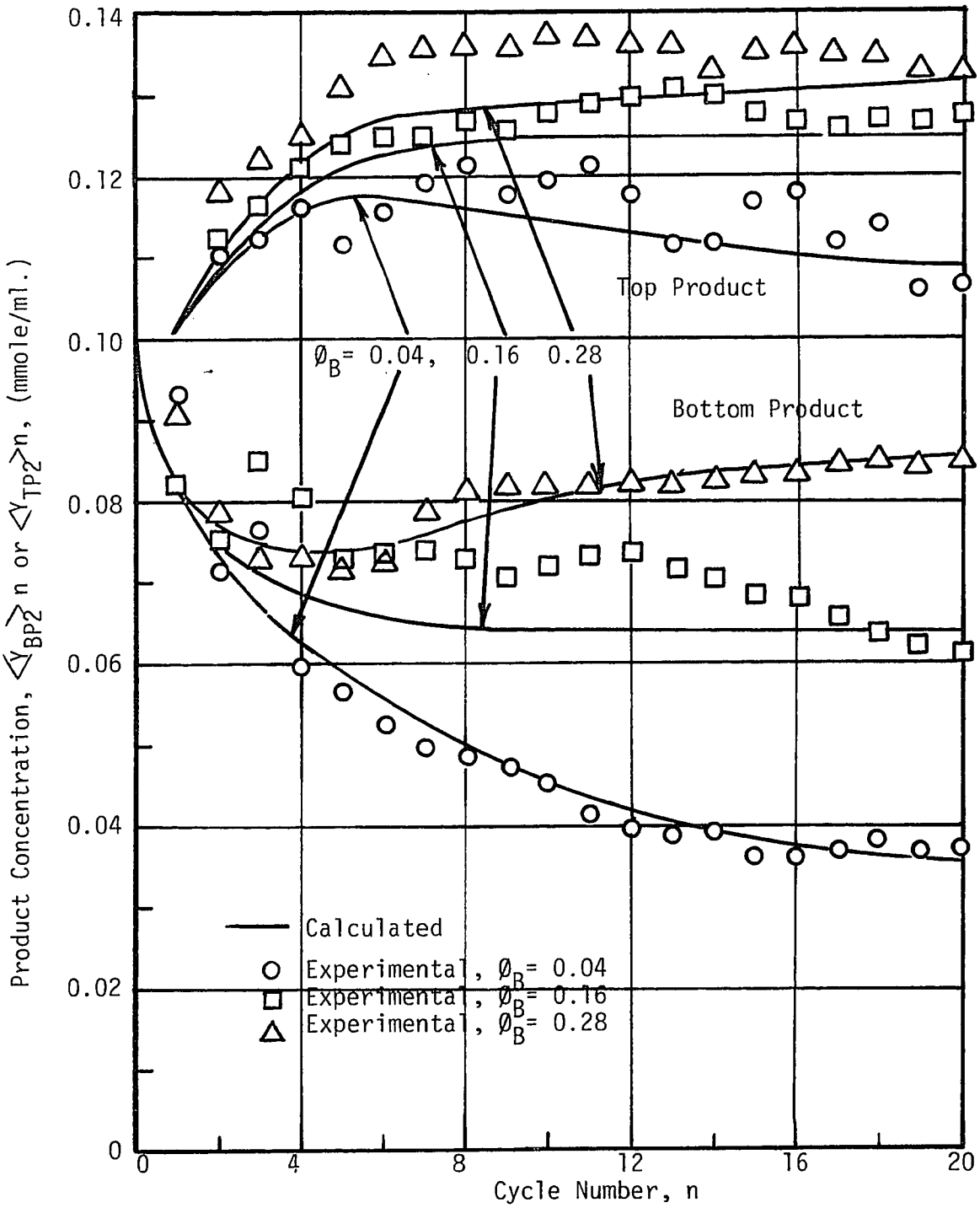

FIGURE 10 - EFFECT OF BOTTOM PRODUCT WITHDRAWAL RATE ON SEPARATION, 90 cm COLUMN

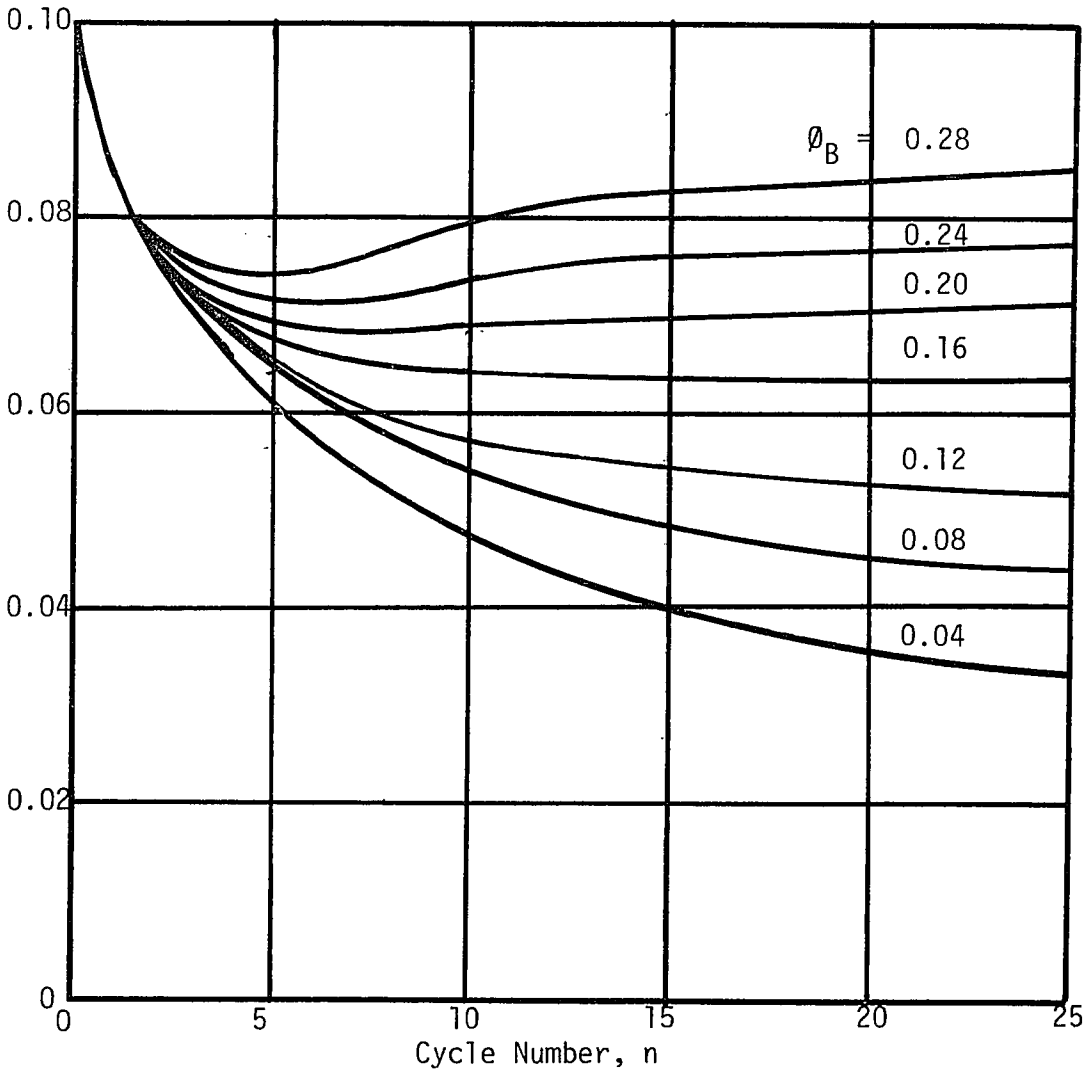

FIGURE 11 - CALCULATED PERFORMANCE CURVES FOR VARIOUS RATES OF BOTTOM PRODUCT WITHDRAWAL, h = 90 cm, h = 90 cm, $Q\tau$ = 25 cm^3, τ = 24 min., $\emptyset_T+\emptyset_B$ = 0.40

TABLE 8

CALCULATED BOTTOM PRODUCT CONCENTRATIONS

VARIABLE BOTTOM PRODUCT WITHDRAWAL RATE

LONG COLUMN

(CONCENTRATIONS IN MOLES NaCl/LITER)

Bottom Product Withdrawal Ratio	0.04	0.08	0.12	0.16	0.20	0.24	0.28
Cycle No.							
1	0.0812	0.0811	0.0811	0.0810	0.0810	0.0809	0.0809
2	0.0728	0.0733	0.0736	0.0744	0.0749	0.0754	0.0761
3	0.0662	0.0675	0.0690	0.0700	0.0713	0.0726	0.0741
4	0.0612	0.0634	0.0655	0.0675	0.0695	0.0715	0.0739
5	0.0572	0.0602	0.0633	0.0660	0.0690	0.0715	0.0748
6	0.0539	0.0578	0.0614	0.0651	0.0685	0.0719	0.0759
7	0.0511	0.0558	0.0601	0.0645	0.0685	0.0726	0.0772
8	0.0487	0.0541	0.0592	0.0642	0.0687	0.0733	0.0785
9	0.0466	0.0528	0.0584	0.0640	0.0695	0.0740	0.0796
10	0.0448	0.0516	0.0578	0.0639	0.0703	0.0747	0.0807
15	0.0387	0.0477	0.0552	0.0638	0.0727	0.0770	0.0840
20	0.0354	0.0457	0.0543	0.0638	0.0738	0.0781	0.0854
25	0.0336	0.0447	0.0531	0.0638	0.0742	0.0786	0.0859

Concentration profiles within the adsorbing column calculated via solution of the model equations illustrate the effect of bottom product withdrawal rate on separation. Figure 12 shows liquid concentrations in the column versus time at the top midpoint, and bottom of the adsorbing column for the lower bottom product withdrawal rate (ϕ_B=0.04). A steadily decreasing liquid phase concentration throughout the column length is predicted by the model, showing a net movement of solute toward the concentrated end of the adsorbing column.

The solid-phase axial concentration profile at the end of each half-cycle is shown on Figure 13, where each division of the ordinate represents the entire column length. With each succeeding cycle of operation, the average solid concentration for the hot half-cycle has decreased steadily as indicated by the downward displacement of each hot half-cycle concentration profile, indicating a net movement of solute out of the system in the concentrated product.

The same series of curves for the higher bottom product withdrawal rate (ϕ_B=0.24) is presented in Figures 14 and 15. From Figure 14, the liquid phase concentration at the column ends and midpoint indicate a developing net movement of solute toward the lean end of the column, rather than toward the concentrated end. The liquid contained within the column volume is apparently accumulating solute with time. The same is true for the solid phase, as shown in Figure 15. Here the solid phase concentration is increasing

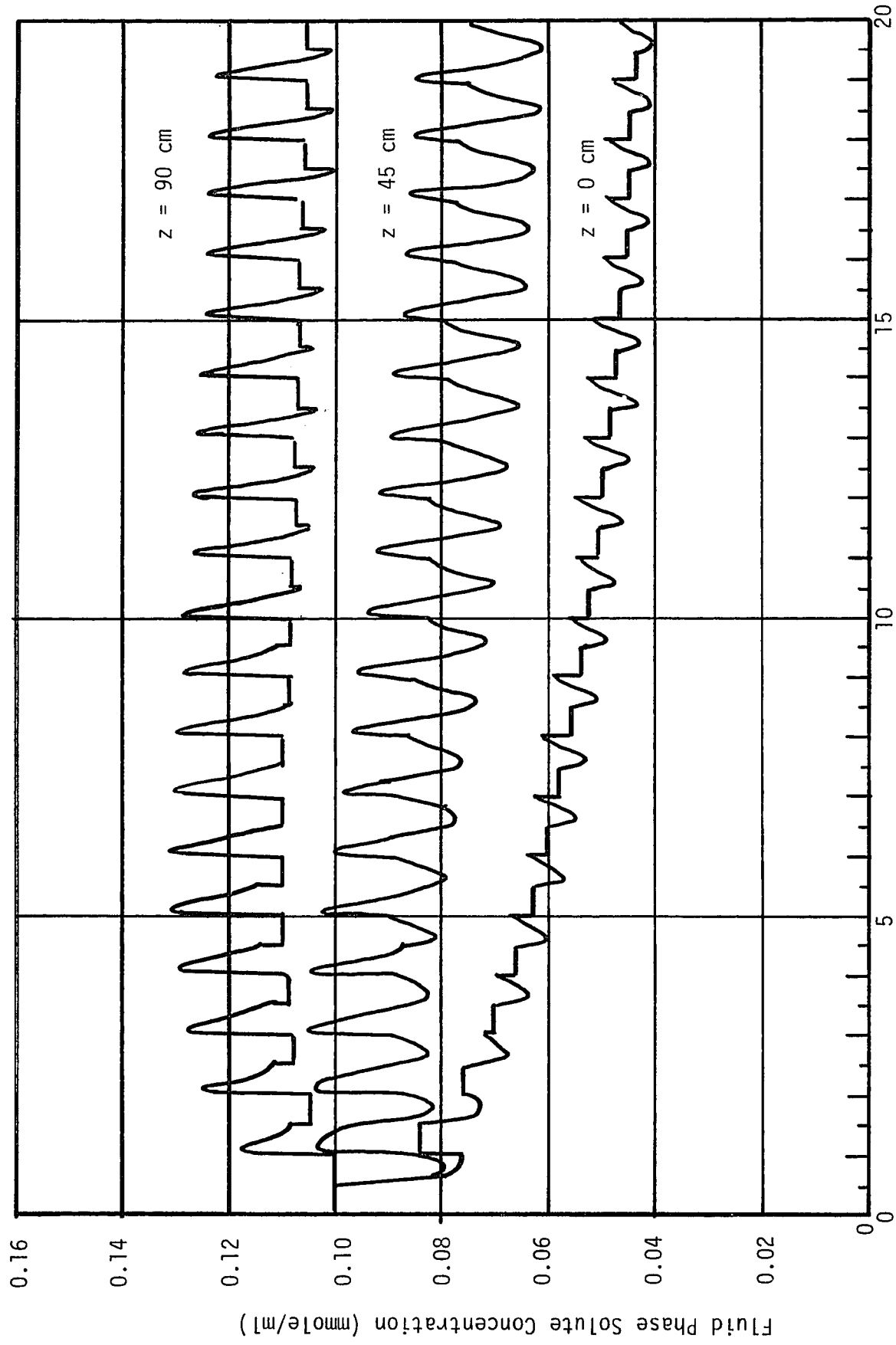

FIGURE 12 - CALCULATED CONCENTRATION PROFILES FOR ϕ_B = 0.04, h = 90 cm

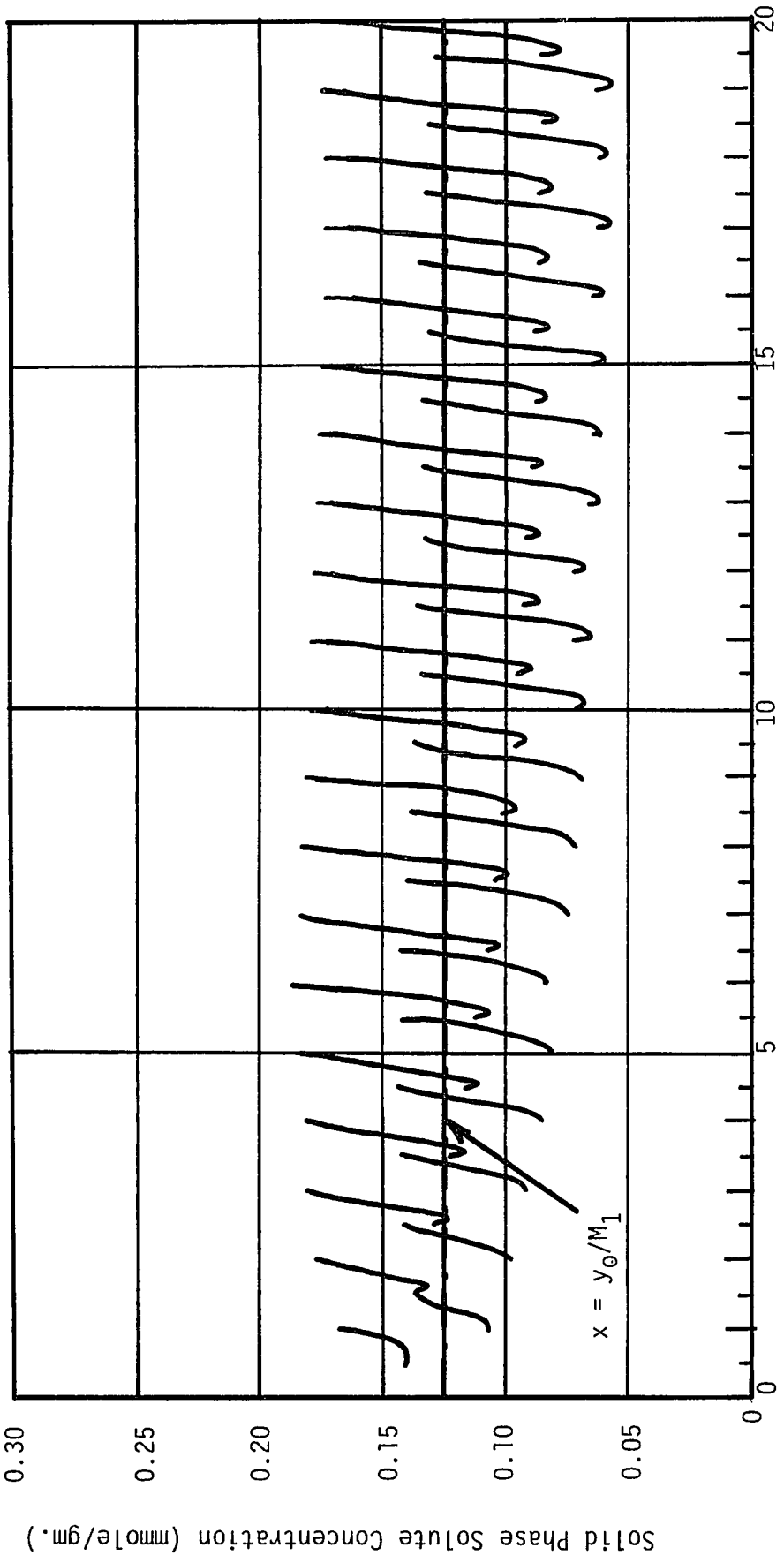

FIGURE 13 - CALCULATED SOLID PHASE CONCENTRATIONS AT END OF HALF CYCLE
$\emptyset_B$ = 0.04, h = 90 cm

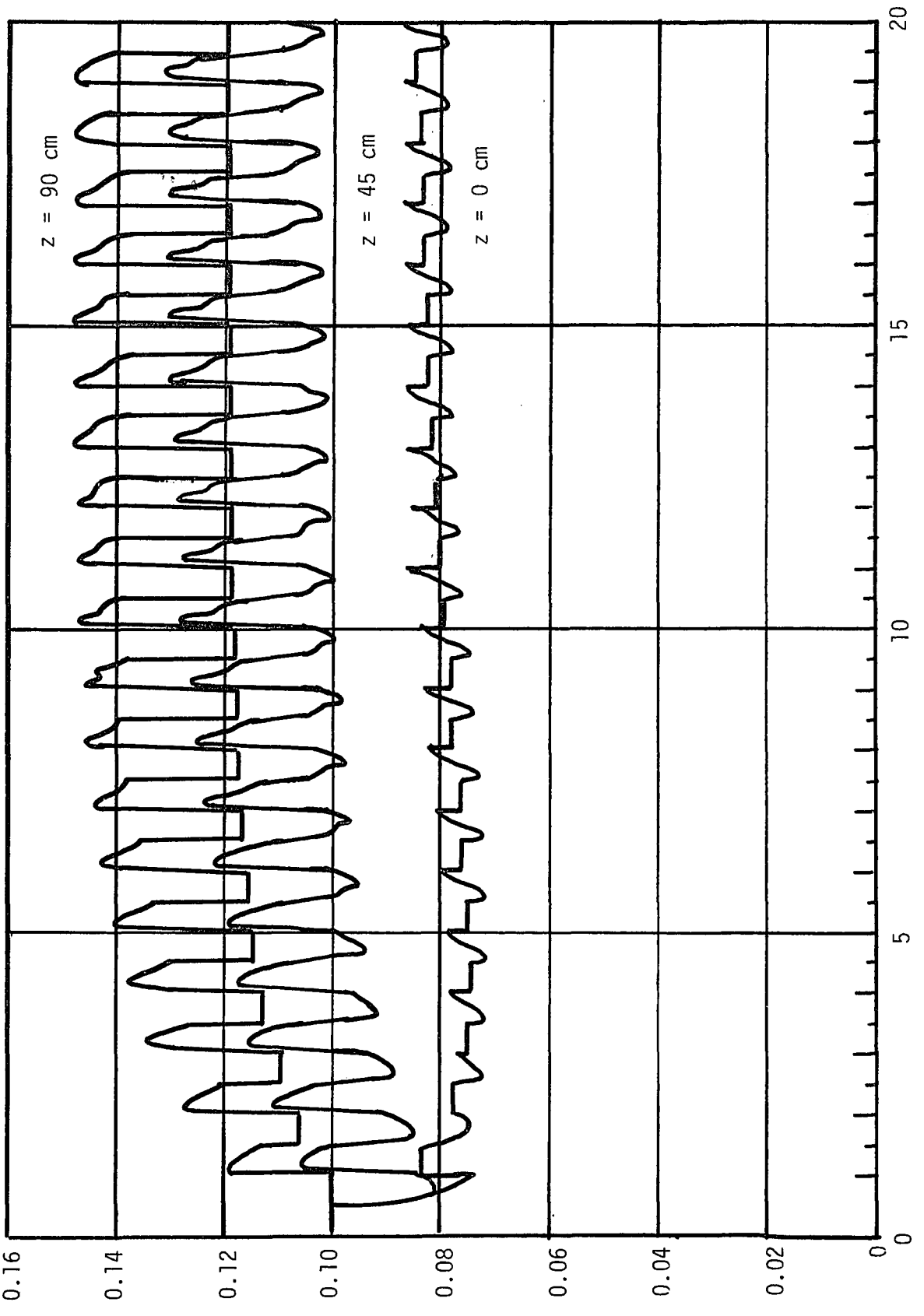

FIGURE 14 - CALCULATED CONCENTRATION PROFILES FOR $\emptyset_B$= 0.24 AT h = 90 cm

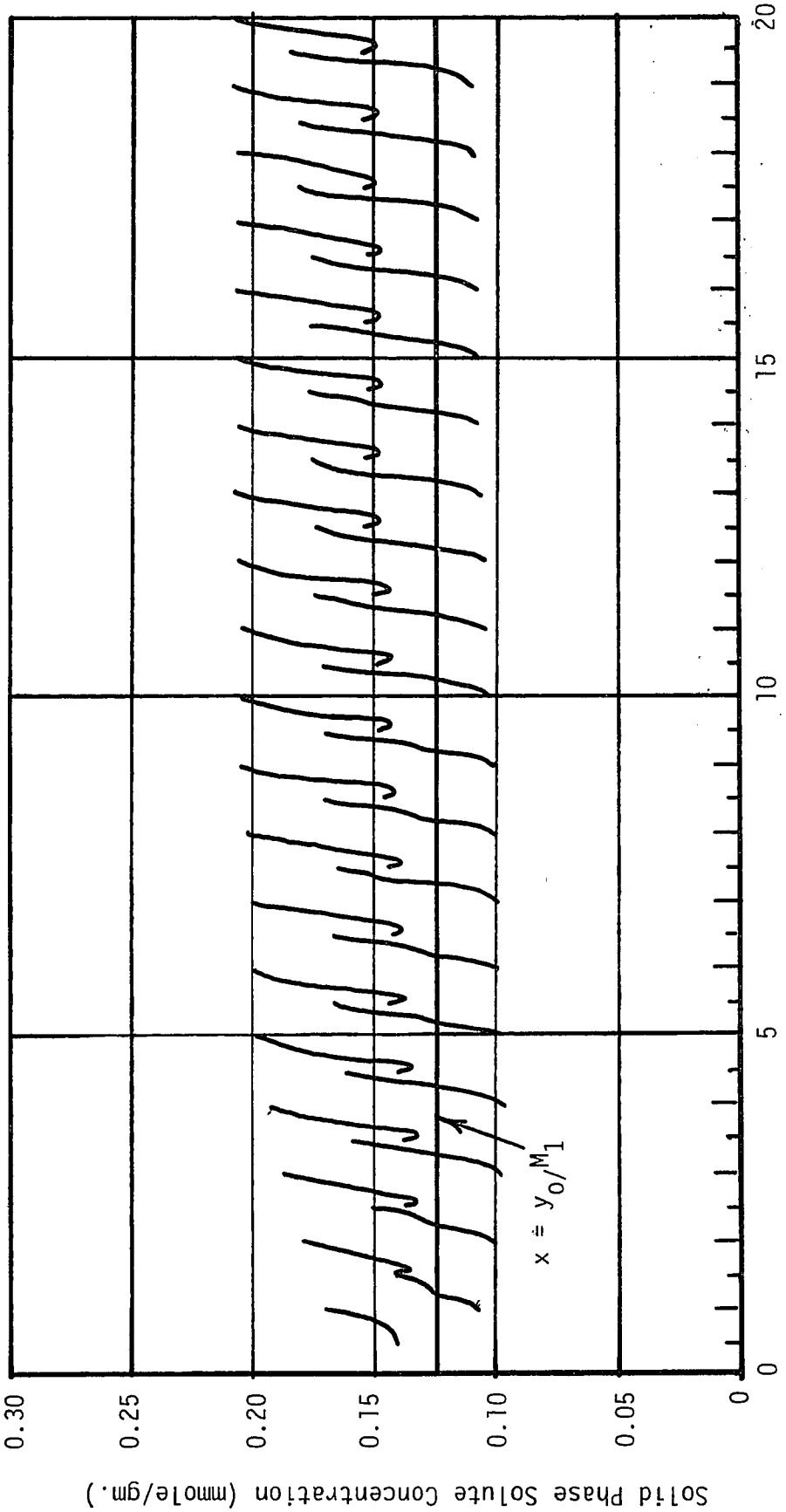

FIGURE 15 - CALCULATED SOLID PHASE CONCENTRATIONS AT END OF HALF-CYCLE
$\emptyset_B = 0.24$, h = 90 cm.

with time along the entire column length. Figure 15 is identical in construction to Figure 13.

The next series of experimental runs were designed to demonstrate the effect of total liquid displacement and column length on separation of solute into lean and concentrated products. The results show that it is the relative fluid displacement between cold and hot half-cycles, rather than total displacement relative to column length, that marks the transition between steadily increasing separation and steadily degrading separation. Operating parameters were again chosen with reference to the equilibrium theory of operation for comparison purposes.

It is apparent from comparing equations (67) and (68) with equations (A-8) and (A-9) that the penetration length for the leading equilibrium theory wave front lags behind total fluid displacement by the factor $(1-b)/(1+m_o)$ for the cold half-cycle and by $(1+b)/(1+m_o)$ for the hot half-cycle. Therefore, equation (69) need not apply, although (A-17) or (A-18) do, to remain within Region I or II for equilibrium operation. For the first set of runs, discussed above, both (69) and (A-17) or (A-18) were true. However, at the operating conditions described on Table 9, with a 60 cm column length and 25 cm^3 reservoir displacement, in contrast with (69),

$$\frac{Q\tau(1+\phi_B)}{\varepsilon A} \gtrless \frac{Q\tau(1-\phi_B)}{\varepsilon A} > h \qquad (70)$$

although, if equilibrium conditions were possible, it was still

TABLE 9

EXPERIMENTAL CONDITIONS FOR RUNS WITH VARIABLE

BOTTOM PRODUCT WITHDRAWAL RATE

(MEDIUM COLUMN)

Operating Variable	Value
Hot Temperature	343° K
Cold Temperature	228° K
Reservoir Displacement	25 cm^3
Feed Rate Ratio ($\phi_B+\phi_T$)	0.400
Dead Volume	4.5 cm^3
Feed Composition	0.100 moles NaCl/liter
Column Height	60 cm
Half-Cycle Time	24 min.

true that $L_1<h$ and $L_2<h$. The experimental results are summarized on Table 10 and appear graphically along with the performance predicted by the model equations (given on Table 11) in Figure 16. Again, a reasonable fit of the model to the experimental data is obtained and the same qualitative behavior shows up. For low bottom product withdrawal rates (ϕ_B=0.08) a steadily decreasing bottom product concentration is shown to exist, but a high bottom product withdrawal rates (ϕ_B=0.24), a minimum in bottom product concentration exists and separation is seen to degrade thereafter with increasing number of cycles.

The model equations were then applied to the operating conditions summarized on Table 9 to generate performance curves for the bottom product concentration at various values of ϕ_B, which are shown on Table 12. Figure 17 shows that performance is similar to that obtained with the previous set of operating conditions. Irrespective of column length relative to liquid displacement, a gradual transition from steadily improving separation to steadily degrading separation is noted with the concentration minimum first appearing within the first 25 cycles of operation at ϕ_B=0.20.

The internal operation of the adsorbant system remains qualitatively the same as for the previous set of operating conditions. Figure 18 gives the liquid phase concentration curves at the top, midpoint, and bottom of the adsorbing column at ϕ_B=0.08. Again the liquid phase solute concentration along the column length is seen

TABLE 10

EXPERIMENTAL RESULTS, VARIABLE BOTTOM PRODUCT RATE, MEDIUM COLUMN

(CONCENTRATIONS IN MOLES NaCl/LITER)

Bottom Product Withdrawal Ratio	0.08		0.16		0.24	
Cycle No.	Top Product	Bottom Product	Top Product	Bottom Product	Top Product	Bottom Product
1	0.100	0.086	0.100	0.087	0.100	0.084
2	0.109	0.072	0.110	0.077	0.107	0.088
3	0.114	0.080	0.116	0.074	0.118	0.071
4	0.122	0.071	0.117	0.071	0.123	0.079
5	0.189	0.064	0.116	0.074	0.124	0.074
6	0.112	0.066	0.118	0.075	0.129	0.076
7	0.114	0.060	0.120	0.071	0.137	0.078
8	0.112	0.062	0.117	0.073	0.137	0.079
9	0.113	0.062	0.123	0.075	0.137	0.083
10	0.113	0.062	0.122	0.074	0.138	0.084
11	0.113	0.065	0.121	0.077	0.137	0.085
12	0.115	0.068	0.120	0.077	0.135	0.084
13	0.116	0.066	0.122	0.077	0.136	0.085
14	0.113	0.057	0.124	0.075	0.139	0.086
15	0.110	0.055	0.120	0.071	0.138	0.087
16	0.114	0.052	0.120	0.067	0.138	0.085
17	0.112	0.158	0.122	0.070	0.136	0.084
18	0.112	0.059	0.122	0.068	0.134	0.083
19	0.113	0.059	0.121	0.069	0.136	0.084
20	0.111	0.060	0.121	0.068	0.130	0.083

TABLE 11

CALCULATED RESULTS, VARIABLE BOTTOM PRODUCT RATE,

MEDIUM COLUMN

(CONCENTRATIONS IN MOLES NaCl/LITER)

Bottom Product Withdrawal Ratio	0.08		0.16		0.24	
Cycle No.	Top Product	Bottom Product	Top Product	Bottom Product	Top Product	Bottom Product
1	0.1000	0.0817	0.1000	0.0819	0.1000	0.0821
2	0.1088	0.0754	0.1092	0.0770	0.1095	0.0787
3	0.1136	0.0709	0.1147	0.0740	0.1156	0.0773
4	0.1156	0.0678	0.1171	0.0725	0.1192	0.0773
5	0.1160	0.0656	0.1191	0.0716	0.1214	0.0777
6	0.1158	0.0639	0.1198	0.0711	0.1228	0.0783
7	0.1153	0.0625	0.1201	0.0708	0.1237	0.0789
8	0.1147	0.0615	0.1202	0.0706	0.1243	0.0794
9	0.1142	0.0606	0.1202	0.0704	0.1247	0.0799
10	0.1138	0.0599	0.1202	0.0703	0.1250	0.0803
11	0.1134	0.0593	0.1201	0.0702	0.1252	0.0806
12	0.1130	0.0588	0.1201	0.0701	0.1254	0.0808
13	0.1127	0.0584	0.1201	0.0701	0.1256	0.0810
14	0.1125	0.0581	0.1201	0.0701	0.1257	0.0812
15	0.1123	0.0578	0.1200	0.0700	0.1258	0.0813
16	0.1121	0.0576	0.1200	0.0699	0.1258	0.0814
17	0.1120	0.0574	0.1200	0.0699	0.1259	0.0815
18	0.1119	0.0573	0.1200	0.0699	0.1259	0.0816
19	0.1118	0.0571	0.1200	0.0699	0.1259	0.0816
20	0.1117	0.0570	0.1200	0.0699	0.1260	0.0817

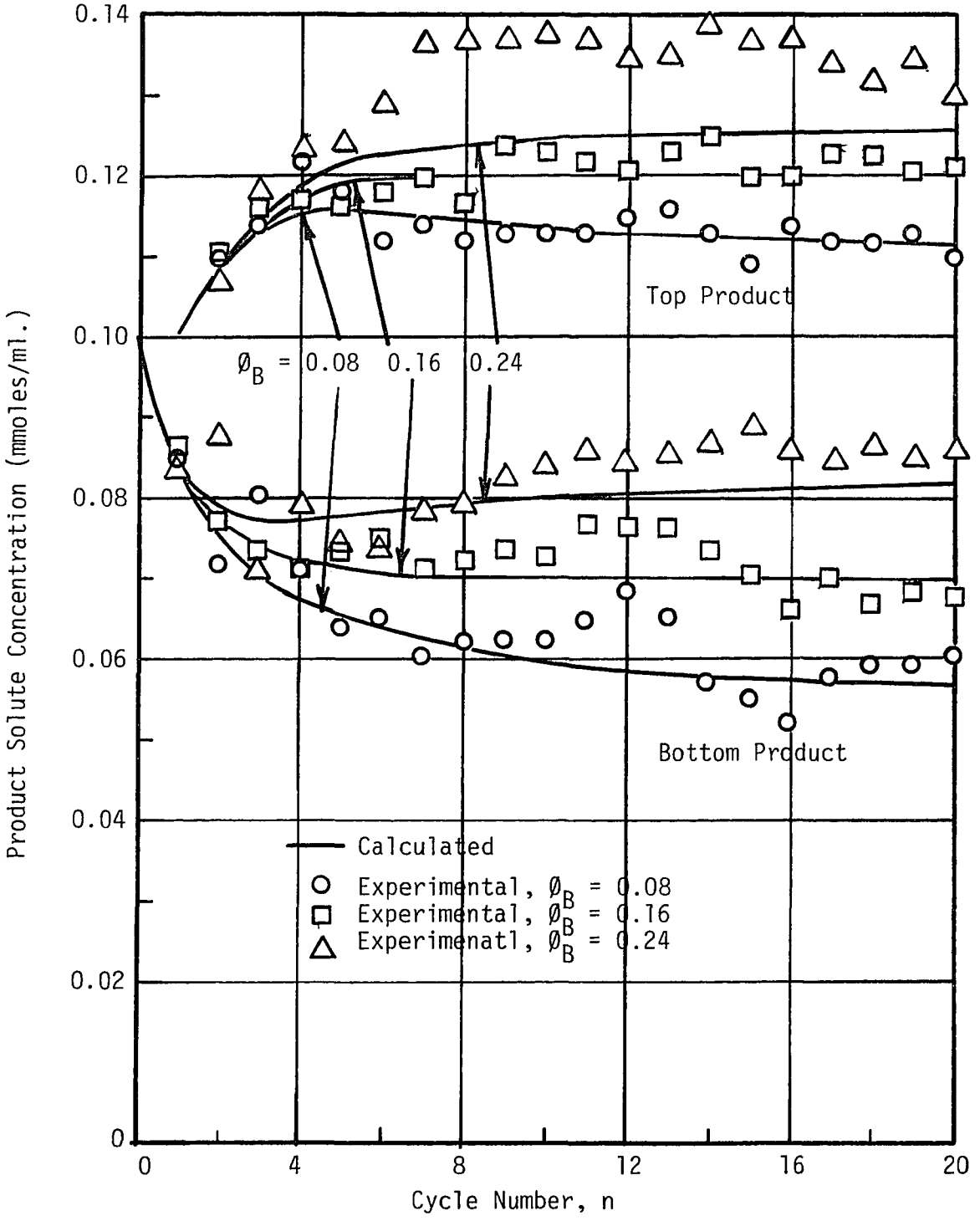

FIGURE 16 - EFFECT OF BOTTOM PRODUCT WITHDRAWAL RATE ON SEPARATION, 60 cm COLUMN

TABLE 12

CALCULATED BOTTOM PRODUCT CONCENTRATIONS

VARIABLE BOTTOM PRODUCT WITHDRAWAL RATE

MEDIUM COLUMN

(CONCENTRATIONS IN MOLES NaCl/LITER)

Bottom Product Withdrawal Ratio	0.04	0.08	0.12	0.16	0.20	0.24	0.28
Cycle No.							
1	0.0817	0.0817	0.0818	0.0819	0.0820	0.0821	0.0822
2	0.0746	0.0754	0.0762	0.0770	0.0778	0.0787	0.0796
3	0.0692	0.0709	0.0725	0.0740	0.0757	0.0773	0.0792
4	0.0653	0.0678	0.0702	0.0725	0.0749	0.0773	0.0799
5	0.0623	0.0656	0.0683	0.0716	0.0747	0.0777	0.0811
6	0.0599	0.0639	0.0675	0.0711	0.0748	0.0783	0.0822
7	0.0580	0.0625	0.0667	0.0708	0.0750	0.0789	0.0833
8	0.0564	0.0615	0.0661	0.0706	0.0752	0.0794	0.0842
9	0.0551	0.0606	0.0656	0.0704	0.0753	0.0799	0.0849
10	0.0540	0.0599	0.0652	0.0703	0.0755	0.0803	0.0855
15	0.0590	0.0578	0.0641	0.0700	0.0760	0.0813	0.0871
20	0.0496	0.0570	0.0637	0.0699	0.0762	0.0817	0.0875
25	0.0491	0.0567	0.0635	0.0699	0.0762	0.0818	0.0877

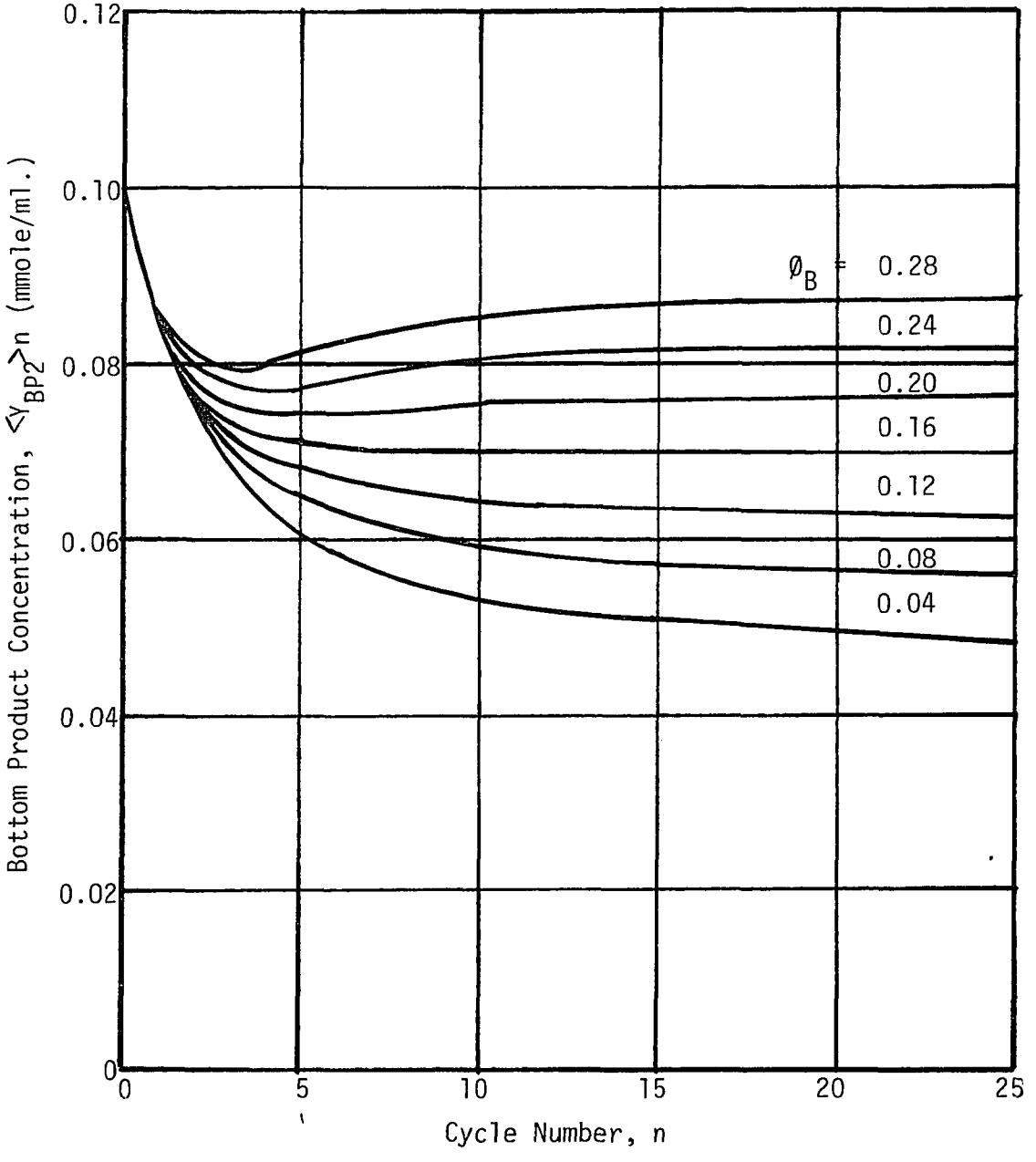

FIGURE 17 - CALCULATED PERFORMANCE CURVES FOR VARIOUS RATES OF BOTTOM PRODUCT WITHDRAWAL, h = 60 cm

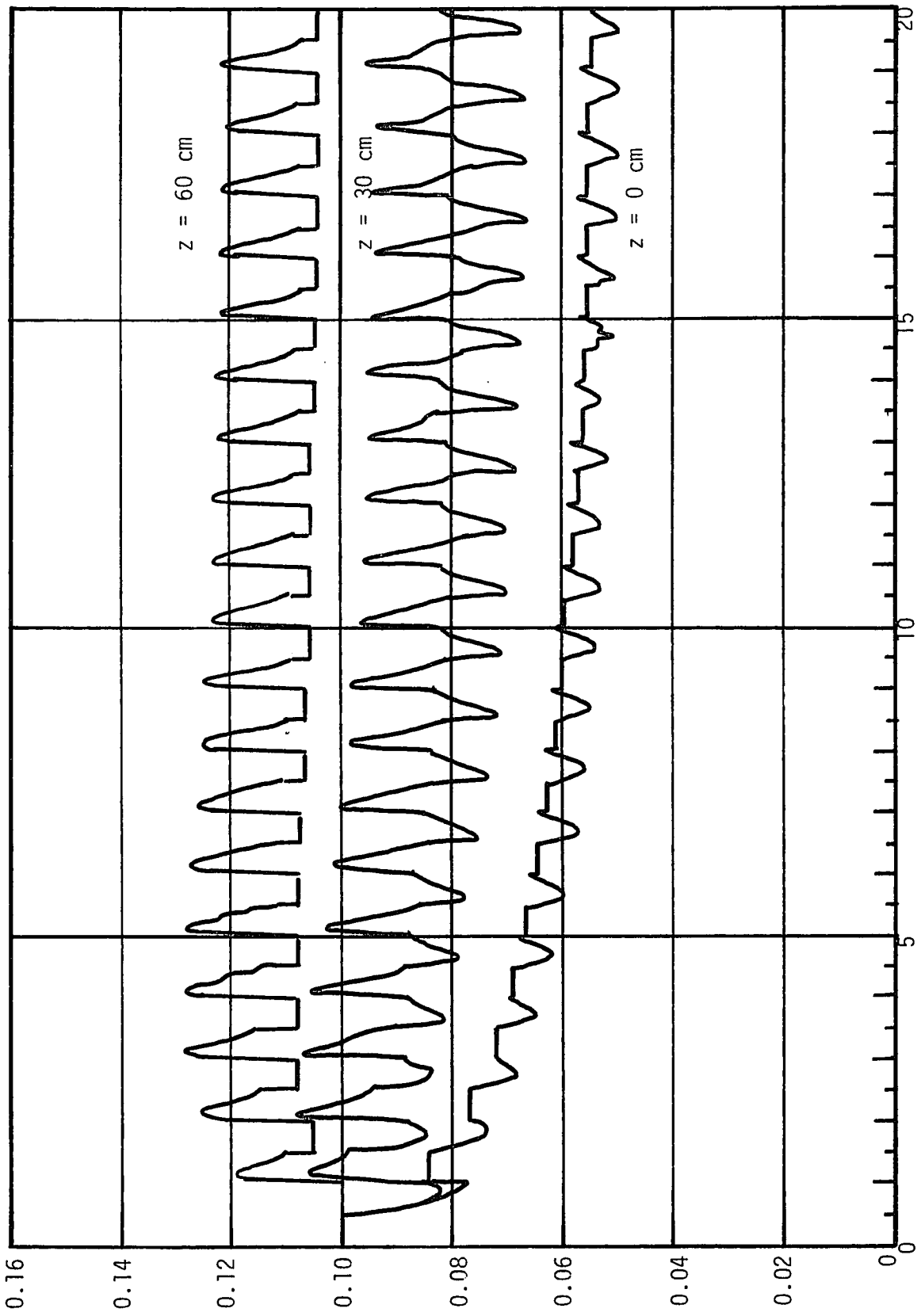

FIGURE 18 - CALCULATED CONCENTRATION PROFILES FOR ϕ_B = 0.08, h = 60 cm

to decrease uniformly from cycle to cycle showing a net removal of solute to the concentrated end of the column. The same is true for the solid phase concentration as seen in Figure 19, which has an identical construction to Figures 13 and 15. Here solid phase concentration throughout the adsorbant column decreases with time showing a net rejection of solids from the system to the concentrated product.

For ϕ_B=0.24, however, the obverse is true. In the liquid phase, as seen in Figure 20, a gradual buildup of solute develops after the first cycle of operation and, by the fourth cycle, has reached the column bottom, and the steadily degenerating separation found in the earlier set of runs appears. Figure 21 shows the solid phase solute concentration in the same manner as Figure 19. Again, solute accumulates on the solid adsorbant with increasing number of cycles rather than being rejected with the concentrated product.

This series of experimental runs, designed to investigate the effect of total liquid displacement and column length on separation, was continued by moving column operation into a region operationally equivalent to equilibrium theory Region III. Here column length was reduced to 30 cm, so that, if equilibrium operation were possible, L_1>h and L_2>h. In equilibrium theory operation, the characteristic shape of the separation curves is not affected by the relative lengths of concentration front penetrations, i.e., no minimum in lean product concentration appears even though $L_2 > L_1$. However, in the non-equilibrium case, the appearance of the

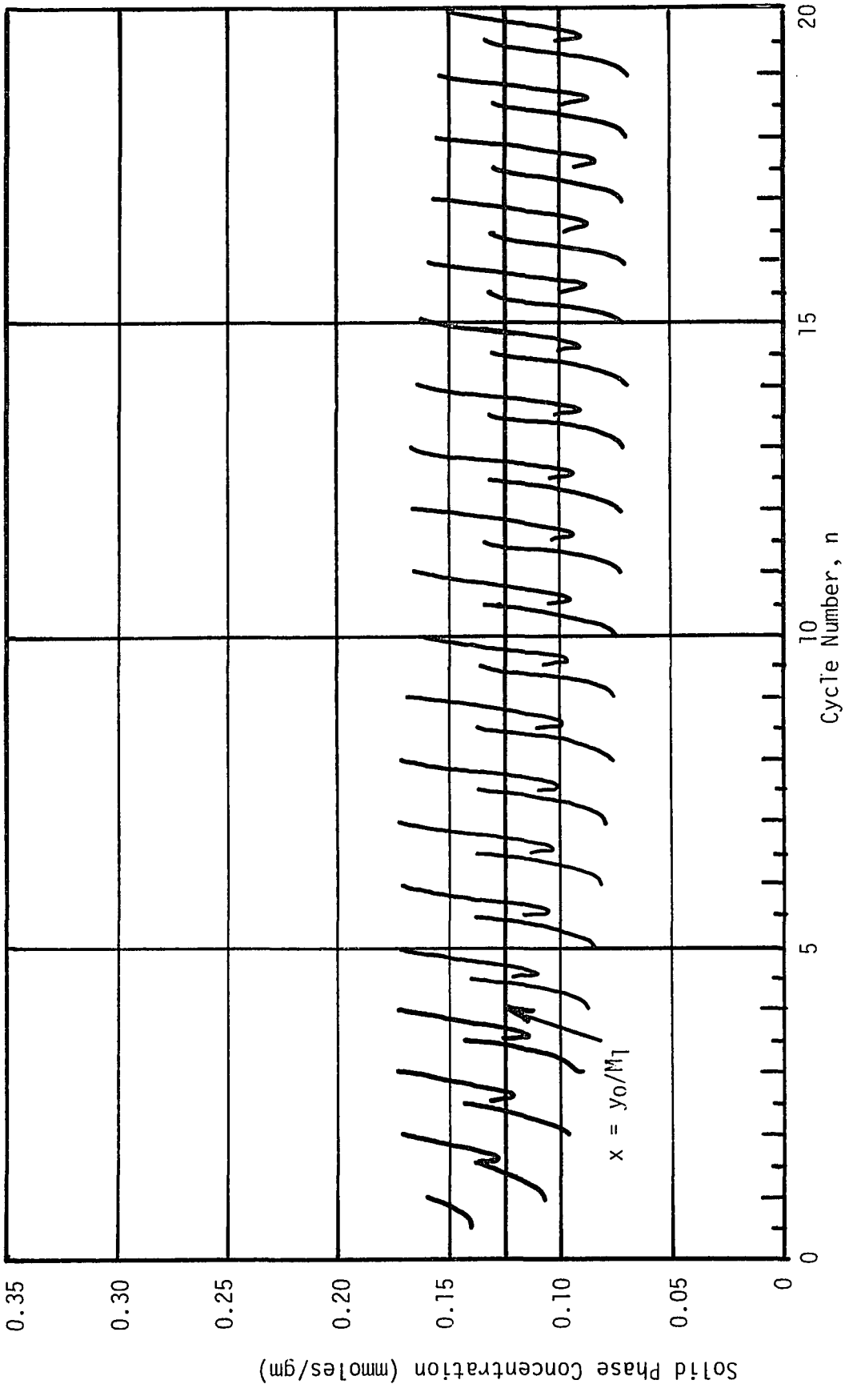

FIGURE 19 - CALCULATED SOLID PHASE CONCENTRATIONS AT END OF HALF-CYCLE, $\phi_B = 0.08$, h = 60 cm.

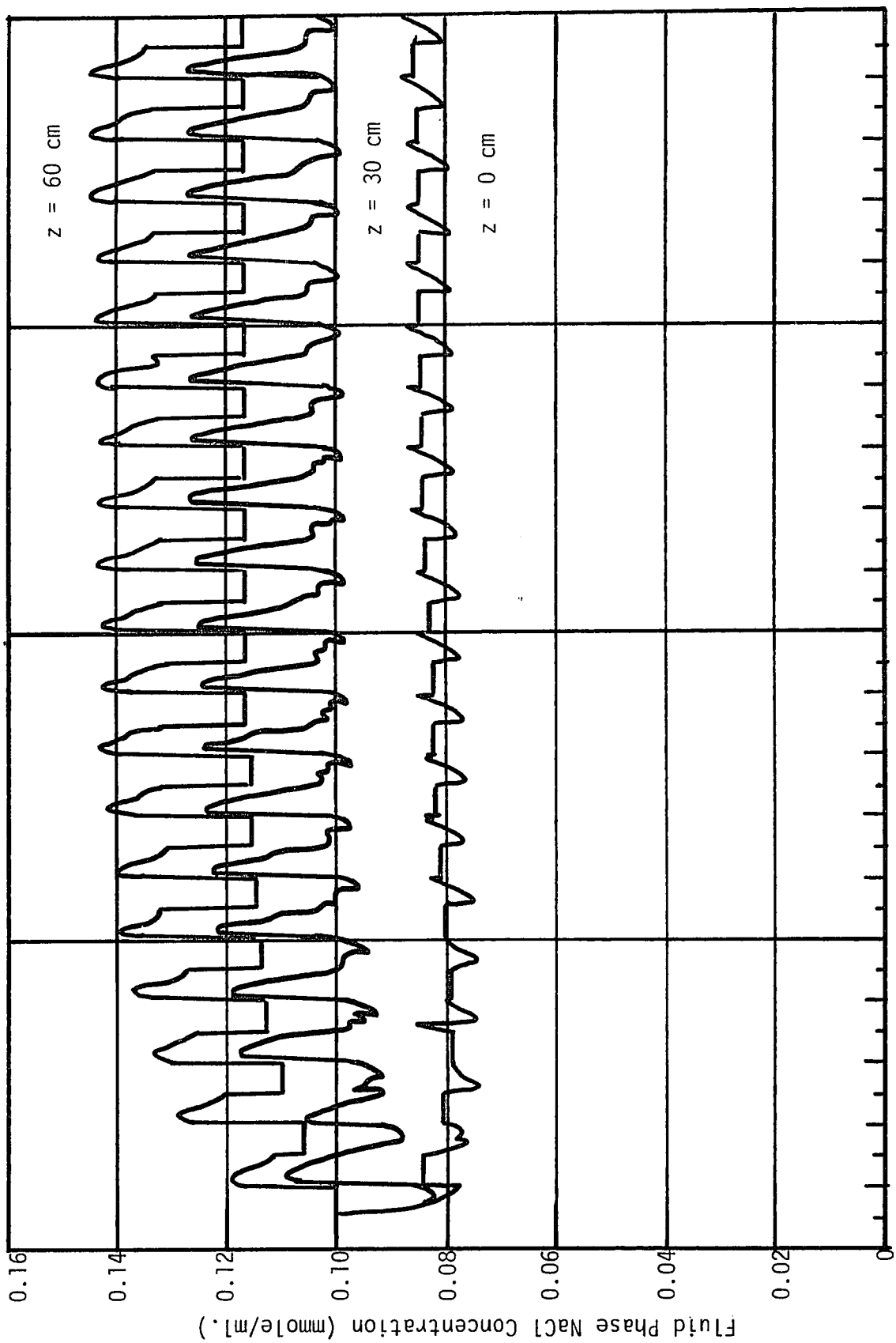

FIGURE 20 - CALCULATED CONCENTRATION PROFILES FOR ϕ_B = 0.24 at h = 60 cm.

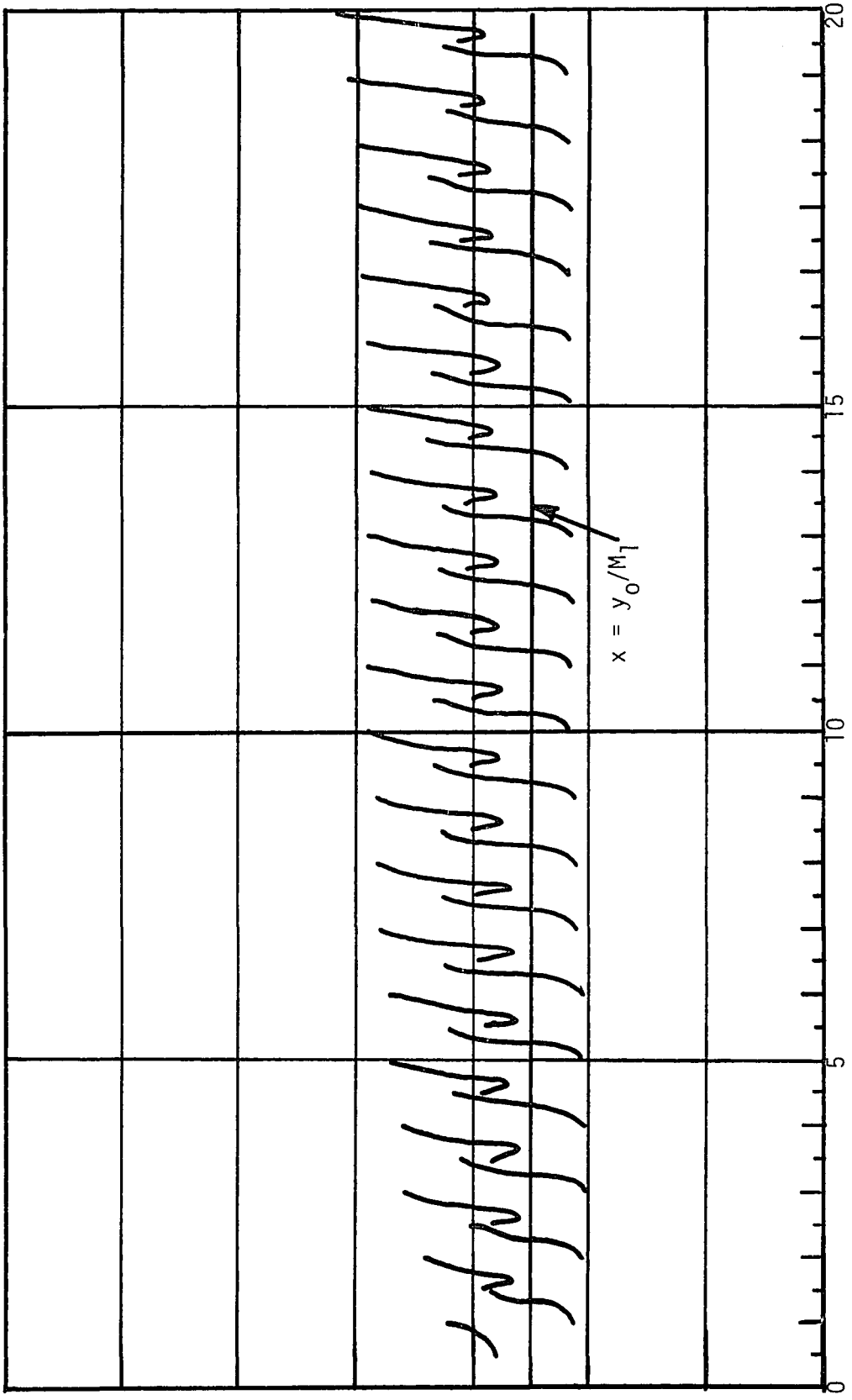

FIGURE 21 - CALCULATED SOLID-PHASE CONCENTRATIONS AT END OF HALF-CYCLE, $\phi_B = 0.24$ h = 60 cm.

minimum occurs even under these operating conditions. In short, the only factor influencing the characteristic shape (minimum or no minimum) of the performance curve for bottom product concentration is the bottom product flow ratio, ϕ_B.

The experimental conditions are summarized on Table 13 and the experimental results appear on Table 14. The experimental results are compared with the performance predicted by the model equations (Table 15) on Figure 22, again showing a reasonable fit of the model to the data and the same qualitative behavior indicated at longer column lengths. For ϕ_B=0.08, the lean product concentration decreases with increasing number of cycles. At ϕ_B=0.24, a minimum in lean product concentration appears early and the degenerating level of separation continues thereafter.

The model equations predict the same behavior for operation with the short column. Figure 23 shows the calculated dependence of lean product concentration on bottom product withdrawal rate given on Table 16, indicating that the minimum in lean product concentration first appears between ϕ_B=0.16 and ϕ_B=0.20, the same behavior as with the longer columns. At ϕ_B=0.08, Figure 24 shows that liquid phase solute concentration throughout the column length decreases with increasing number of cycles and Figure 25 shows that the same holds true for the solid phase. However, at ϕ_B=0.24, Figures 26 and 27 show that solute accumulates in the adsorbant column with time in both liquid and solid phases as was the case with the longer columns.

TABLE 13

EXPERIMENTAL CONDITIONS FOR RUNS WITH VARIABLE

BOTTOM PRODUCT WITHDRAWAL RATE

(SHORT COLUMN)

Operating Variable	Value
Hot Temperature	343° K
Cold Temperature	278° K
Reservoir Displacement	25 cm^3
Feed Rate Ratio ($\phi_B+\phi_T$)	0.400
Dead Volume	4.5 cm^3
Feed Composition	0.100 moles NaCl/liter
Column Height	30 cm
Half-Cycle Time	24 min.

TABLE 14

EXPERIMENTAL RESULTS, VARIABLE BOTTOM PRODUCT RATE,

SHORT COLUMN

(CONCENTRATIONS IN MOLES NaCl/LITER)

Bottom Product Withdrawal Ratio	0.08		0.16		0.24	
Cycle No.	Top Product	Bottom Product	Top Product	Bottom Product	Top Product	Bottom Product
1	0.100	0.090	0.100	0.092	0.100	0.088
2	0.109	0.092	0.107	0.094	0.105	0.095
3	0.111	0.086	0.107	0.087	0.108	0.091
4	0.106	0.080	0.107	0.083	0.109	0.094
5	0.104	0.075	0.109	0.081	0.106	0.088
6	0.102	0.080	0.106	0.083	0.110	0.086
7	0.104	0.077	0.109	0.085	0.107	0.085
8	0.106	0.075	0.106	0.082	0.108	0.086
9	0.104	0.074	0.107	0.086	0.107	0.088
10	0.106	0.073	0.112	0.086	0.109	0.089
11	0.104	0.072	0.112	0.087	0.118	0.088
12	0.102	0.071	0.109	0.087	0.109	0.092
13	0.108	0.073	0.110	0.086	0.108	0.088
14	0.105	0.071	0.111	0.087	0.108	0.088
15	0.106	0.073	0.110	0.087	0.106	0.088
16	0.103	0.071	0.109	0.086	0.108	0.092
17	0.106	0.070	0.111	0.087	0.107	0.092
18	0.103	0.072	0.108	0.086	0.106	0.095
19	0.107	0.072	0.106	0.085	0.108	0.094
20	0.111	0.070	0.105	0.086	0.106	0.093

TABLE 15

CALCULATED RESULTS, VARIABLE BOTTOM PRODUCT RATE,

SHORT COLUMN

(CONCENTRATIONS IN MOLES NaCl/LITER)

Bottom Product Withdrawal Ratio	0.08		0.16		0.24	
Cycle No.	Top Product	Bottom Product	Top Product	Bottom Product	Top Product	Bottom Product
1	0.1000	0.0862	0.1000	0.0867	0.1000	0.0871
2	0.1073	0.0830	0.1081	0.0847	0.1088	0.0865
3	0.1089	0.0809	0.1108	0.0837	0.1126	0.0865
4	0.1086	0.0797	0.1116	0.0833	0.1141	0.0870
5	0.1081	0.0788	0.1117	0.0831	0.1150	0.0875
6	0.1075	0.0782	0.1117	0.0830	0.1154	0.0879
7	0.1071	0.0778	0.1116	0.0830	0.1157	0.0881
8	0.1068	0.0775	0.1116	0.0829	0.1160	0.0883
9	0.1065	0.0772	0.1116	0.0829	0.1161	0.0885
10	0.1064	0.0771	0.1115	0.0828	0.1162	0.0886
11	0.1062	0.0769	0.1115	0.0828	0.1163	0.0887
12	0.1061	0.0769	0.1115	0.0828	0.1164	0.0887
13	0.1061	0.0768	0.0115	0.0828	0.1164	0.0888
14	0.1060	0.0767	0.1115	0.0828	0.1164	0.0888
15	0.1060	0.0767	0.1115	0.0828	0.1165	0.0888
16	0.1059	0.0767	0.1115	0.0828	0.1165	0.0888
17	0.1059	0.0767	0.1115	0.0828	0.1165	0.0888
18	0.1059	0.0766	0.1115	0.0828	0.1165	0.0888
19	0.1059	0.0766	0.1115	0.0828	0.1165	0.0888
20	0.1059	0.0766	0.1115	0.0828	0.1165	0.0888

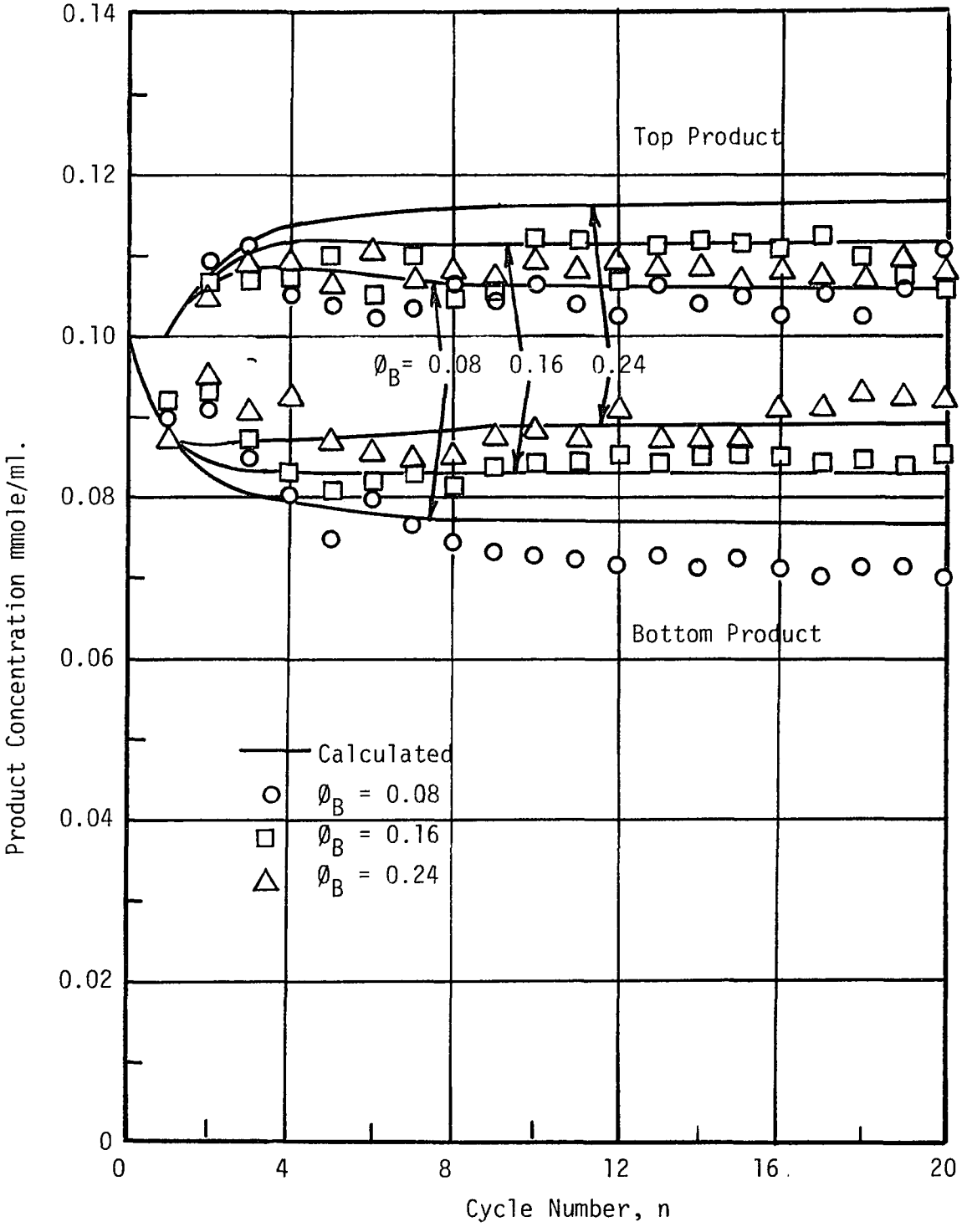

FIGURE 22 - EFFECT OF BOTTOM PRODUCT WITHDRAWAL RATE ON SEPARATION, 30 cm COLUMN - h = 30 cm, Q_τ = 25 cm^3, τ = 24 min. $\emptyset_T+\emptyset_B$ = 0.40

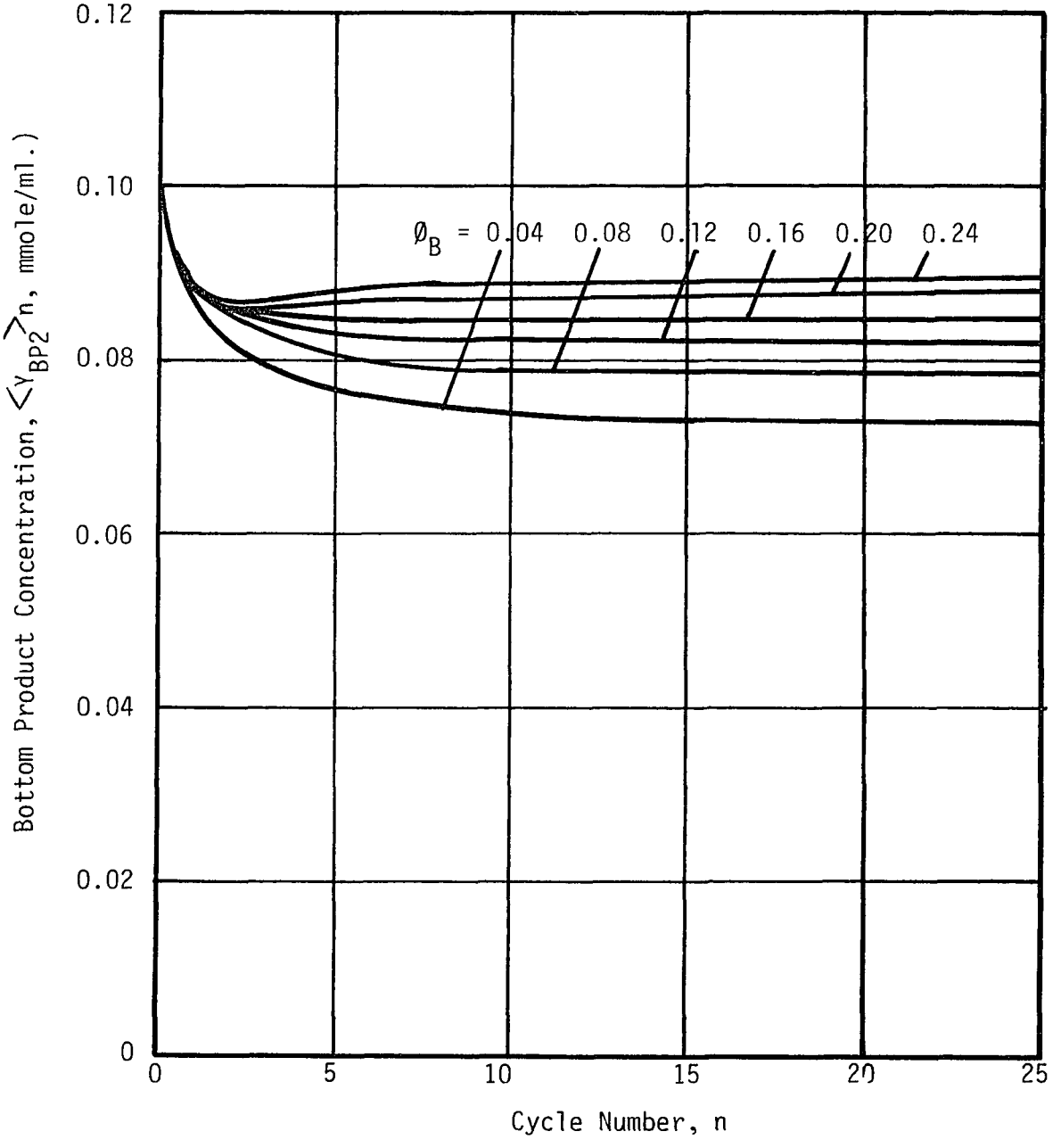

FIGURE 23 - CALCULATED PERFORMANCE CURVES FOR VARIOUS RATES OF BOTTOM PRODUCT WITHDRAWAL - h = 30 cm, $Q\tau$ = 25 cm^3, τ = 24 min., $\emptyset_T+\emptyset_B$ = 0.40

TABLE 16

CALCULATED BOTTOM PRODUCT CONCENTRATIONS

VARIABLE BOTTOM PRODUCT WITHDRAWAL RATE

MEDIUM COLUMN

(CONCENTRATIONS IN MOLES NaCl/LITER)

Bottom Product Withdrawal Ratio	0.04	0.08	0.12	0.16	0.20	0.24	0.28
Cycle No.							
1	0.0860	0.0862	0.0865	0.0867	0.0869	0.0871	0.0873
2	0.0819	0.0830	0.0839	0.0847	0.0853	0.0865	0.0867
3	0.0785	0.0809	0.0821	0.0837	0.0847	0.0865	0.0869
4	0.0772	0.0797	0.0811	0.0833	0.0850	0.0870	0.0877
5	0.0763	0.0788	0.0798	0.0831	0.0853	0.0875	0.0880
10	0.0743	0.0771	0.0782	0.0828	0.0857	0.0886	0.0890
15	0.0732	0.0767	0.0798	0.0828	0.0857	0.0888	0.0890
20	0.0730	0.0766	0.0796	0.0828	0.0857	0.0888	0.0890
25	0.0730	0.0766	0.0796	0.0828	0.0857	0.0888	0.0890

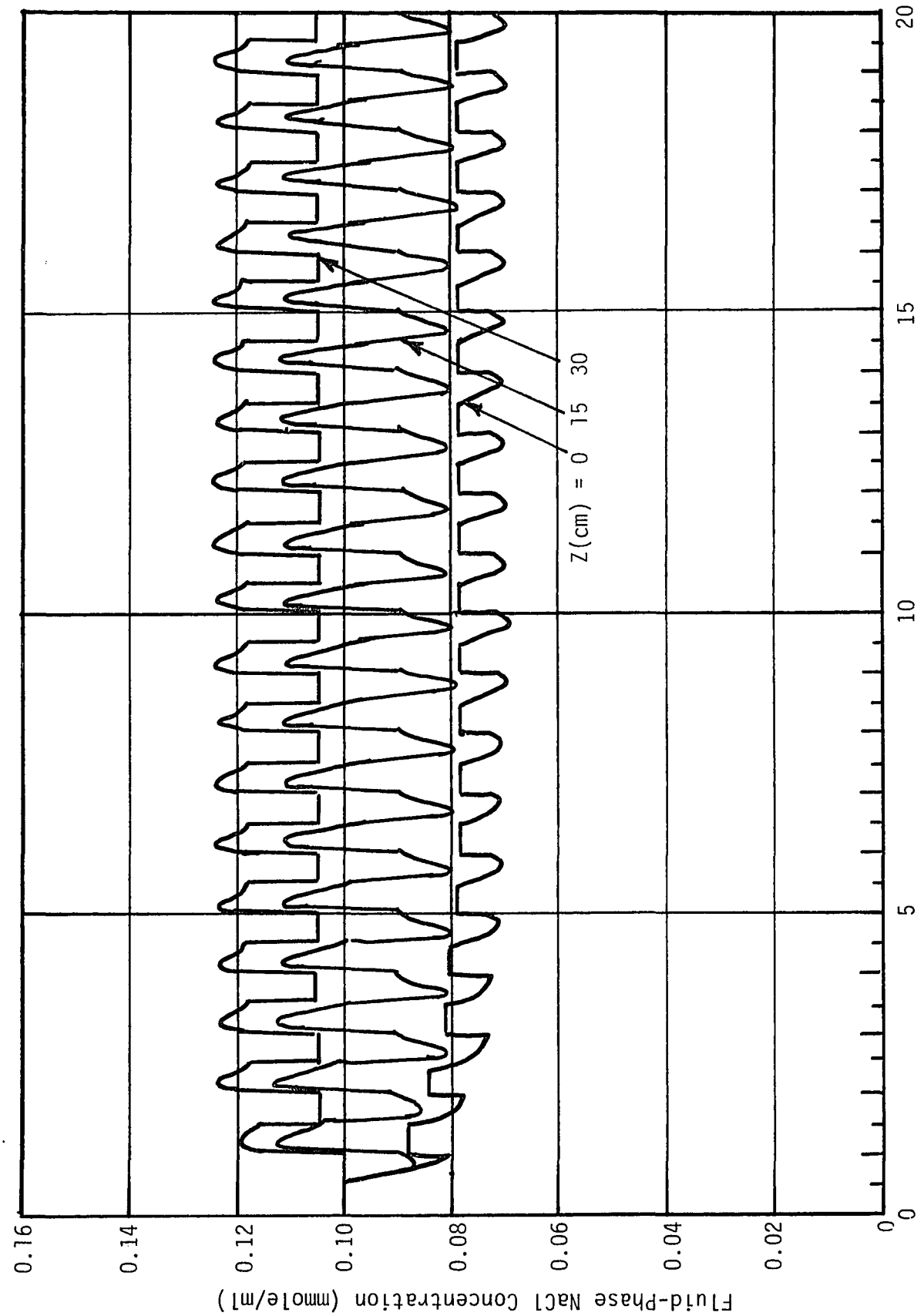

FIGURE 24 - CALCULATED CONCENTRATION PROFILES FOR $\emptyset_B$ = 0.08 AND h = 30 cm

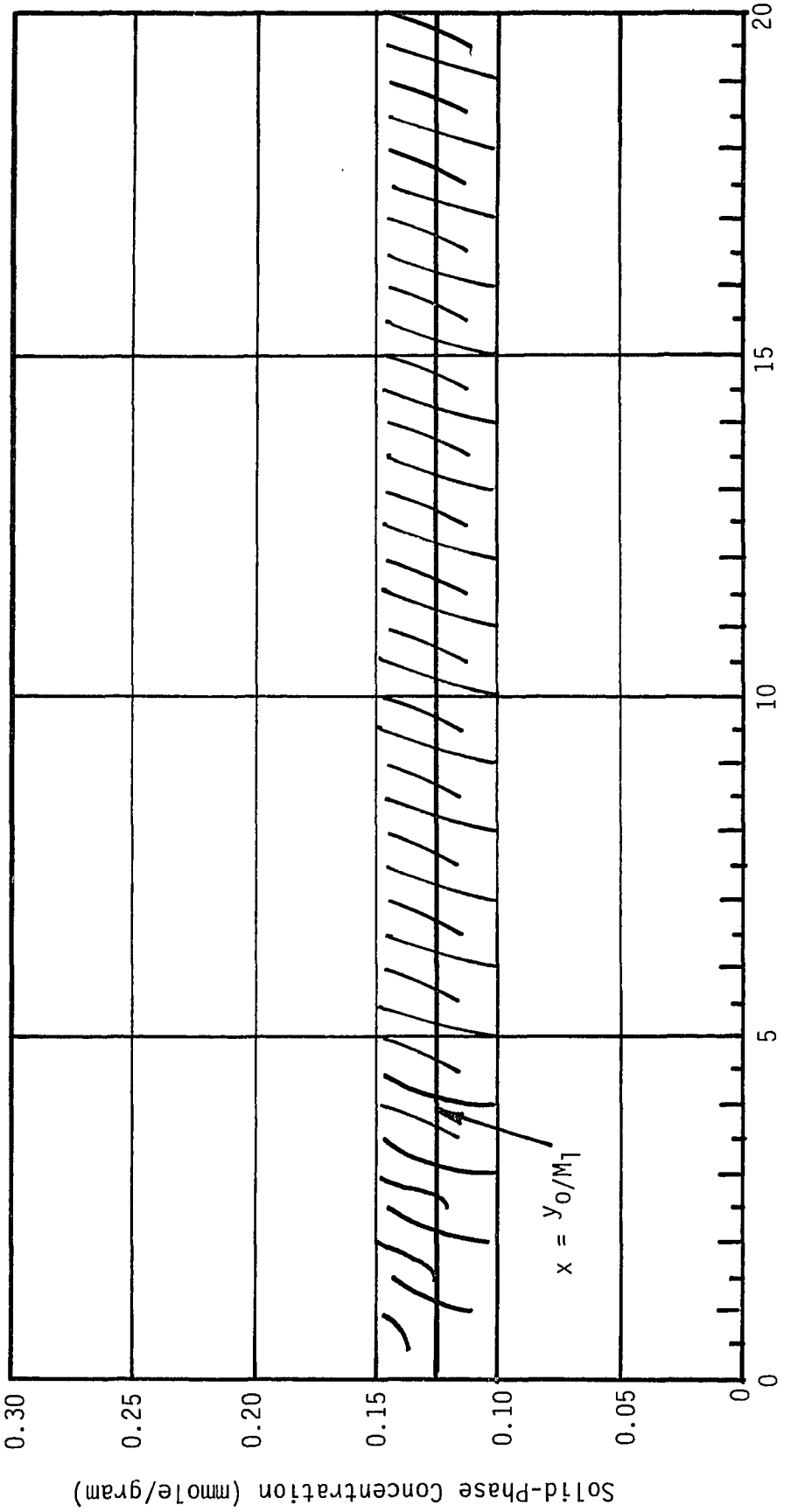

FIGURE 25 - CALCULATED SOLID PHASE CONCENTRATIONS AT END OF HALF-CYCLE, $\emptyset_B$ = 0.08 AND h = 30 cm

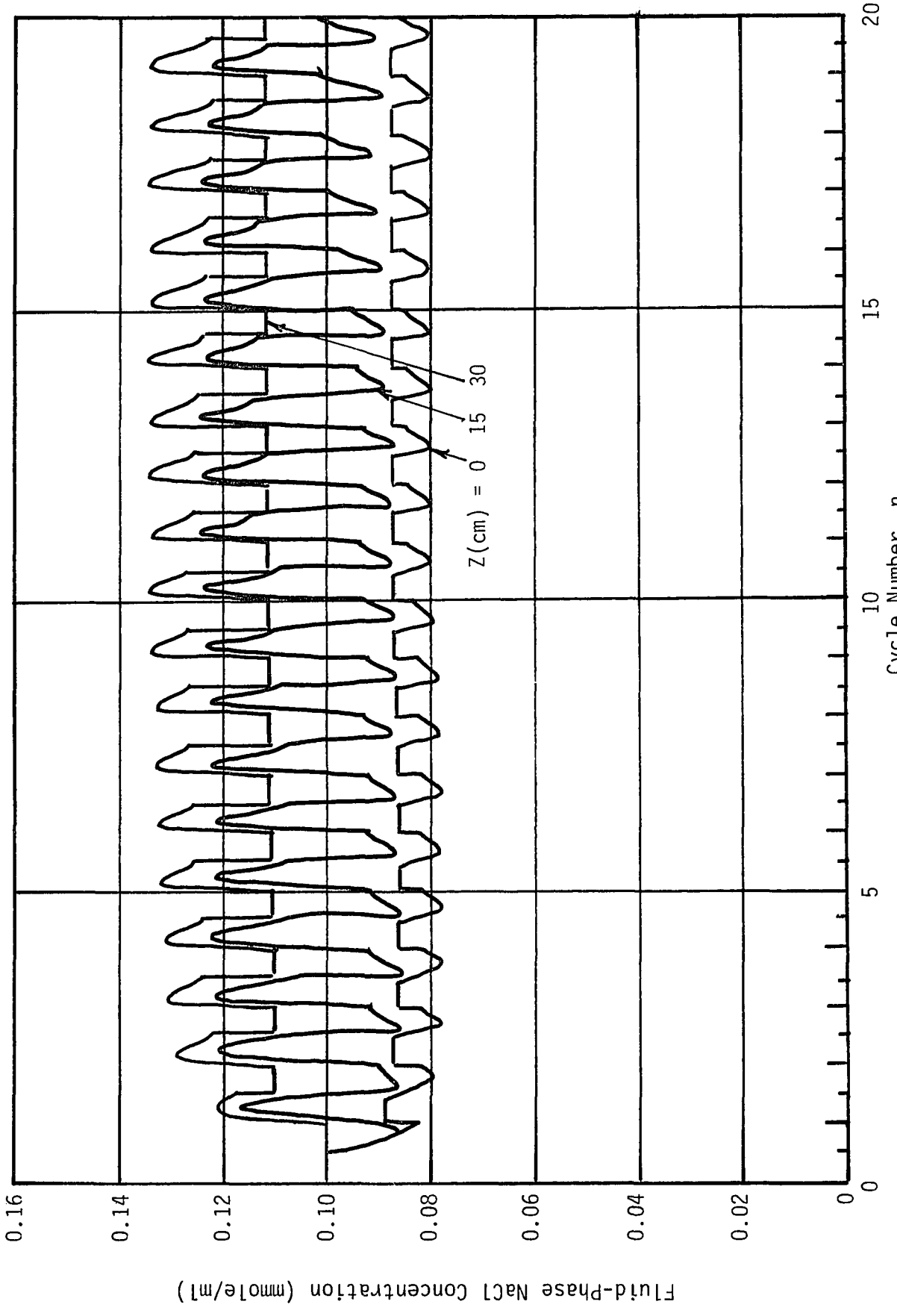

FIGURE 26 - CALCULATED CONCENTRATION PROFILES FOR $\emptyset_B$ = 0.24 AND h = 30 cm

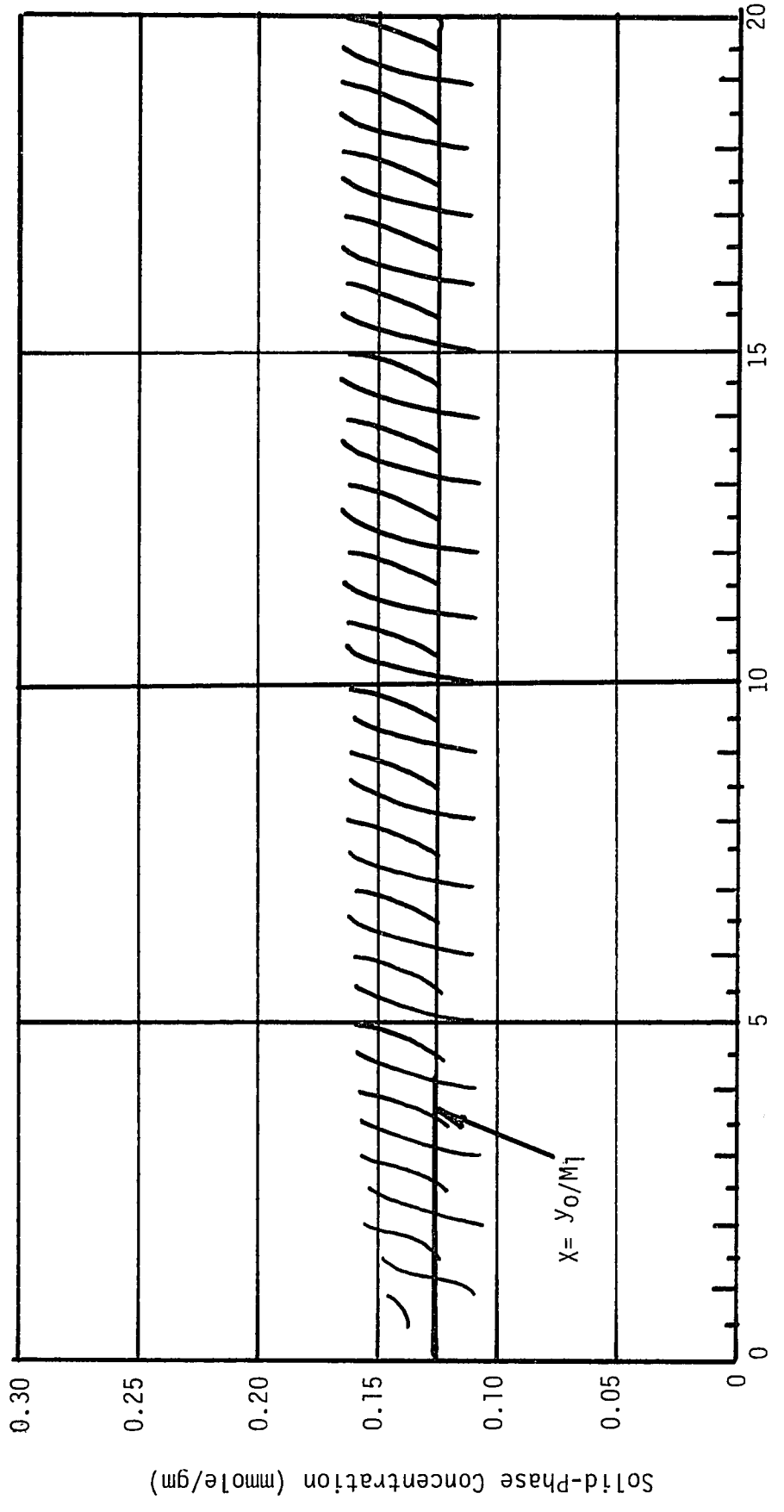

FIGURE 27 - CALCULATED SOLID PHASE CONCENTRATION AT END OF HALF-CYCLE, $\emptyset_B = 0.24$, h = 30 cm

The effect of column height on separation is summarized on Table 17 and Figure 28. Here, lean product concentration is shown as a function of cycle number and column height for ϕ_B=0.08 and ϕ_B=0.24. The characteristic shape of the curve is not changed by decreasing column length but is strongly affected by bottom product withdrawal rate.

D. Effect of Reservoir Displacement, Q_T

A final series of experiments were conducted at ϕ_B=0.04 for various reservoir displacements holding the column length constant at 90 cm. The operating conditions are summarized on Table 18 and the experimental results appear on Table 19. Figure 29 compares the experimental results with the model equations and shows a good agreement between experimental and predicted results. Figure 30 shows the effect of reservoir displacement on separation from the calculated results appearing on Table 20. Here lean product concentration is shown as a function of cycle number and reservoir displacement for ϕ_B=0.04 and 0.24. Again, reservoir displacement does not determine whether or not a minimum in lean product concentration will occur but bottom product withdrawal rate does.

Sweed has reported an interesting aspect of batch non-equilibrium parametric pump operation. He has shown that the ultimate separation factor, defined as the ratio of top product solute concentration to bottom product solute concentration after many cycles of operation is maximized at a particular value of reservoir displacement. For his direct mode batch parametric pumps, the

TABLE 17

CALCULATED BOTTOM PRODUCT CONCENTRATIONS

VARIABLE COLUMN LENGTH

$\phi_T+\phi_B=0.40$, $Q\tau=25cm^3$, $\tau=24$ min.

(CONCENTRATIONS IN MOLES NaCl/LITER)

ϕ_B =	0.08			0.24		
Column Height	30	60	90	30	60	90
Cycle No.						
1	0.0862	0.0817	0.0811	0.0871	0.0821	0.0809
2	0.0830	0.0754	0.0733	0.0865	0.0787	0.0754
3	0.0809	0.0709	0.0675	0.0865	0.0773	0.0726
4	0.0897	0.0678	0.0634	0.0870	0.0273	0.0715
5	0.0788	0.0656	0.0602	0.0875	0.0777	0.0715
6	0.0782	0.0639	0.0578	0.0879	0.0783	0.0719
7	0.0778	0.0625	0.0558	0.0881	0.0789	0.0726
8	0.0775	0.0615	0.0541	0.0883	0.0794	0.0733
9	0.0772	0.0606	0.0528	0.0885	0.0799	0.0740
10	0.0771	0.0599	0.0516	0.0886	0.0803	0.0747
15	0.0767	0.0578	0.0477	0.0888	0.0813	0.0770
20	0.0766	0.0570	0.0457	0.0888	0.0817	0.0781
25	0.0766	0.0567	0.0447	0.0888	0.0818	0.0786

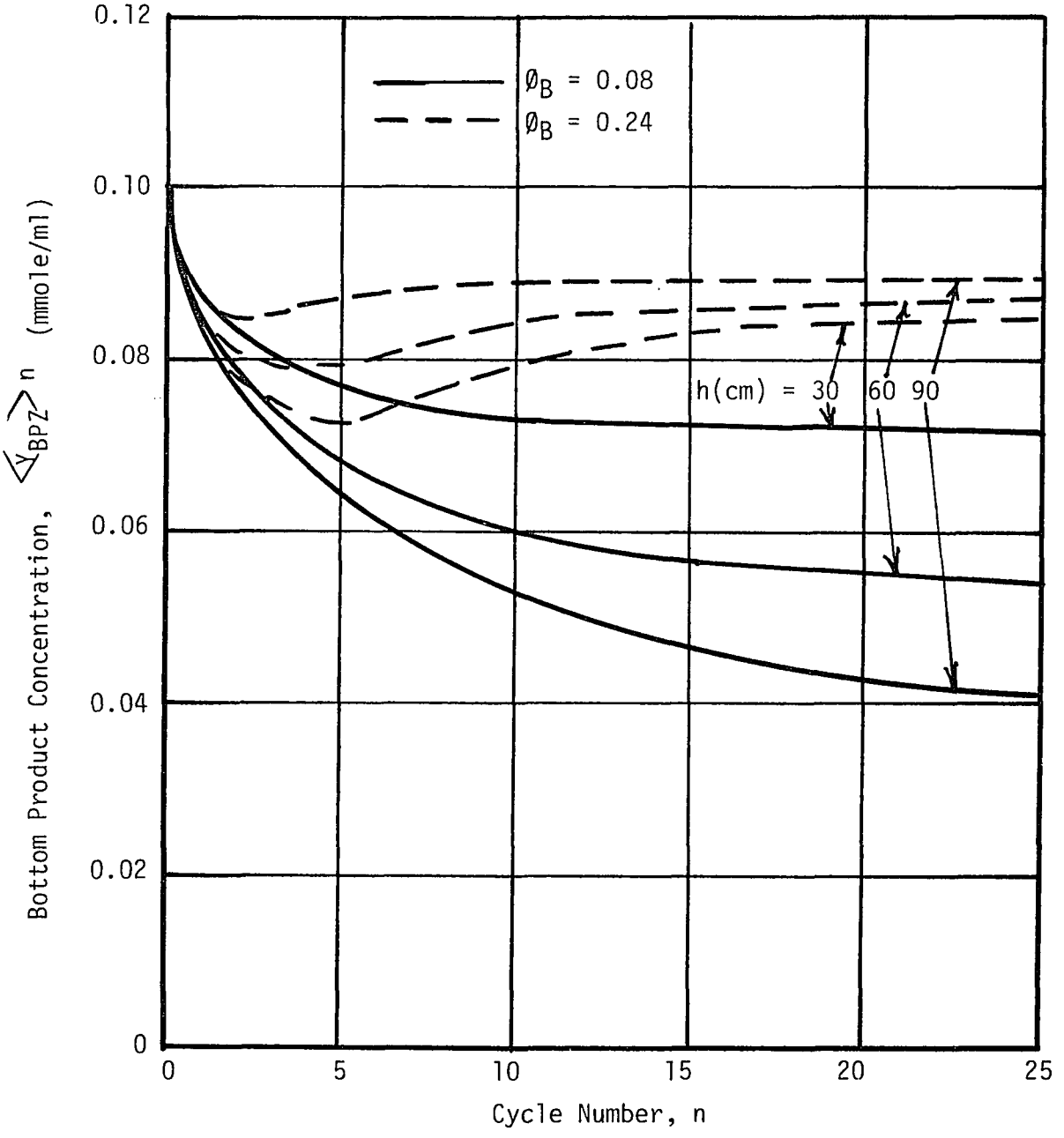

FIGURE 28 - CALCULATED BOTTOM PRODUCT PERFORMANCE CURVES, VARIABLE COLUMN LENGTH
$Q\tau$ = 25 cm^3, τ = 24 min.

TABLE 18

EXPERIMENTAL CONDITIONS FOR RUNS WITH

VARIABLE RESERVOIR DISPLACEMENT

Operating Variable	Value
Hot Temperature	343° K
Cold Temperature	278° K
Half-Cycle Time	24 min.
Feed Rate Ratio ($\phi_B+\phi_T$)	0.400
Bottom Product Withdrawal (ϕ_B)	0.040
Dead Volume	4.5 cm^3
Feed Composition	0.100 moles naCl/liter
Column Height	90 cm

TABLE 19

EXPERIMENTAL RESULTS, VARIABLE RESERVOIR DISPLACEMENT,

LONG COLUMN

(CONCENTRATIONS IN MOLES NaCl/LITER)

Reservoir Displacement (cm^3)	25		35		45	
Cycle No.	Top Product	Bottom Product	Top Product	Bottom Product	Top Product	Bottom Product
1	0.100	0.0930	0.100	0.0851	0.100	0.0890
2	0.110	0.0727	0.113	0.0769	0.117	0.0870
3	0.112	0.0768	0.120	0.0687	0.122	0.0735
4	0.116	0.0600	0.188	0.0620	0.120	0.0648
5	0.112	0.0580	0.123	0.0640	0.124	0.0671
6	0.115	0.0560	0.120	0.0617	0.122	0.0592
7	0.119	0.0500	0.121	0.0499	0.125	0.0585
8	1.121	0.0498	0.127	0.0519	0.130	0.0581
9	0.118	0.0495	1.120	0.0493	0.124	0.0609
10	0.112	0.0475	0.121	0.0495	0.128	0.0593
11	0.113	0.0413	0.117	0.0450	0.127	0.0542
12	0.117	0.0399	0.119	0.0492	0.123	0.0590
13	0.118	0.0383	0.123	0.0486	0.128	0.0585
14	0.112	0.0390	0.120	0.0463	0.126	0.0590
15	0.117	0.0377	0.119	0.0472	0.128	0.0580
16	0.118	0.0368	0.120	0.0461	0.122	0.0583
17	0.112	0.0376	0.119	0.0455	0.124	0.0581
18	0.115	0.0365	0.116	0.0427	0.124	0.0579
19	0.108	0.0365	0.114	0.0421	0.120	0.0582
20	0.109	0.0366	0.110	0.0438	0.121	0.1577

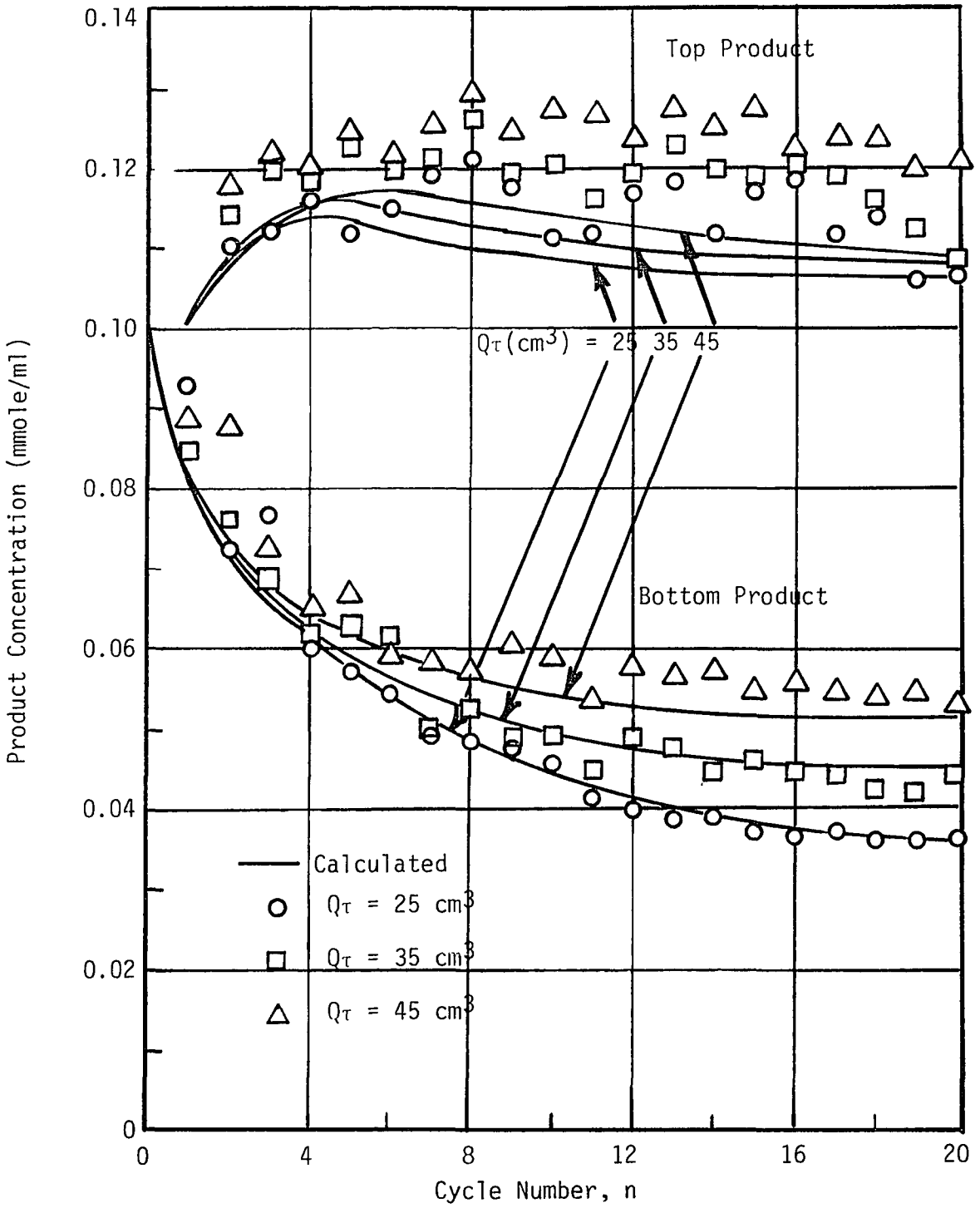

FIGURE 29 - EFFECT OF RESERVOIR DISPLACEMENT ON SEPARATION
h = 90 cm, τ = 24 min., ϕ_B = 0.04, ϕ_B = 0.36

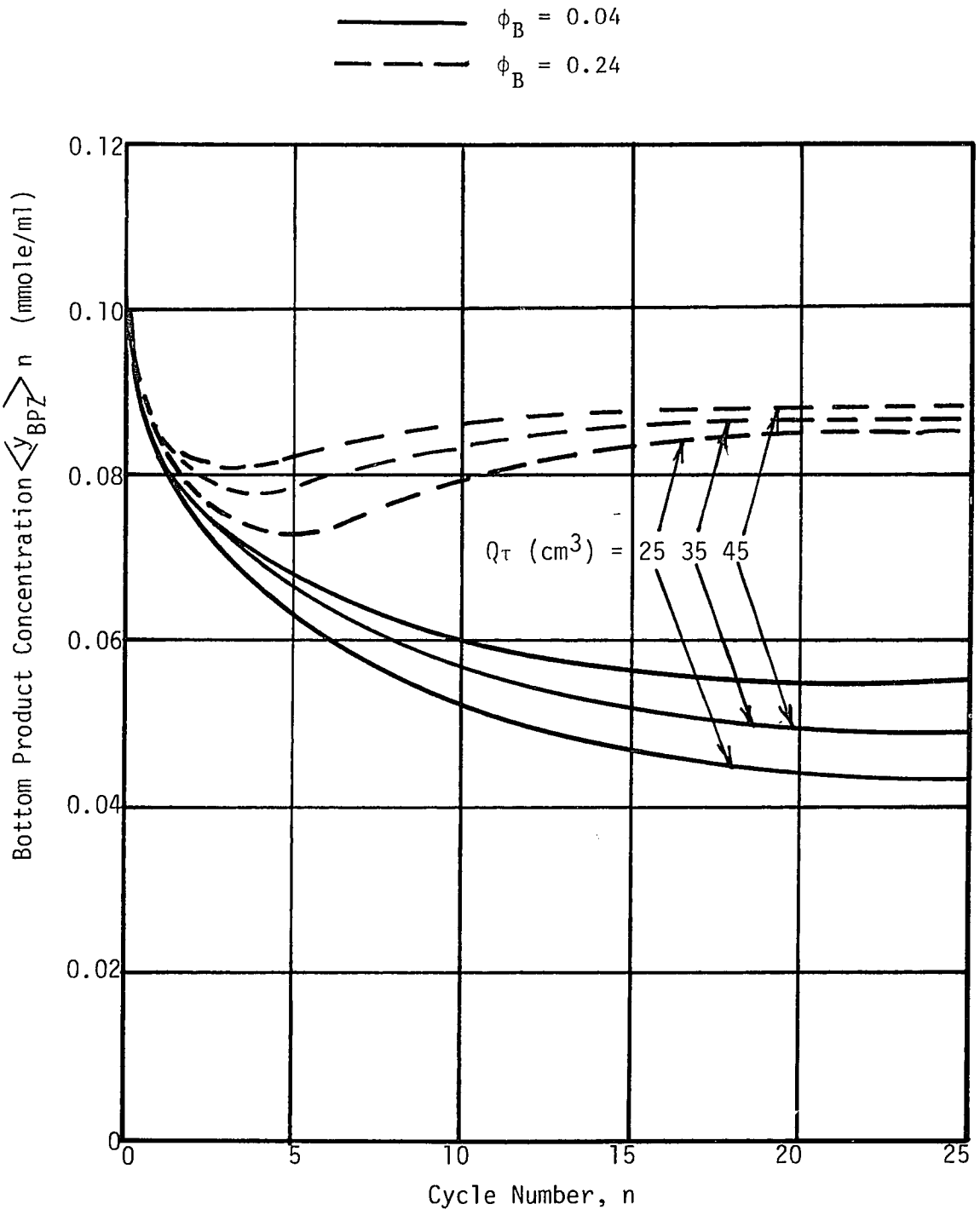

FIGURE 30 - CALCULATED BOTTOM PRODUCT PERFORMANCE CURVES, VARIABLE RESERVOIR DISPLACEMENT

h = 90 cm, τ = 24 min.

TABLE 20

CALCULATED BOTTOM PRODUCT CONCENTRATIONS

VARIABLE RESERVOIR DISPLACEMENT

h=90cm, τ=24 min., $\phi_T+\phi_B$= 0.40

(CONCENTRATIONS IN MOLES NaCl/LITER)

ϕ_B=	0.04			0.24		
Reservoir Displacement	25	35	45	25	35	45
Cycle No.						
1	0.0812	0.0809	0.0815	0.0809	0.0812	0.0822
2	0.0728	0.0727	0.0737	0.0754	0.0768	0.0787
3	0.0662	0.0667	0.0683	0.0725	0.0752	0.0779
4	0.0612	0.0624	0.0645	0.0715	0.0751	0.0782
5	0.0572	0.0590	0.0617	0.0715	0.0756	0.0789
6	0.0539	0.0563	0.0595	0.0719	0.0764	0.0796
7	0.0511	0.0541	0.0578	0.0726	0.0771	0.0802
8	0.0487	0.0523	0.0564	0.0733	0.0778	0.0808
9	0.0466	0.0508	0.0553	0.0740	0.0783	0.0812
10	0.0448	0.0496	0.0545	0.0747	0.0788	0.0815
15	0.0386	0.0458	0.0522	0.0770	0.0802	0.0823
20	0.0354	0.0443	0.0514	0.0781	0.0807	0.0825
25	0.0336	0.0437	0.0512	0.0786	0.0808	0.0826

maximum separation appears to occur where the reservoir displacement equals the column void volume. At reservoir displacements greater than the column void volume, separation diminishes because fluid breakthrough occurs from one end of the column to the other. The poorer separations at reservoir displacements less than the column void space are not explained.

Similar results have been obtained in the continuous case by using the model equations to calculate product concentrations at various reservoir displacements. Table 21 shows the conditions chosen for the calculations, where, all other variables held constant, the reservoir displacement is made to change over the range 45 cm^3 to 5.0 cm^3 for a 1.0 cm diameter by 90 cm long column (void volume = 27 cm^3). The calculated results are shown in Table 22 and pictured graphically on Figures 31 and 32. The limiting condition at zero reservoir displacement is obtained by inference. At zero reservoir displacement and zero feed rate to the column, the reservoir contents cannot change in composition, assuming diffusion is negligible. From Figure 32, it is apparent that the separation factor is maximized at a reservoir displacement of 10.0 cm^3, about 2/5 the column void space for the continuous non-equilibrium parametric pump.

Table 23 shows the calculated parametric pump performance on a cycle-by-cycle basis, from which an interpretation of the above result can be derived. The steadily decreasing separation factor for $Q_T > 25 cm^3$ is apparently due to breakthrough of solute from the concentrated to the lean end of the column during the cold half-

TABLE 21

CONSTANT PARAMETERS FOR CALCULATION OF THE

EFFECT OF RESERVOIR DISPLACEMENT ON SEPARATION

Operating Variable	Value
Hot Temperature, T_1	343° K
Cold Temperature, T_2	278° K
Half-Cycle Time, τ	24 min.
Feed Rate Ratio, $(\phi_T+\phi_B)$	0.40
Bottom Product Withdrawal (ϕ_B)	0.08
Dead Volume Ratio $(C_T=C_B)$	0.18
Feed Composition	0.100 mole NaCl/liter
Column Height	90 cm

TABLE 22

SEPARATION AS A FUNCTION OF RESERVOIR DISPLACEMENT

τ=24 min., ϕ_T=0.32, ϕ_B=0.08, h=90 cm, n=cycles

Reservoir Displacement (cm^3)	Steady State Product Concentration (mole/l.)		Separation Factor ($\langle YTP2\rangle_n / \langle YBP2\rangle_n$)
	Top	Bottom	
5	0.1218	0.0351	3.47
10	0.1201	0.0310	3.87
15	0.1174	0.0342	3.43
20	0.1159	0.0394	2.94
25	0.1151	0.0447	2.58
35	0.1127	0.0517	2.18
45	0.1103	0.0571	1.93

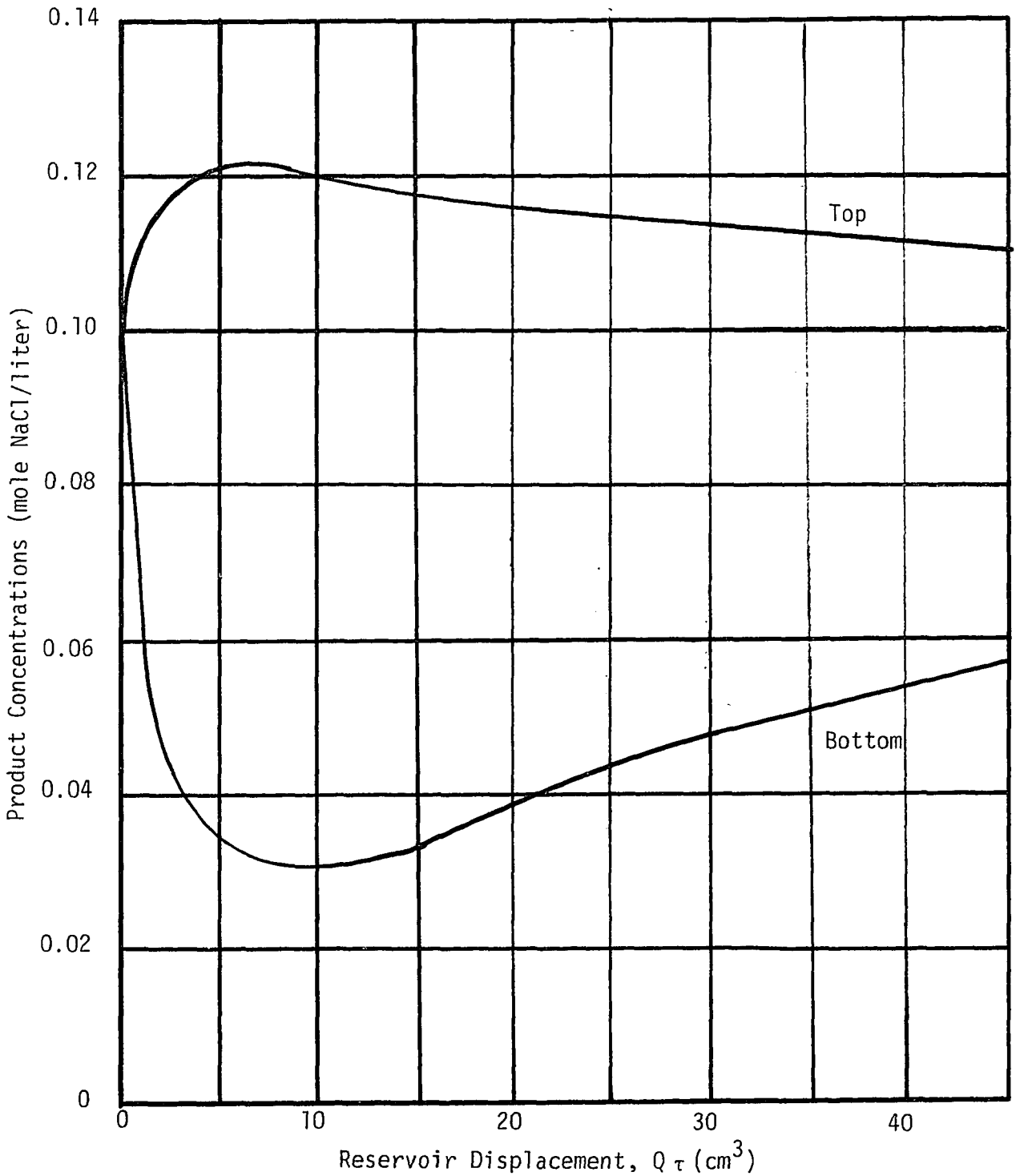

FIGURE 31 - PRODUCT CONCENTRATIONS AT n = 50 CYCLES FOR VARIOUS RESERVOIR DISPLACEMENTS

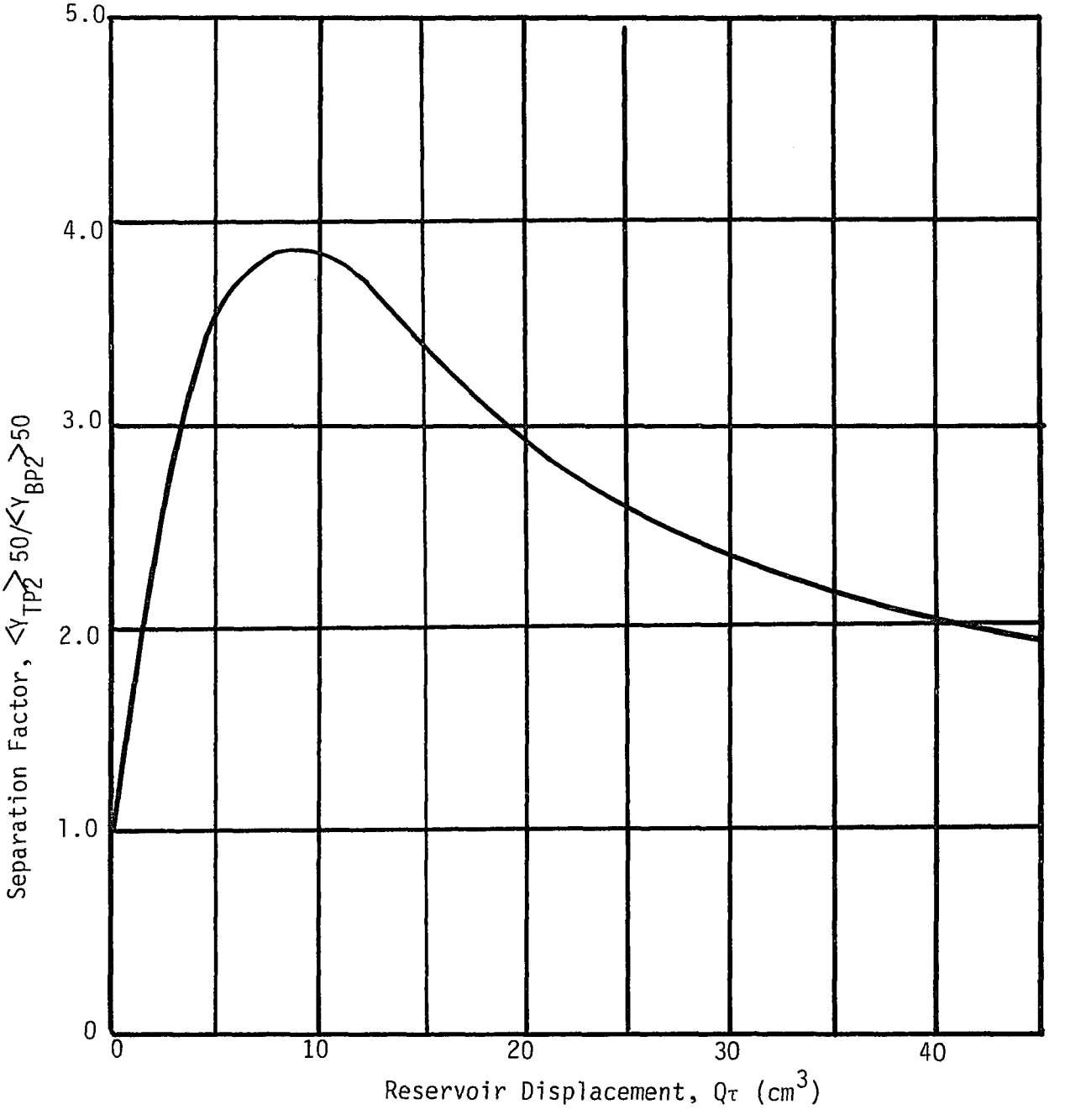

FIGURE 32 - SEPARATION FACTOR AS A FUNCTION OF RESERVOIR DISPLACEMENT

TABLE 23

PRODUCT CONCENTRATIONS AS A FUNCTION OF CYCLE NUMBER AT VARIOUS RESERVOIR DISPLACEMENTS

Reservoir Displacement (cm^3)	5		10		15		20	
Cycle No.	Top	Bottom	Top	Bottom	Top	Bottom	Top	Bottom
1	0.1000	0.0838	0.1000	0.0825	0.1000	0.0818	0.1000	0.0814
2	0.1065	0.0777	0.1074	0.0755	0.1000	0.0743	0.1084	0.0736
3	0.1105	0.0728	0.1120	0.0700	0.1129	0.0685	0.1134	0.0678
4	0.1131	0.0688	0.1149	0.0656	0.1159	0.0639	0.1166	0.0635
5	0.1148	0.0656	0.1168	0.0620	0.1179	0.0602	0.1186	0.0601
6	0.1160	0.0628	0.1182	0.0589	0.1194	0.0572	0.1198	0.0574
7	0.1169	0.0603	0.1192	0.0563	0.1203	0.0547	0.1204	0.0551
8	0.1177	0.0582	0.1200	0.0540	0.1210	0.0526	0.1207	0.0533
9	0.1182	0.0563	0.1206	0.0520	0.1214	0.0508	0.1207	0.0517
10	0.1187	0.0546	0.1211	0.0502	0.1216	0.0492	0.1205	0.0504
15	0.1202	0.0479	0.1223	0.0439	0.1212	0.0438	0.1191	0.0458
20	0.1210	0.0434	0.1224	0.0399	0.1202	0.0405	0.1179	0.0432
25	0.1215	0.0400	0.1221	0.0373	0.1193	0.0385	0.1171	0.0416
30	0.1218	0.0374	0.1216	0.0353	0.1186	0.0369	0.1166	0.0406
35	0.1219	0.0361	0.1212	0.0338	0.1181	0.0358	0.1163	0.0400
40	0.1220	0.0356	0.1208	0.0327	0.1178	0.0351	0.1161	0.0397
45	0.1219	0.0353	0.1204	0.0317	0.1176	0.0346	0.1160	0.0395
50	0.1218	0.0351	0.1201	0.0310	0.1174	0.0342	0.1159	0.0394

TABLE 23 (Cont'd)

PRODUCT CONCENTRATIONS AS A FUNCTION OF CYCLE NUMBER AT VARIOUS RESERVOIR DISPLACEMENTS

Reservoir Displacement	25		35		45	
Cycle No.	Top	Bottom	Top	Bottom	Top	Bottom
1	0.1000	0.0811	0.1000	0.0812	0.1000	0.0816
2	0.1087	0.0733	0.1091	0.0739	0.1094	0.0751
3	0.1139	0.0678	0.1143	0.0690	0.1139	0.0707
4	0.1170	0.0640	0.1167	0.0655	0.1153	0.0677
5	0.1186	0.0606	0.1175	0.0629	0.1154	0.0654
6	0.1194	0.0581	0.1175	0.0609	0.1148	0.0637
7	0.1196	0.0561	0.1171	0.0592	0.1142	0.0624
8	0.1194	0.0544	0.1166	0.0579	0.1135	0.0613
9	0.1191	0.0530	0.1160	0.0568	0.1129	0.0605
10	0.1187	0.0518	0.1155	0.0560	0.1124	0.0600
15	0.1169	0.0478	0.1138	0.0533	0.1110	0.0580
20	0.1157	0.0458	0.1130	0.0522	0.1105	0.0573
25	0.1151	0.0447	0.1127	0.0517	0.1103	0.0571

cycle. Figure 33 shows the bottom product concentration transient for the first five cycles of operation. There is clearly a change in the shape of the transient curves as the reservoir displacement decreases from 45 cm^3. For reservoir displacements both greater than 25 cm^3 and less than 25 cm^3, the transient is initially less steep than the 25 cm^3 curve. In the former case, solute breakthrough has occurred; in the latter case, mass transfer resistance is greater due to lower fluid velocity.

However, as Figure 34 indicates, whereas the transient is always less steep for reservoir displacements greater than 25 cm^3, the transient becomes steeper for the smaller reservoir displacements beyond 5 cycles of operation. Obviously, where the reservoir displacement is less than the column void space, the fluid contained in the column has more than one "pass" across the adsorbant surface, which it undergoes on successive cold half-cycles. Since it has been shown earlier that a steadily decreasing solid and liquid phase concentration gradient exists in the column at the chosen value of bottom product withdrawal, ϕ_B, it is clear that proportionately more solute can be transferred from the liquid to the solid as it is subject to more extensive contact with the liquid phase.

However, it has been pointed out that as reservoir displacement (an hence, fluid velocity) is decreased, resistance to interphase mass transfer is increased since λ is proportional to $v^{0.3}$. At reservoir displacements less than 10 cm^3, this effect is seen to predominate. Figures 35 through 38 show the liquid phase axial

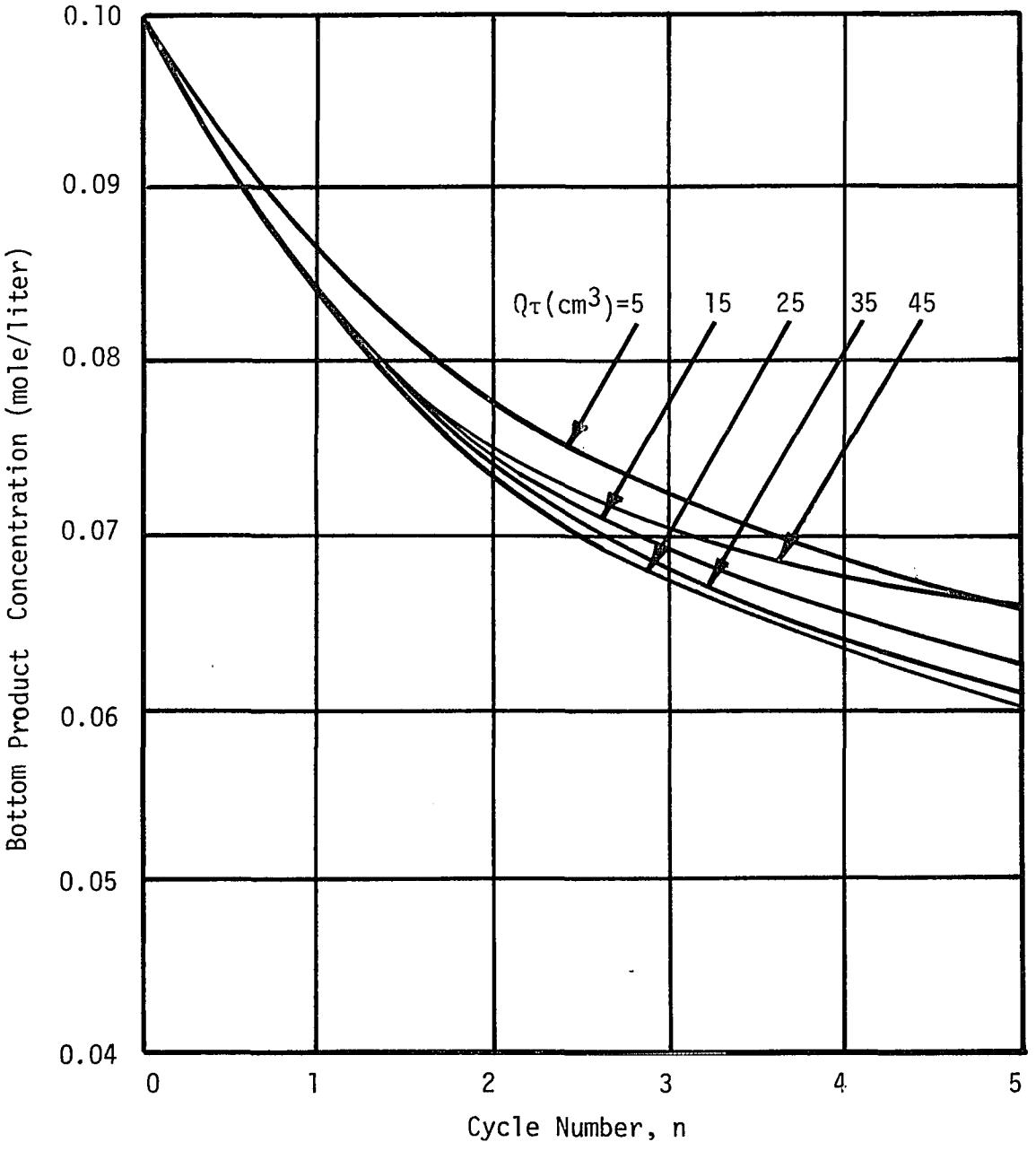

FIGURE 33 - CONCENTRATION TRANSIENTS FOR FIRST FIVE CYCLES OF OPERATION AT VARIABLE RESERVOIR DISPLACEMENT.

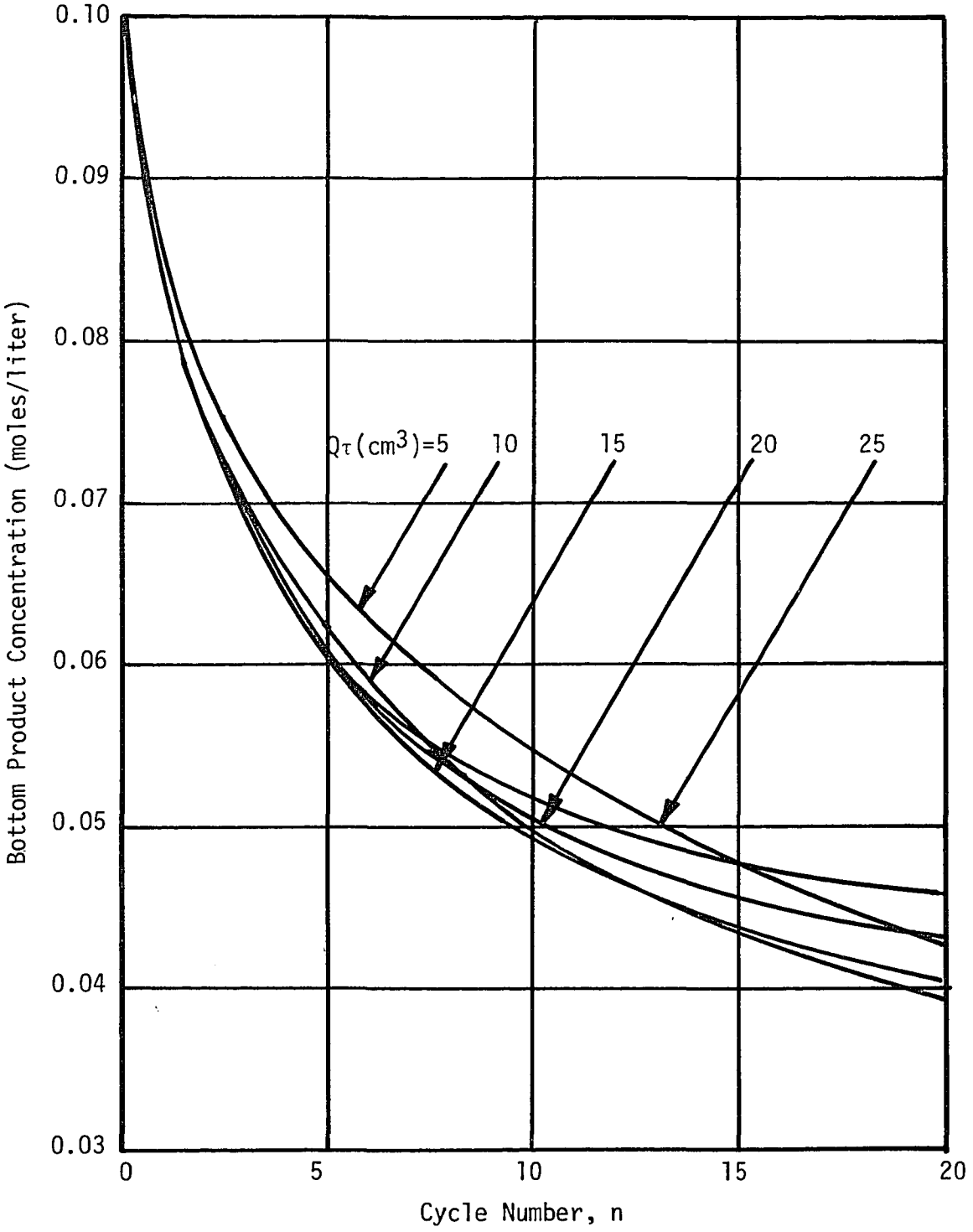

FIGURE 34 - CONCENTRATION TRANSIENTS FOR FIRST 20 CYCLES OF OPERATION AT VARIABLE RESERVOIR DISPLACEMENT

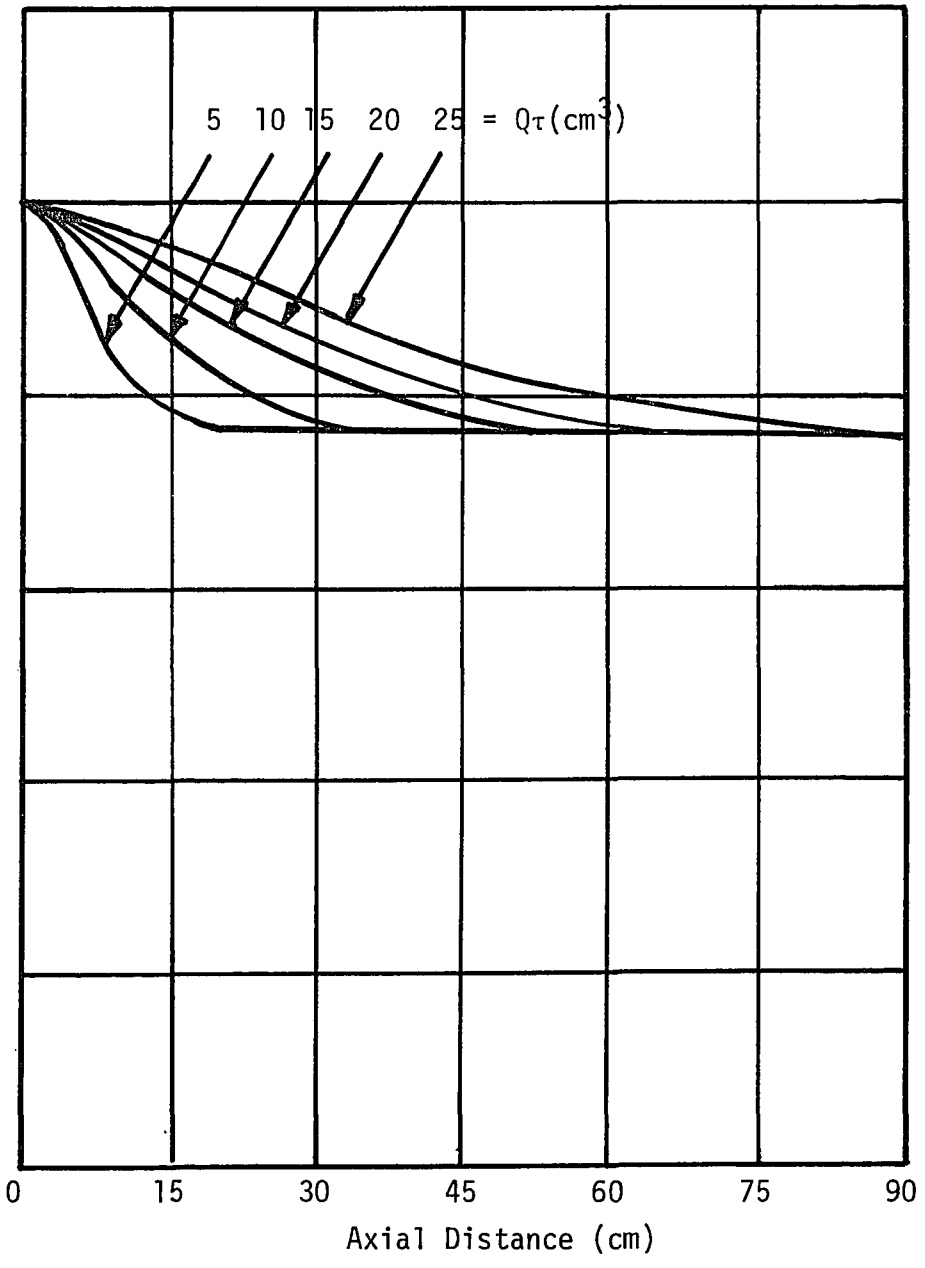

FIGURE 35 - CONCENTRATION GRADIENTS AT n = 1,
VARIABLE RESERVOIR DISPLACMENT

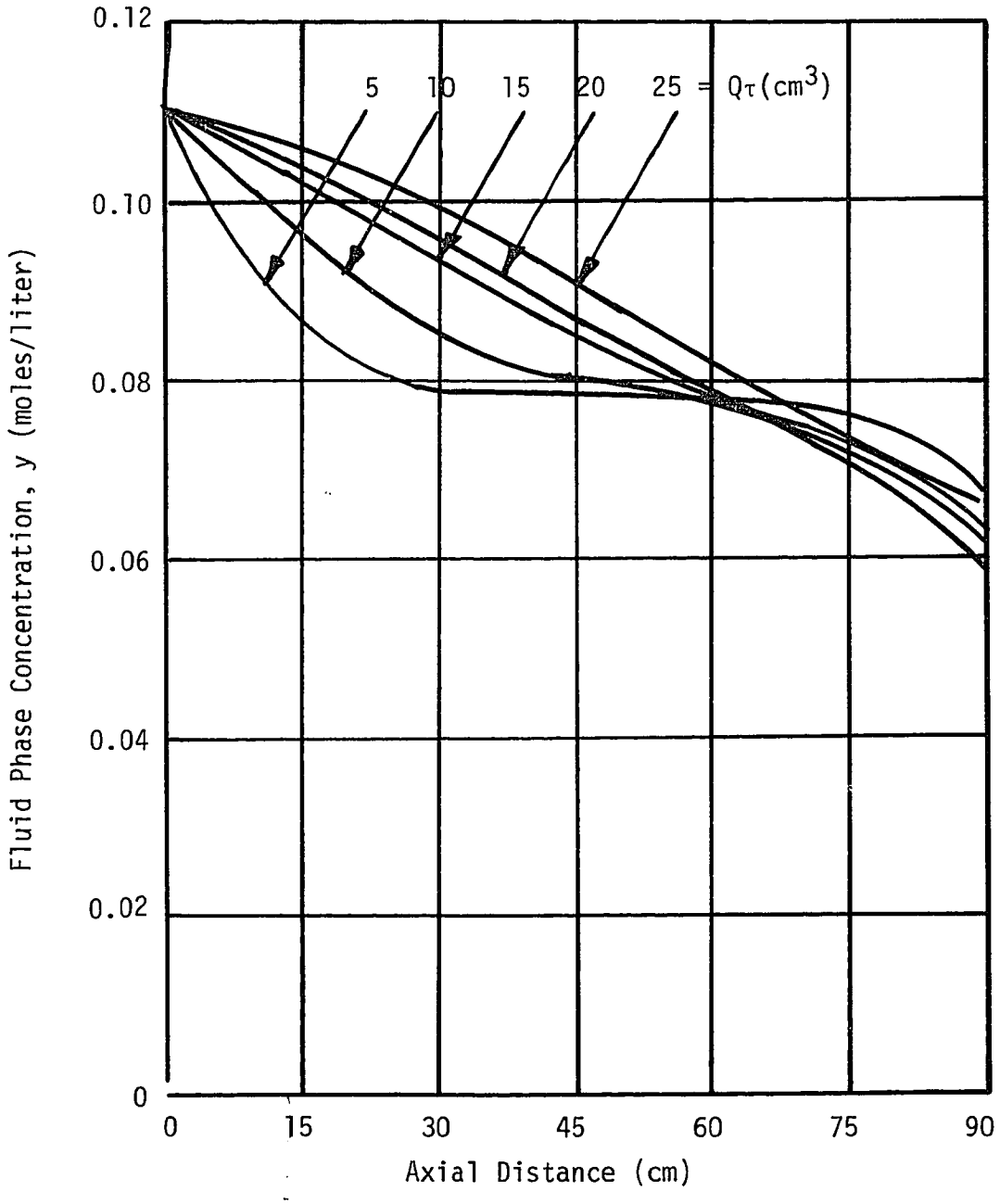

FIGURE 36 - CONCENTRATION GRADIENTS AT n = 5,
VARIABLE RESERVOIR DISPLACEMENT

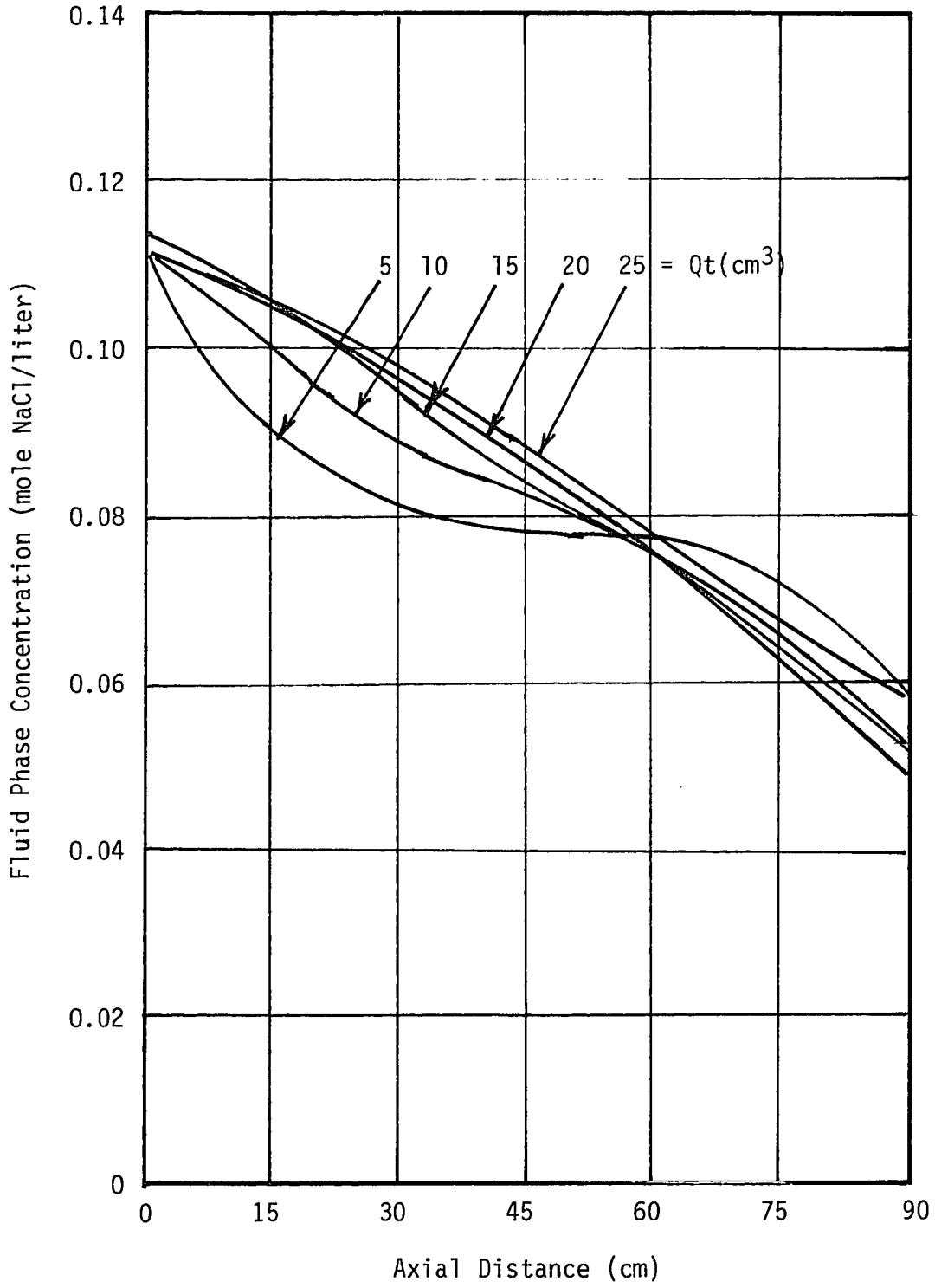

FIGURE 37 - CONCENTRATION GRADIENTS AT n = 10
VARIABLE RESERVOIR DISPLACEMENT

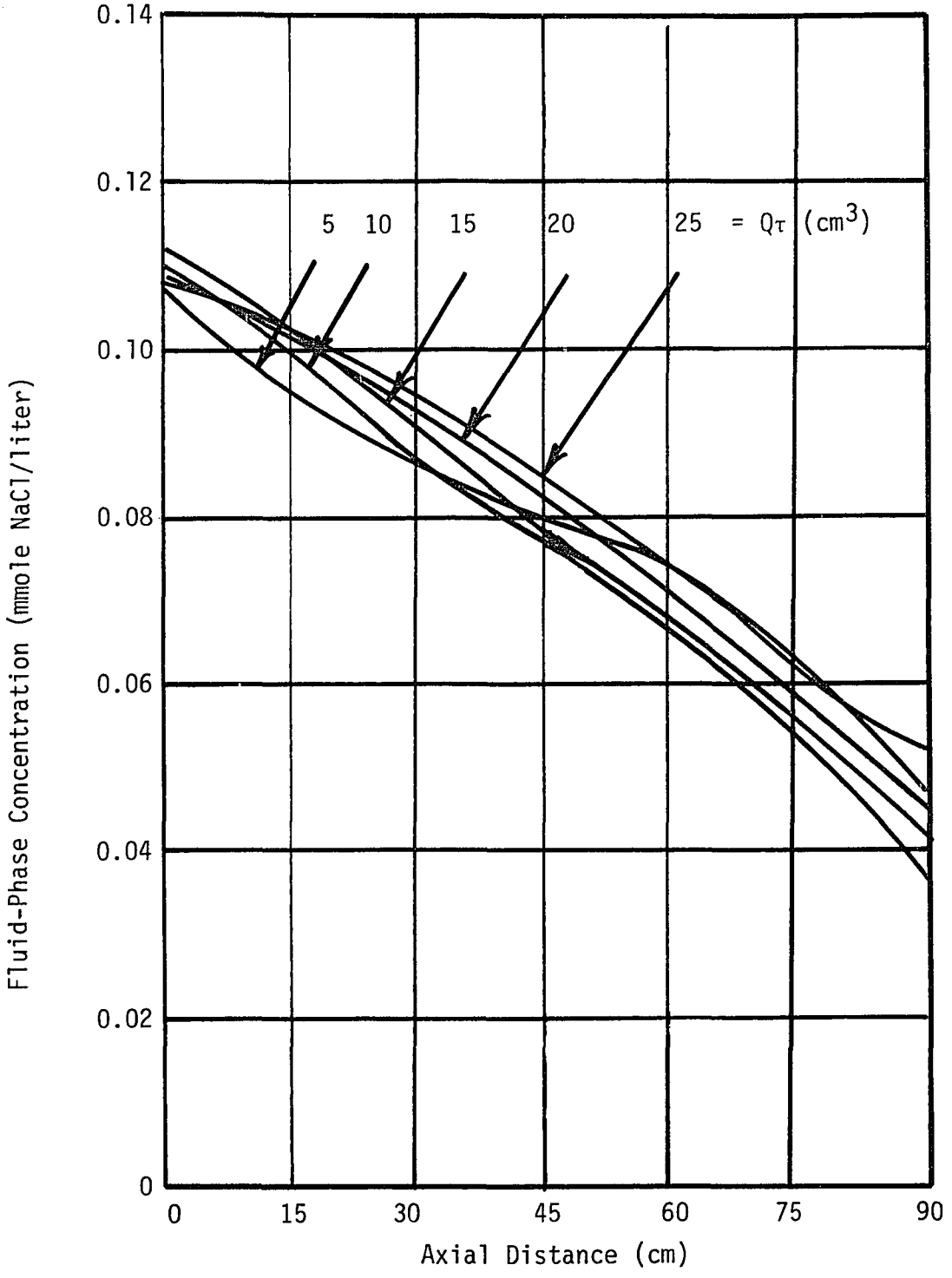

FIGURE 38 - CONCENTRATION GRADIENTS AT n = 25
VARIABLE RESERVOIR DISPLACEMENT

concentration gradient as a function of reservoir displacement after 1, 5, 10 and 25 cycles of operation for reservoir displacements less than 25 cm^3. Except for the column top where the driving force for mass transfer is greatest, the axial concentration gradient is reduced substantially at 5 cm^3 reservoir displacement. Figure 39 is a representation of the solid phase concentration transient at the column mid-point at the end of the hot half cycle. Due to the substantial increase in mass transfer resistance at 5 cm^3 reservoir displacement, it is apparent that removal of solute from the solid on the hot half-cycle is markedly less effective. There are much less available sites for adsorption on the next half-cycle, i.e., the driving force for mass transfer to the solid for the cold half-cycle is reduced, in addition to the obvious increase in mass transfer resistance due to lower velocities. The combination of these two effects work to reduce separation at this low reservoir displacement.

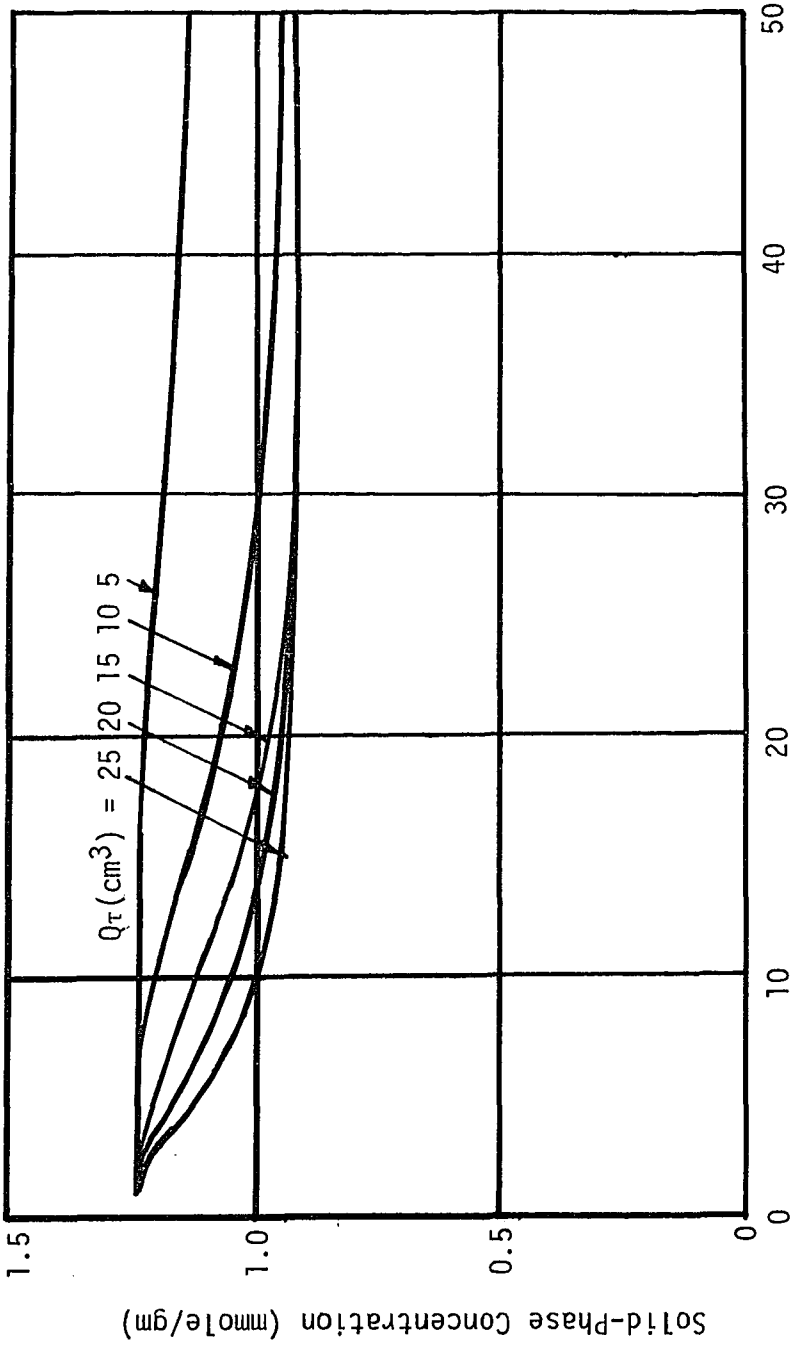

FIGURE 39 - SOLID-PHASE CONTRATION TRANSIENT AT COLUMN MIDPOINT (HOT HALF-CYCLE), VARIABLE RESERVOIR DISPLACEMENT

SUMMARY OF CONCLUSIONS

A. The Theoretical Model

This work establishes the reliability of the model equations for predicting the behavior of continuous non-equilibrium parametric pumps. The model is based on the equations of change for the liquid-solid system with the diffusion term of negligible importance, a liquid-film controlling mass transfer rate expression, and a linear equilibrium relation between the liquid and solid phases. Gregory had previously established the reliability of the same model equations for batch and semi-continuous parametric pumps.

This work further establishes the reliability of the method of characteristics for resolving the model equations into a set of four algebraic relations governing liquid boundary conditions and a set of two finite-difference expressions governing internal column operation. Gregory's study of batch and semi-continuous parametric pumps made use of a STOP-GO algorithm for solution of the internal equations and a set of material balance realtions for the external equations, which were particular to his experimental set-up.

There is little to choose between the two computational schemes. The method of characteristics is more fundamental, but may be less efficient computationally than the STOP-GO algorithm at longer half-

cycle times, especially when the approach to equilibrium is close.

The agreement between the experimental results and the behavior predicted by the model equations is good. The qualitative differences between separations achieved under varying operating conditions is correctly predicted by the model equations. Investigation of internal pump operation using the model equations leads to meaningful interpretation of the behavioral differences noted from experiment to experiment.

B. Qualitative Behavior

This study examines the effect of cycle time, relative displacement of fluid on cold and hot half-cycles of operation, and total fluid displacement relative to column volume on separation of a feed stream into two products, one lean and the other concentrated in solute. The following effects are noted:

1. Better separation, i.e., leaner bottom product and more concentrated top product, is achieved at longer half-cycle times. However, for the experimental system under study, which is characterized by slow interphase mass transfer rates, half-cycle times in excess of four hours would be required to achieve equilibrium operation and, hence, maximum separations. Gregory had previously established the beneficial effect of longer half-cycle times on separation in his work with batch and semi-continuous operation.

2. Poorer separation is achieved when the reservoir liquid displacement per half-cycle exceeds the liquid volume in the absorbant bed. Although a much wider range of relative displacements is studied in this work, this conclusion matches that of Gregory for his batch and semi-continuous operation.

3. Separation is greatly affected by the relative amounts of liquid fed to the adsorbant bed on the cold and hot half-cycles. This work establishes the fact that sufficient fluid must be fed to the bed on the hot half-cycle to remove all the solute adsorbed on the bed during the previous cold half-cycle. When the above is true, a steadily improving separation is achieved with increasing number of cycles of operation. When an insufficient amount of fluid is delivered to the column on the hot half-cycle, separation improves momentarily but then soon degenerates to a steadily worsening separation due to accumulation of solute in both the liquid and solid portions of the adsorbant bed. This effect is found to depend on the relative amounts of hot and cold half-cycle displacement and not at all on total displacement relative to column liquid volume. This phenomenon is not treated in earlier works.

The nature of the parametric pumping process is such that no simple relation exists which predicts what the relative displacement of cold and hot half-cycle liquid must be to avoid the situation of worsening separation with time. The limiting lean product withdrawal rate is a complex function of position of equilibrium (a function of temperature and composition), resistance to

interphase mass transfer (a function of temperature and fluid velocity), and the driving force for interphase mass transfer (a function of half-cycle time and temperature), among other factors. Prediction of the operability of a particular parametric pumping application, if it is characterized by slow mass transfer rates, must rely on evaluation of the individual mass transfer relation, equilibrium isotherms, and concentration region.

This aspect of parametric pumping operation has not been treated by other workers in the field and provides fertile ground for future research efforts.

NOMENCLATURE

A	cross-sectional area of solid bed (cm^2)
a	constant defined by equation (68)
b	constant defined by equation (72)
C	dead volume ratio (dimensionless)
e	error (dimensionless)
h	height of adsorbant bed (cm)
i	index for $\bar{z}$-calculation
j	index for t-calculation
k	number of iteration
L	penetration distance (cm)
M	equilibrium constant, see equation (17)
m	equilibrium constant, see equation (66)
N	number of intervals
n	cycle number
Q	reservoir displacement rate (cm^3/min)
R	number of intervals
r	index for time intervals
T	temperature (°C)
t	time (minutes)
	constant defined by equation (A-5)
V	dead volume, cm^3
v	fluid velocity (cm/min)

X soled-phase concentration (m moles/gm)

Y liquid phase concentration (moles/liter)

Z axial distance (cm)

Greek Letters

α constant defined by equation (83)

β constant defined by equation (83)

δ finite difference interval (min)

ε void space (dimensionless)

λ mass transfer rate constant (min^{-1})

μ constant defined by equation (85)

ρ density (gm/cm^3)

τ half-cycle time (min)

ϕ product withdrawal flow ratio (dimensionless)

ψ thermondyamic property

ω a frequency (min^{-1})

Other Symbols and Subscripts

<> average value

n cycle number

T top

B bottom

P product

0 initial condition

1 hot upflow half-cycle

2 cold downflow half-cycle

S solid phase

APPENDIX I

COMPUTER PROGRAM FOR CONTINUOUS NON-EQUILIBRIUM PARAMETRIC PUMP SIMULATION

The following material is appended to this work to detail the computational operations discussed in the Theory Section. There follows, in order,

Table A-1, Nomenclature for Computer Program Input and Output

Exhibit A, The Computer Program

Exhibit B, Sample Input

Exhibit C, Sample Output, First 5 Cycles of Operation

Exhibit D, Sample Output Summary

TABLE A-1

NOMENCLATURE FOR COMPUTER PROGRAM INPUT AND OUTPUT

Program Symbol	Text Symbol	Designation
N	n	number of cycles
NNZ	m	number of distance intervals
NCASE	--	number of cases to be run
NITER	--	maximum number of iterations
AM	M_o	constants in eq. (66) used to
BM	μ^o	calculate equilibrium coefficients
H	h	column height
TIME	τ	half-cycle time
YO	Y_o	feed concentration
Q	$Q\tau$	reservoir displacement
VT	V_T	top reservoir dead volume
VB	V_B	bottom reservoir dead volume
TEMP1	T_1	hot temperature
TEMP2	T_2	cold temperature
VOID	ε	column void fraction
AK2	β_2	
BK	α^2	constants in eq. (64) used to calculate λ
AK1	β_1	
DENS	ρ_s	solid density
ERR	e^s	error limits on iteration
A	--	cross-sectional area of bed
PHOT	ϕ_T	top product flow ratio
PHOB	ϕ_B	bottom product flow ratio
V1	V_1	hot half-cycle fluid velocity
V2	V_2^1	cold half-cycle fluid velocity
DT1	δ_1^2	hot half cycle finite difference interval
DT2	δ_2^1	cold half cycle finite difference interval
YTP1	<YTP1>	average top product concentration (hot)
YT2	YT2	influent concentration at column top

TABLE A-1 (Cont'd)

Program Symbol	Text Symbol	Designation
TIME	t	time (no. of intervals)
DIST	Z	distance (axial, no. of intervals)
YY	Y	fluid phase concentration
XX	X	solid phase concentration
M	n	cycle number
YTP2	<YTP2>	average top product concentration (cold)
YBP2	<YBP2>	average bottom product concentration (cold)
YBP1	<YBP1>	average bottom product concentration (hot)

PLEASE NOTE:

Print on some pages is small and indistinct. Filmed in the best possible way.

UNIVERSITY MICROFILMS.

EXHIBIT A

```
FORTRAN IV (VER 45 ) SOURCE LISTING:                    10/01/77  08:53:14  PAGE 0001

    1          DIMENSION PHOT(10),PHOB(10),X2(500),YTP2(500),Y2(500),YBP2(500)
    2         1,XX2(500),YY2(500),XX(500),YY(500),XT(500),XXS(500),YYS(500)
    3         2,NTR(500),TT(500)
    4          READ 10,N,NNZ,NCASE,NITER
    5 10       FORMAT(4I10)
    6          READ 16,AM,BM
    7 16       FORMAT(4E20.5)
    8          READ 15,H,TIME,YO,Q,VT,VB,TEMP1,TEMP2,VOID,AK2,BK,AK1,DENS,ERR,A
    9 15       FORMAT( 8F10.4)
   10          READ 20,(PHOT(I),PHOB(I),I=1,NCASE)
   11 20       FORMAT(2F10.4)
   12          DO 600 I=1,NCASE
   13 2020     FORMAT ( '1' )
   14 11       FORMAT(///)
   15          PRINT 2020
   16          PRINT 3030
   17 3030     FORMAT(9X,'N',8X,'NNZ',5X,'NCASE',5X,'NITER'//)
   18          PRINT 10,N,NNZ,NCASE,NITER
   19          PRINT 11
   20          PRINT 4040
   21 4040     FORMAT(15X,'AM',20X,'BM'//)
   22          PRINT 16,AM,BM
   23          PRINT 11
   24          PRINT 5050
   25 5050     FORMAT    (5X,'H',7X,'TIME',/X,'YO',9X,'Q',8X,'VT',8X,'VB',6X,
   26         1'TEMP1',6X,'TEMP2'//)
   27          PRINT 15,H,TIME,YO,Q,VT,VB,TEMP1,TEMP2
   28          PRINT 11
   29          PRINT 6060
   30 6060     FORMAT(3X,'VOID',7X,'AK2',7X,'BK',8X,'AK1',6X,'DENS',7X,'ERR',
   31         18X,'A'//)
   32          PRINT 15,VOID,AK2,BK,AK1,DENS,ERR,A
   33          PRINT 11
   34          PRINT 7070
   35 7070     FORMAT(3X,'PHOT',6X,'PHOB'//)
   36          PRINT 20,PHOT(I),PHOB(I)
   37          PRINT 2020
   38          V1=(1.-PHOB(I))*Q/(A*VOID*TIME)
   39          V2=(1.+PHOB(I))*Q/(A*VOID*TIME)
   40          DT1=H/(NNZ*V1)
   41          DT2=H/(NNZ*V2)
   42          PRINT 111,V1, V2, DT1, DT2
   43 111      FORMAT (15X,'V1',19X,'V2',15X,'DT1',15X,'DT2'//4(10X,F10.5))
   44          NZ=NNZ+1
   45          YT1=YO
   46          DO 30 J=1,NZ
   47          Y2(J)=YO
   48 30       X2(J)=YO*(AM-BM*TEMP1)
   49          M=1
   50          IF(M-1)31,31,32
```

```
      YTP22=YO
      GO TO 33
   32 YTP22=YTP2(M-1)
   33 YTP1=((PHOT(I)+PHOB(I))*YO+(1.-PHOB(I))*YT1)/(1.+PHOT(I))
      IND=2
      YTP2(M)=(Q*YTP1+VT*YTP22)/(VT+Q)
      YT2=((PHOT(I)+PHOB(I))*YO+(1.-PHOT(I))*YTP2(M))/(1.+PHOB(I))
      YIN=YT2
C
      PRINT 222,YTP1,YT2
  222 FORMAT('-',5X,'YTP1',E20.5,10X,'YT2',E20.5///)
      CALL XYCAL(VOID,DENS,AK1,AK2,BK,AM,BM,TEMP1,TEMP2,V1,V2,IND,DT1,
     1DT2,NITER,X2,Y2,YIN,TIME,NZ,XX,YY,YB,M,ERR )
      YBP2(M)=YB
      PRINT 800,M,YTP2(M),YBP2(M)
  800 FORMAT(5X,'M',I20,10X,'YTP2',E20.5,10X,'YBP2',E20.5/)
      IF(M-N)50,500,500
   50 IF(M-1)51,51,52
   51 YBP22=YO
      GO TO 53
   52 YBP22=YBP1
   53 YBP1=(Q*YBP2(M)+VB*YBP22)/(Q+VB)
      PRINT 333,YBP1
  333 FORMAT('0',5X,'YBP1',E20.5)
      M=M+1
      YIN=YBP1
      DO 60 L=1,NZ
      LL=L-1
      X2(L)=XX(NZ-LL)
   60 Y2(L)=YY(NZ-LL)
      IND=1
C
      CALL XYCAL(VOID,DENS,AK1,AK2,BK,AM,BM,TEMP1,TEMP2,V1,V2,IND,DT1,
     1DT2,NITER,X2,Y2,YIN,TIME,NZ,XX,YY,YT1,M,ERR )
      DO 70 L=1,NZ
      LL=L-1
      X2(L)=XX(NZ-LL)
   70 Y2(L)=YY(NZ-LL)
      GO TO 32
  500 PRINT 510,(M,YTP2(M),YBP2(M),M=1,N)
  510 FORMAT('-',18X,'M',12X,'YTP2',16X,'YBP2'//(10X,I10,2E20.5))
  600 CONTINUE
      STOP
      END
C
C
C
C
```

```
      SUBROUTINE XYCAL(VOID,DENS,AK1,AK2,BK,AM,BM,TEMP1,TEMP2,V1,V2,
     1IND,DT1,DT2,NITER,X2,Y2,YIN,TIME,NZ,XX,YY,YYAV,M,ERR )
C
      DIMENSION X2(500),Y2(500),XX(500),YY(500),XT(500),YYS(500),XXS(500
     1),XX2(500),YY2(500),NTR(500),TT(500)
      SUM = Y2(NZ)
      IF((-1)**IND)20,10,10
10    CK=AK2*V2**BK
      CM=AM-BM*TEMP2
      DT=DT2
      T=TEMP2
      GO TO 30
20    CK=AK1*V1**BK
      CM=AM-BM*TEMP1
      DT=DT1
      T=TEMP1
30    CNST=-(1.-VOID)*DENS*CK/VOID
      XT(1)=X2(1)
      DO 22 L=1,NZ
      XX2(L)=X2(L)
22    YY2(L)=Y2(L)
      K=1
155   CNK=K
      TT(K)=DT*CNK
      YY(1)=YIN
      XT(K+1)=CM*YY(1)-(CM*YIN-XT(1))*EXP(-CK*TT(K)/CM)
      XX(1)=XT(K+1)
      I=2
C
85    ITER=1
      NTR(1)=1
      YYS(I) = YY2(I-1)+CNST*DT*(YY2(I-1)-XX2(I-1)/CM)
      XXS(I)=XX2(I)+CK*DT*(YY2(I)-XX2(I)/CM)
100   YY(I) = YY2(I-1)+(DT/2.)*CNST*(YYS(I)-XXS(I)/CM+YY2(I-1)-XX2(I-1)/
     1CM)
      XX(I)=XX2(I)+(CK*DT/2.)*(YYS(I)-XXS(I)/CM+YY2(I)-XX2(I)/CM)
      DEVY=(YY(I)-YYS(I))/YYS(I)
      IF(ABS(DEVY)-ERR)50,50,60
50    DEVX=(XX(I)-XXS(I))/XXS(I)
      IF(ABS(DEVX)-ERR)70,70,60
60    IF(ITER-NITER)80,70,70
80    YYS(I)=YY(I)
      XXS(I)=XX(I)
      ITER=ITER+1
      GO TO 100
70    NTR(I)=ITER
      IF(I-NZ)81,90,90
81    I=I+1
      GO TO 85
C
```

```
   51 90     SUM=SUM+YY(NZ)
   52        IF(TT(K)-TIME)150,200,200
   53 150    DO 151 L=1,NZ
   54        YY2(L)=YY(L)
   55 151    XX2(L)=XX(L)
   56        NNZ=NZ-1
   57            DO 2000 MMM=1,NNZ,8
   58        IF(K.EQ.MMM) GO TO 1001
   59 2000   CONTINUE
   60        GO TO 4000
   61 1001   PRINT 1000,(MMM,NNN,YY(NNN),XX(NNN),NNN=2, NZ,8)
   62 1000   FORMAT(2X,'TIME',2X,'DIST',11X,'YY',20X,'XX'/(I5,4X,I4,4X,2E20.8))
   63 4000   K=K+1
   64        GO TO 155
   65 200    TOTK=K+1
   66        YYAV=SUM/TOTK
   67        RETURN
   68        END
```

EXHIBIT B

N	NNZ	NCASE	NITER
25	65	1	90

AM	BM
0.46347E 01	0.99300E-02

H	TIME	YO	Q	VT	VB	TEMP1	TEMP2
90.0000	24.0000	0.0001	50.0000	0.9000	0.9000	343.1599	278.1599

VOID	AK2	BK	AK1	DENS	ERR	A
0.3800	0.0736	0.3000	0.3280	0.7610	0.0001	0.7850

PHOI	PHOB
0.3200	0.0800

EXHIBIT C

V1	V2	DT1	DT2
6.4253	7.54274	0.21549	0.18357

YTP1 0.10000E-03 YT2 0.10000E-03

TIME	DIST	YY	XX
1	2	0.98962686E-04	0.12354767E-03
1	10	0.98962686E-04	0.12354767E-03
1	18	0.98962686E-04	0.12354767E-03
1	26	0.98962686E-04	0.12354767E-03
1	34	0.98962686E-04	0.12354767E-03
1	42	0.98962686E-04	0.12354767E-03
1	50	0.98962686E-04	0.12354767E-03
1	58	0.98962686E-04	0.12354767E-03
1	66	0.98962686E-04	0.12354767E-03
TIME	DIST	YY	XX
9	2	0.99065320E-04	0.12976026E-03
9	10	0.92119909E-04	0.12905868E-03
9	18	0.92119909E-04	0.12905868E-03
9	26	0.92119909E-04	0.12905868E-03
9	34	0.92119909E-04	0.12905868E-03
9	42	0.92119909E-04	0.12905868E-03
9	50	0.92119909E-04	0.12905868E-03
9	58	0.92119909E-04	0.12905868E-03
9	66	0.92119909E-04	0.12905868E-03
TIME	DIST	YY	XX
17	2	0.99157841E-04	0.13536730E-03
17	10	0.92809990E-04	0.13348811E-03
17	18	0.87307169E-04	0.13293473E-03
17	26	0.87307169E-04	0.13293473E-03
17	34	0.87307169E-04	0.13293473E-03
17	42	0.87307169E-04	0.13293473E-03
17	50	0.87307169E-04	0.13293473E-03
17	58	0.87307169E-04	0.13293473E-03
17	66	0.87307169E-04	0.13293473E-03
TIME	DIST	YY	XX
25	2	0.99241180E-04	0.14042779E-03
25	10	0.93440117E-04	0.13759668E-03
25	18	0.88281827E-04	0.13609737E-03
25	26	0.83922393E-04	0.13566071E-03
25	34	0.83922393E-04	0.13566071E-03
25	42	0.83922393E-04	0.13566071E-03
25	50	0.83922393E-04	0.13566071E-03
25	58	0.83922393E-04	0.13566071E-03
25	66	0.83922393E-04	0.13566071E-03
TIME	DIST	YY	XX
33	2	0.99316283E-04	0.14499496E-03
33	10	0.94015354E-04	0.14140584E-03
33	18	0.89184220E-04	0.13911841E-03
33	26	0.84995757E-04	0.13792167E-03
33	34	0.81542602E-04	0.13757727E-03
33	42	0.81542602E-04	0.13757727E-03
33	50	0.81542602E-04	0.13757727E-03
33	58	0.81542602E-04	0.13757727E-03
33	66	0.81542602E-04	0.13757727E-03
TIME	DIST	YY	XX
41	2	0.99384109E-04	0.14911624E-03
41	10	0.94541319E-04	0.14493513E-03
41	18	0.90019399E-04	0.14199867E-03

41	26	0.96030079E-04	0.14015111E-03
41	34	0.92603932E-04	0.13919709E-03
41	42	0.79868535E-04	0.13892546E-03
41	50	0.79868535E-04	0.13892546E-03
41	58	0.79868535E-04	0.13892546E-03
41	66	0.79868535E-04	0.13892546E-03
TIME	DIST	YY	XX
49	2	0.99445038E-04	0.15283554E-03
49	10	0.95020834E-04	0.14820433E-03
49	18	0.90791974E-04	0.14474080E-03
49	26	0.86947722E-04	0.14234011E-03
49	34	0.83614446E-04	0.14084898E-03
49	42	0.80857600E-04	0.14008801E-03
49	50	0.78690907E-04	0.13987382E-03
49	58	0.78690907E-04	0.13987382E-03
49	66	0.78690907E-04	0.13987382E-03
TIME	DIST	YY	XX
57	2	0.99499957E-04	0.15619237E-03
57	10	0.95458104E-04	0.15123143E-03
57	18	0.91505862E-04	0.14734728E-03
57	26	0.87833148E-04	0.14448128E-03
57	34	0.84575192E-04	0.14252026E-03
57	42	0.81813181E-04	0.14131668E-03
57	50	0.79578603E-04	0.14070989E-03
57	58	0.77862481E-04	0.14054093E-03
57	66	0.77862481E-04	0.14054093E-03
TIME	DIST	YY	XX
65	2	0.99549419E-04	0.15922205E-03
65	10	0.95857263E-04	0.15403320E-03
65	18	0.92165602E-04	0.14982108E-03
65	26	0.88662214E-04	0.14656859E-03
65	34	0.85487714E-04	0.14419980E-03
65	42	0.82734361E-04	0.14259841E-03
65	50	0.80449099E-04	0.14162734E-03
65	58	0.78638884E-04	0.14114342E-03
65	66	0.77279735E-04	0.14101020E-03

M 1 YTP2 0.10000E-03 YBP2 0.82006E-

YBP1 0.82324E-04

TIME	DIST	YY	XX
1	2	0.87814449E-04	0.14281526E-03
1	10	0.89655251E-04	0.14483325E-03
1	18	0.91733891E-04	0.14732368E-03
1	26	0.94010931E-04	0.15030516E-03
1	34	0.96427160E-04	0.15377007E-03
1	42	0.98904056E-04	0.15767828E-03
1	50	0.10134636E-03	0.16195241E-03
1	58	0.10364666E-03	0.16647486E-03
1	66	0.10569220E-03	0.17109029E-03
TIME	DIST	YY	XX
9	2	0.84725252E-04	0.12201630E-03
9	10	0.10338498E-03	0.13231482E-03
9	18	0.10524507E-03	0.13474841E-03
9	26	0.10742301E-03	0.13759523E-03
9	34	0.10990107E-03	0.14083099E-03
9	42	0.11263936E-03	0.14440218E-03
9	50	0.11557399E-03	0.14822348E-03
9	58	0.11861663E-03	0.15217729E-03
9	66	0.12165650E-03	0.15611720E-03
TIME	DIST	YY	XX
17	2	0.83461010E-04	0.11149289E-03
17	10	0.96787334E-04	0.12664848E-03
17	18	0.10637424E-03	0.13227153E-03
17	26	0.10841448E-03	0.13496882E-03
17	34	0.11077709E-03	0.13805427E-03

17	42	0.11343535E-03	0.14148229E-03
17	50	0.11633866E-03	0.14517693E-03
17	58	0.11941118E-03	0.14903067E-03
17	66	0.12253896E-03	0.15290541E-03
TIME	DIST	YY	XX
25	2	0.82861908E-04	0.10621693E-03
25	10	0.91912210E-04	0.12032937E-03
25	18	0.10249429E-03	0.12985313E-03
25	26	0.10784534E-03	0.13370518E-03
25	34	0.11007946E-03	0.13663839E-03
25	42	0.11262203E-03	0.13993079E-03
25	50	0.11543247E-03	0.14351797E-03
25	58	0.11844540E-03	0.14730451E-03
25	66	0.12157005E-03	0.15116464E-03
TIME	DIST	YY	XX
33	2	0.82578568E-04	0.10358822E-03
33	10	0.88488115E-04	0.11477244E-03
33	18	0.98332428E-04	0.12599316E-03
33	26	0.10566814E-03	0.13216423E-03
33	34	0.10922580E-03	0.13544950E-03
33	42	0.11164628E-03	0.13859989E-03
33	50	0.11435110E-03	0.14207045E-03
33	58	0.11728474E-03	0.14577793E-03
33	66	0.12036652E-03	0.14960839E-03
TIME	DIST	YY	XX
41	2	0.82444530E-04	0.10228487E-03
41	10	0.86193569E-04	0.11041640E-03
41	18	0.94479022E-04	0.12153870E-03
41	26	0.10274394E-03	0.12969063E-03
41	34	0.10779902E-03	0.13415079E-03
41	42	0.11069103E-03	0.13734758E-03
41	50	0.11328337E-03	0.14069155E-03
41	58	0.11612663E-03	0.14430544E-03
41	66	0.11915009E-03	0.14808736E-03
TIME	DIST	YY	XX
49	2	0.82381127E-04	0.10164139E-03
49	10	0.84705883E-04	0.10723837E-03
49	18	0.91238078E-04	0.11716060E-03
49	26	0.99476252E-04	0.12644565E-03
49	34	0.10578087E-03	0.13237397E-03
49	42	0.10954203E-03	0.13608352E-03
49	50	0.11225637E-03	0.13936574E-03
49	58	0.11500044E-03	0.14287293E-03
49	66	0.11795276E-03	0.14658854E-03
TIME	DIST	YY	XX
57	2	0.82351558E-04	0.10132375E-03
57	10	0.83766484E-04	0.10503147E-03
57	18	0.88679517E-04	0.11326198E-03
57	26	0.96229079E-04	0.12277003E-03
57	34	0.10327689E-03	0.13001509E-03
57	42	0.10804417E-03	0.13461066E-03
57	50	0.11118098E-03	0.13806639E-03
57	58	0.11391296E-03	0.14148300E-03
57	66	0.11678299E-03	0.14511636E-03
TIME	DIST	YY	XX
65	2	0.82337079E-04	0.10116759E-03
65	10	0.83185863E-04	0.10355409E-03
65	18	0.86734959E-04	0.11002290E-03
65	26	0.93254682E-04	0.11901773E-03
65	34	0.10048796E-03	0.12713966E-03
65	42	0.10614886E-03	0.13278349E-03
65	50	0.10993505E-03	0.13669644E-03
65	58	0.11283089E-03	0.14012966E-03
65	66	0.11564567E-03	0.14367666E-03

YTP1 0.11412E-03 YT2 0.10689E-03

TIME	DIST	YY	XX
1	2	0.10689597E-03	0.13513953E-03
1	10	0.10237913E-03	0.12998021E-03
1	18	0.96870528E-04	0.12349854E-03
1	26	0.91073423E-04	0.11619984E-03
1	34	0.86207262E-04	0.10948801E-03
1	42	0.83155304E-04	0.10479285E-03
1	50	0.81839592E-04	0.10248880E-03
1	58	0.81504578E-04	0.10179856E-03
1	66	0.81470352E-04	0.10171013E-03
TIME	DIST	YY	XX
9	2	0.10594391E-03	0.14149320E-03
9	10	0.99395314E-04	0.13589104E-03
9	18	0.95165174E-04	0.12914892E-03
9	26	0.90023633E-04	0.12154355E-03
9	34	0.84641127E-04	0.11452123E-03
9	42	0.80151861E-04	0.10957291E-03
9	50	0.77357966E-04	0.10711230E-03
9	58	0.76165626E-04	0.10635439E-03
9	66	0.75866701E-04	0.10624860E-03
TIME	DIST	YY	XX
17	2	0.10603793E-03	0.14721561E-03
17	10	0.99301207E-04	0.14086053E-03
17	18	0.93446520E-04	0.13390940E-03
17	26	0.89285138E-04	0.12619580E-03
17	34	0.84383325E-04	0.11890310E-03
17	42	0.79448291E-04	0.11354980E-03
17	50	0.75491552E-04	0.11068974E-03
17	58	0.73117626E-04	0.10967180E-03
17	66	0.72137409E-04	0.10946178E-03
TIME	DIST	YY	XX
25	2	0.10612284E-03	0.15237986E-03
25	10	0.99968747E-04	0.14545201E-03
25	18	0.93896203E-04	0.13802550E-03
25	26	0.88449261E-04	0.13023286E-03
25	34	0.84302198E-04	0.12282362E-03
25	42	0.79707344E-04	0.11710482E-03
25	50	0.75347197E-04	0.11373778E-03
25	58	0.72013805E-04	0.11227641E-03
25	66	0.70079142E-04	0.11181302E-03
TIME	DIST	YY	XX
33	2	0.10619914E-03	0.15703989E-03
33	10	0.10057774E-03	0.14970242E-03
33	18	0.94907169E-04	0.14191883E-03
33	26	0.89246008E-04	0.13382340E-03
33	34	0.84085288E-04	0.12632237E-03
33	42	0.80060388E-04	0.12036854E-03
33	50	0.75917996E-04	0.11653430E-03
33	58	0.72208014E-04	0.11454745E-03
33	66	0.69473622E-04	0.11368452E-03
TIME	DIST	YY	XX
41	2	0.10626786E-03	0.16124580E-03
41	10	0.10113292E-03	0.15363547E-03
41	18	0.95841343E-04	0.14560398E-03
41	26	0.90461981E-04	0.13728411E-03
41	34	0.85101710E-04	0.12951487E-03
41	42	0.80267389E-04	0.12335701E-03
41	50	0.76535536E-04	0.11916811E-03
41	58	0.72939132E-04	0.11668893E-03
41	66	0.69852001E-04	0.11535743E-03
TIME	DIST	YY	XX
49	2	0.10632981E-03	0.16504180E-03

49	10	0.10163958E-03	0.15727336E-03
49	18	0.96704025E-04	0.14908788E-03
49	26	0.91598980E-04	0.14061836E-03
49	34	0.86434927E-04	0.13264010E-03
49	42	0.81409772E-04	0.12614817E-03
49	50	0.77014032E-04	0.12164032E-03
49	58	0.73693692E-04	0.11876004E-03
49	66	0.70640264E-04	0.11698094E-03
TIME	DIST	YY	XX
57	2	0.10638562E-03	0.16846780E-03
57	10	0.10210200E-03	0.16063702E-03
57	18	0.97500989E-04	0.15237786E-03
57	26	0.92661357E-04	0.14382447E-03
57	34	0.87695254E-04	0.13569521E-03
57	42	0.82795289E-04	0.12892205E-03
57	50	0.78206270E-04	0.12400211E-03
57	58	0.74326089E-04	0.12075345E-03
57	66	0.71442700E-04	0.11859486E-03
TIME	DIST	YY	XX
65	2	0.10643591E-03	0.17155985E-03
65	10	0.10252398E-03	0.16374607E-03
65	18	0.98237142E-04	0.15548155E-03
65	26	0.93653958E-04	0.14690170E-03
65	34	0.88885572E-04	0.13867383E-03
65	42	0.84118510E-04	0.13167196E-03
65	50	0.79589372E-04	0.12638865E-03
65	58	0.75507792E-04	0.12270187E-03
65	66	0.72144233E-04	0.12018804E-03

M 2 YTP2 0.11095E-03 YBP2 0.746

YBP1 0.74799E-04

TIME	DIST	YY	XX
1	2	0.85714054E-04	0.13247046E-03
1	10	0.89373716E-04	0.13751182E-03
1	18	0.93239315E-04	0.14332301E-03
1	26	0.97196811E-04	0.14990149E-03
1	34	0.10109069E-03	0.15706352E-03
1	42	0.10474536E-03	0.16439226E-03
1	50	0.10800773E-03	0.17140868E-03
1	58	0.11078980E-03	0.17779709E-03
1	66	0.11305521E-03	0.18347340E-03
TIME	DIST	YY	XX
9	2	0.77113960E-04	0.11236536E-03
9	10	0.98756499E-04	0.12683462E-03
9	18	0.10284028E-03	0.13218848E-03
9	26	0.10734767E-03	0.13810970E-03
9	34	0.11218464E-03	0.14443460E-03
9	42	0.11714165E-03	0.15083280E-03
9	50	0.12193464E-03	0.15691936E-03
9	58	0.12631886E-03	0.16242440E-03
9	66	0.13017884E-03	0.16725146E-03
TIME	DIST	YY	XX
17	2	0.75894800E-04	0.10203291E-03
17	10	0.90022091E-04	0.11981092E-03
17	18	0.10263255E-03	0.12893911E-03
17	26	0.10702366E-03	0.13460811E-03
17	34	0.11182415E-03	0.14071602E-03
17	42	0.11687067E-03	0.14699317E-03
17	50	0.12189834E-03	0.15307819E-03
17	58	0.12663072E-03	0.15866739E-03
17	66	0.13088176E-03	0.16361344E-03
TIME	DIST	YY	XX
25	2	0.75317337E-04	0.96863688E-04
25	10	0.88804589E-04	0.11253980E-03
25	18	0.97323834E-04	0.12514938E-03

25	26	0.10546790E-03	0.13221432E-03
25	34	0.11011458E-03	0.13814472E-03
25	42	0.11507835E-03	0.14434740E-03
25	50	0.12013358E-03	0.15049493E-03
25	58	0.12500468E-03	0.15626306E-03
25	66	0.12947015E-03	0.16144510E-03

TIME	DIST	YY	XX
33	2	0.75044212E-04	0.94292176E-04
33	10	0.81189456E-04	0.10638591E-03
33	18	0.92405287E-04	0.12007792E-03
33	26	0.10211689E-03	0.12939777E-03
33	34	0.10829834E-03	0.13577522E-03
33	42	0.11313851E-03	0.14187023E-03
33	50	0.11816037E-03	0.14803853E-03
33	58	0.12310737E-03	0.15395449E-03
33	66	0.12773639E-03	0.15936622E-03

TIME	DIST	YY	XX
41	2	0.74915005E-04	0.93018898E-04
41	10	0.78788900E-04	0.10167014E-03
41	18	0.88012457E-04	0.11465460E-03
41	26	0.98255841E-04	0.12567587E-03
41	34	0.10581090E-03	0.13325020E-03
41	42	0.11122439E-03	0.13945335E-03
41	50	0.11617514E-03	0.14559308E-03
41	58	0.12115239E-03	0.15160866E-03
41	66	0.12590768E-03	0.15721965E-03

TIME	DIST	YY	XX
49	2	0.74853873E-04	0.92390968E-04
49	10	0.77244170E-04	0.98280215E-04
49	18	0.84397848E-04	0.10954287E-03
49	26	0.94204777E-04	0.12129656E-03
49	34	0.10280294E-03	0.13023843E-03
49	42	0.10907026E-03	0.13699886E-03
49	50	0.11421468E-03	0.14316115E-03
49	58	0.11918186E-03	0.14922608E-03
49	66	0.12402514E-03	0.15499721E-03

TIME	DIST	YY	XX
57	2	0.74825453E-04	0.92081972E-04
57	10	0.76274300E-04	0.95950948E-04
57	18	0.81582038E-04	0.10511241E-03
57	26	0.90339788E-04	0.11664563E-03
57	34	0.99392011E-04	0.12668553E-03
57	42	0.10657933E-03	0.13431706E-03
57	50	0.11217534E-03	0.14072203E-03
57	58	0.11721472E-03	0.14682423E-03
57	66	0.12210725E-03	0.15271176E-03

TIME	DIST	YY	XX
65	2	0.74811439E-04	0.91929483E-04
65	10	0.75677453E-04	0.94404138E-04
65	18	0.79481629E-04	0.10150312E-03
65	26	0.86889180E-04	0.11209265E-03
65	34	0.95811046E-04	0.12270402E-03
65	42	0.10372575E-03	0.13128716E-03
65	50	0.10995523E-03	0.13818424E-03
65	58	0.11521895E-03	0.14440829E-03
65	66	0.12016972E-03	0.15038023E-03

YTP1 0.11456E-03 YT2 0.10913E-03

TIME	DIST	YY	XX
1	2	0.10617269E-03	0.13523111E-03
1	10	0.99466793E-04	0.12727373E-03
1	18	0.92069400E-04	0.11825915E-03

1	26	0.84890838E-04	0.10898428E-03
1	34	0.79217541E-04	0.10101646E-03
1	42	0.75820425E-04	0.95723633E-04
1	50	0.74406445E-04	0.93225287E-04
1	58	0.74057723E-04	0.92502377E-04
1	66	0.74023191E-04	0.92412883E-04
TIME	DIST	YY	XX
9	2	0.10811801E-03	0.14195144E-03
9	10	0.98664619E-04	0.13312583E-03
9	18	0.92403119E-04	0.12373133E-03
9	26	0.85515232E-04	0.11404949E-03
9	34	0.78860539E-04	0.10569989E-03
9	42	0.73633214E-04	0.10011237E-03
9	50	0.70926031E-04	0.97439813E-04
9	58	0.69245652E-04	0.96644143E-04
9	66	0.68934692E-04	0.96536634E-04
TIME	DIST	YY	XX
17	2	0.10821788E-03	0.14803704E-03
17	10	0.10089071E-03	0.13863973E-03
17	18	0.92399714E-04	0.12868609E-03
17	26	0.86365165E-04	0.11876108E-03
17	34	0.79892706E-04	0.11000330E-03
17	42	0.73844988E-04	0.10389928E-03
17	50	0.69261106E-04	0.10076043E-03
17	58	0.66628112E-04	0.99677141E-04
17	66	0.65977012E-04	0.99458760E-04
TIME	DIST	YY	XX
25	2	0.10830763E-03	0.15352838E-03
25	10	0.10161533E-03	0.14375875E-03
25	18	0.94733652E-04	0.13345339E-03
25	26	0.86902262E-04	0.12313112E-03
25	34	0.81068006E-04	0.11409490E-03
25	42	0.75109550E-04	0.10746533E-03
25	50	0.69815665E-04	0.10369910E-03
25	58	0.65969958E-04	0.10210670E-03
25	66	0.63827625E-04	0.10161070E-03
TIME	DIST	YY	XX
33	2	0.10838851E-03	0.15848454E-03
33	10	0.10227578E-03	0.14849391E-03
33	18	0.95857365E-04	0.13797429E-03
33	26	0.89250868E-04	0.12740420E-03
33	34	0.81966951E-04	0.11797155E-03
33	42	0.76467273E-04	0.11092940E-03
33	50	0.71176124E-04	0.10653843E-03
33	58	0.66700406E-04	0.10431235E-03
33	66	0.63553525E-04	0.10336198E-03
TIME	DIST	YY	XX
41	2	0.10846139E-03	0.16295764E-03
41	10	0.10287852E-03	0.15287232E-03
41	18	0.96894858E-04	0.14224426E-03
41	26	0.90630754E-04	0.13152629E-03
41	34	0.84274957E-04	0.12181516E-03
41	42	0.77990244E-04	0.11427957E-03
41	50	0.72602153E-04	0.10936199E-03
41	58	0.68054825E-04	0.10650474E-03
41	66	0.64345411E-04	0.10499643E-03
TIME	DIST	YY	XX
49	2	0.10852706E-03	0.16699471E-03
49	10	0.10342854E-03	0.15691943E-03
49	18	0.97853189E-04	0.14627297E-03
49	26	0.91919631E-04	0.13548520E-03
49	34	0.85812411E-04	0.12557780E-03
49	42	0.79814359E-04	0.11765050E-03
49	50	0.73836519E-04	0.11215280E-03
49	58	0.69462330E-04	0.10874259E-03
49	66	0.65627056E-04	0.10667126E-03

TIME	DIST	YY	XX
57	2	0.10858623E-03	0.17063822E-03
57	10	0.10393046E-03	0.16065898E-03
57	18	0.98738106E-04	0.15007029E-03
57	26	0.93123497E-04	0.13928076E-03
57	34	0.87263819E-04	0.12924349E-03
57	42	0.81430291E-04	0.12099986E-03
57	50	0.75937059E-04	0.11500990E-03
57	58	0.70719950E-04	0.11100683E-03
57	66	0.66957974E-04	0.10842817E-03
TIME	DIST	YY	XX
65	2	0.10863955E-03	0.17392654E-03
65	10	0.10438840E-03	0.16411321E-03
65	18	0.99555181E-04	0.15364619E-03
65	26	0.94247385E-04	0.14291388E-03
65	34	0.88633532E-04	0.13280615E-03
65	42	0.82971222E-04	0.12430959E-03
65	50	0.77562770E-04	0.11789601E-03
65	58	0.72664639E-04	0.11337041E-03
65	66	0.68177236E-04	0.11024892E-03

M 3 YTP2 0.11449E-03 YRP2 0.70446E-

YBp1 0.70523E-04

TIME	DIST	YY	XX
1	2	0.03434337E-04	0.12612618E-03
1	10	0.87788866E-04	0.13219040E-03
1	18	0.92369387E-04	0.13914845E-03
1	26	0.97038850E-04	0.14699128E-03
1	34	0.10161365E-03	0.15551950E-03
1	42	0.10588352E-03	0.16427033E-03
1	50	0.10966427E-03	0.17266627E-03
1	58	0.11283689E-03	0.18027746E-03
1	66	0.11535638E-03	0.18692423E-03
TIME	DIST	YY	XX
9	2	0.72766473E-04	0.10662129E-03
9	10	0.99232200E-04	0.12246925E-03
9	18	0.10011376E-03	0.12886561E-03
9	26	0.10547870E-03	0.13591014E-03
9	34	0.11121745E-03	0.14341991E-03
9	42	0.11709305E-03	0.15102171E-03
9	50	0.12277528E-03	0.15825628E-03
9	58	0.12795824E-03	0.16476457E-03
9	66	0.13246108E-03	0.17038052E-03
TIME	DIST	YY	XX
17	2	0.71584698E-04	0.96531453E-04
17	10	0.85791994E-04	0.11503517E-03
17	18	0.99376571E-04	0.12537834E-03
17	26	0.10461576E-03	0.13212978E-03
17	34	0.11032098E-03	0.13938476E-03
17	42	0.11631193E-03	0.14683601E-03
17	50	0.12228044E-03	0.15406267E-03
17	58	0.12789181E-03	0.16067832E-03
17	66	0.13289480E-03	0.16646067E-03
TIME	DIST	YY	XX
25	2	0.71025031E-04	0.91487527E-04
25	10	0.80526922E-04	0.10751364E-03
25	18	0.93993742E-04	0.12111702E-03
25	26	0.10269672E-03	0.12932940E-03
25	34	0.10822873E-03	0.13637987E-03
25	42	0.11412414E-03	0.14374343E-03
25	50	0.12012605E-03	0.15104315E-03
25	58	0.12590640E-03	0.15787936E-03
25	66	0.13117988E-03	0.16396839E-03
TIME	DIST	YY	XX
33	2	0.70760303E-04	0.88979941E-04

33	10	0.76896511E-04	0.10122893E-03
33	18	0.88461703E-04	0.11565730E-03
33	26	0.98940538E-04	0.12605738E-03
33	34	0.10605807E-03	0.13356944E-03
33	42	0.11181226E-03	0.14080918E-03
33	50	0.11777518E-03	0.14813300E-03
33	58	0.12364719E-03	0.15515015E-03
33	66	0.12912510E-03	0.16153193E-03

TIME	DIST	YY	XX
41	2	0.70635069E-04	0.87738968E-04
41	10	0.74494266E-04	0.96450719E-04
41	18	0.83931183E-04	0.10994618E-03
41	26	0.94777438E-04	0.12190765E-03
41	34	0.10319181E-03	0.13059414E-03
41	42	0.10953554E-03	0.13793923E-03
41	50	0.11541690E-03	0.14523035E-03
41	58	0.12132569E-03	0.15236886E-03
41	66	0.12696022E-03	0.15900176E-03

TIME	DIST	YY	XX
49	2	0.70975813E-04	0.87127278E-04
49	10	0.72952607E-04	0.93033857E-04
49	18	0.80230529E-04	0.10463291E-03
49	26	0.90488872E-04	0.11715695E-03
49	34	0.99843775E-04	0.12714126E-03
49	42	0.10701030E-03	0.13503215E-03
49	50	0.11308775E-03	0.14234251E-03
49	58	0.11898631E-03	0.14954188E-03
49	66	0.12472965E-03	0.15637495E-03

TIME	DIST	YY	XX
57	2	0.70547772E-04	0.86826810E-04
57	10	0.71986694E-04	0.90695102E-04
57	18	0.77363554E-04	0.10006882E-03
57	26	0.86445274E-04	0.11220176E-03
57	34	0.96133604E-04	0.12317530E-03
57	42	0.10416299E-03	0.13190217E-03
57	50	0.11067803E-03	0.13944863E-03
57	58	0.11665032E-03	0.14669092E-03
57	66	0.12245546E-03	0.15366920E-03

TIME	DIST	YY	XX
65	2	0.70534704E-04	0.86678133E-04
65	10	0.71393194E-04	0.89146618E-04
65	18	0.75234420E-04	0.96374074E-04
65	26	0.82865779E-04	0.10741124E-03
65	34	0.92301037E-04	0.11882429E-03
65	42	0.10097590E-03	0.12843817E-03
65	50	0.10809368E-03	0.13645852E-03
65	58	0.11428485E-03	0.14382355E-03
65	66	0.12015663E-03	0.15090591E-03

YTP1 0.11479E-03 YT2 0.10931E-03

TIME	DIST	YY	XX
1	2	0.10409663E-03	0.13301114E-03
1	10	0.96605625E-04	0.12402523E-03
1	18	0.88577580E-04	0.11414308E-03
1	26	0.80974001E-04	0.10424158E-03
1	34	0.75078263E-04	0.95914700E-04
1	42	0.71601636E-04	0.90474641E-04
1	50	0.70173584E-04	0.87941734E-04
1	58	0.69825255E-04	0.87217951E-04
1	66	0.69791174E-04	0.87129519E-04

TIME	DIST	YY	XX
9	2	0.10826357E-03	0.13995651E-03

9	10	0.96711373E-04	0.12975442E-03
9	18	0.89722321E-04	0.11945062E-03
9	26	0.82252183E-04	0.10910918E-03
9	34	0.75208095E-04	0.10037831E-03
9	42	0.69777262E-04	0.94632254E-04
9	50	0.66598309E-04	0.91921290E-04
9	58	0.65305430E-04	0.91124005E-04
9	66	0.64994892E-04	0.91017573E-04
TIME	DIST	YY	XX
17	2	0.10836702E-03	0.14626971E-03
17	10	0.10070422E-03	0.13554927E-03
17	18	0.90421817E-04	0.12440041E-03
17	26	0.83723934E-04	0.11376373E-03
17	34	0.76733485E-04	0.10457644E-03
17	42	0.70349633E-04	0.98278556E-04
17	50	0.65594780E-04	0.95082650E-04
17	58	0.62903578E-04	0.93991882E-04
17	66	0.61842714E-04	0.93773807E-04
TIME	DIST	YY	XX
25	2	0.10846002E-03	0.15196696E-03
25	10	0.10146134E-03	0.14094677E-03
25	18	0.94171657E-04	0.12947133E-03
25	26	0.84814455E-04	0.11819325E-03
25	34	0.78392113E-04	0.10866567E-03
25	42	0.71990361E-04	0.10178740E-03
25	50	0.66417982E-04	0.97927390E-04
25	58	0.62434337E-04	0.96310090E-04
25	66	0.60245889E-04	0.95809577E-04
TIME	DIST	YY	XX
33	2	0.10854383E-03	0.15710892E-03
33	10	0.10215158E-03	0.14593829E-03
33	18	0.95354815E-04	0.13429220E-03
33	26	0.88305518E-04	0.12276456E-03
33	34	0.79732533E-04	0.11262747E-03
33	42	0.73727336E-04	0.10527161E-03
33	50	0.68067514E-04	0.10073479E-03
33	58	0.63365703E-04	0.98451841E-04
33	66	0.60108606E-04	0.97482945E-04
TIME	DIST	YY	XX
41	2	0.10861934E-03	0.16174967E-03
41	10	0.10278153E-03	0.15055266E-03
41	18	0.96447154E-04	0.13884276E-03
41	26	0.89766792E-04	0.12718266E-03
41	34	0.82967206E-04	0.11674310E-03
41	42	0.75205694E-04	0.10870927E-03
41	50	0.69792949E-04	0.10358532E-03
41	58	0.64943436E-04	0.10062667E-03
41	66	0.61051454E-04	0.99074066E-04
TIME	DIST	YY	XX
49	2	0.10868738E-03	0.16593805E-03
49	10	0.10335633E-03	0.15481688E-03
49	18	0.97456024E-04	0.14313376E-03
49	26	0.91131456E-04	0.13142261E-03
49	34	0.84601502E-04	0.12077850E-03
49	42	0.78183933E-04	0.11231557E-03
49	50	0.71314934E-04	0.10645577E-03
49	58	0.66588268E-04	0.10289236E-03
49	66	0.62506267E-04	0.10074042E-03
TIME	DIST	YY	XX
57	2	0.10874869E-03	0.16971810E-03
57	10	0.10388084E-03	0.15875623E-03
57	18	0.98387536E-04	0.14717616E-03
57	26	0.92405825E-04	0.13548476E-03
57	34	0.86143991E-04	0.12470718E-03
57	42	0.79905366E-04	0.11590424E-03
57	50	0.74030263E-04	0.10951041E-03

57	58	0.68079447E-04	0.10522614E-03
57	66	0.64025938E-04	0.10252401E-03
TIME	DIST	YY	XX
65	2	0.10880393E-03	0.17312961E-03
65	10	0.10435938E-03	0.16239425E-03
65	18	0.99247496E-04	0.15098097E-03
65	26	0.93595328E-04	0.13937046E-03
65	34	0.87599153E-04	0.12852307E-03
65	42	0.81546444E-04	0.11944655E-03
65	50	0.75764211E-04	0.11260061E-03
65	58	0.70525769E-04	0.10775351E-03
65	66	0.65435320E-04	0.10440455E-03

M 4 YTP2 0.11478E-03 YBP2 0.67707

YBP1 0.67757E-04

TIME	DIST	YY	XX
1	2	0.81500940E-04	0.12180750E-03
1	10	0.86151499E-04	0.12829357E-03
1	18	0.91040317E-04	0.13572858E-03
1	26	0.96020856E-04	0.14410015E-03
1	34	0.10089832E-03	0.15320395E-03
1	42	0.10544879E-03	0.16256273E-03
1	50	0.10947307E-03	0.17156653E-03
1	58	0.11283910E-03	0.17974089E-03
1	66	0.11549423E-03	0.18686708E-03
TIME	DIST	YY	XX
9	2	0.69944027E-04	0.10278756E-03
9	10	0.92578469E-04	0.11913573E-03
9	18	0.97794720E-04	0.12596929E-03
9	26	0.10352240E-03	0.13348830E-03
9	34	0.10964576E-03	0.14150140E-03
9	42	0.11591840E-03	0.14962415E-03
9	50	0.12199346E-03	0.15736838E-03
9	58	0.12754052E-03	0.16434159E-03
9	66	0.13235406E-03	0.17034616E-03
TIME	DIST	YY	XX
17	2	0.68792054E-04	0.92915419E-04
17	10	0.82894315E-04	0.11157985E-03
17	18	0.96808769E-04	0.12240345E-03
17	26	0.10240455E-03	0.12961160E-03
17	34	0.10849460E-03	0.13735272E-03
17	42	0.11488803E-03	0.14531166E-03
17	50	0.12126772E-03	0.15304015E-03
17	58	0.12727319E-03	0.16012452E-03
17	66	0.13262818E-03	0.16630978E-03
TIME	DIST	YY	XX
25	2	0.68246532E-04	0.87982232E-04
25	10	0.77659584E-04	0.10401418E-03
25	18	0.90857429E-04	0.11795807E-03
25	26	0.10033013E-03	0.12664177E-03
25	34	0.10623588E-03	0.13416642E-03
25	42	0.11252875E-03	0.14202877E-03
25	50	0.11893963E-03	0.14983115E-03
25	58	0.12512303E-03	0.15714804E-03
25	66	0.13076766E-03	0.16366399E-03
TIME	DIST	YY	XX
33	2	0.67988512E-04	0.85530467E-04
33	10	0.74058494E-04	0.97730473E-04
33	18	0.85674648E-04	0.11236678E-03
33	26	0.96417192E-04	0.12318272E-03
33	34	0.10391523E-03	0.13116960E-03
33	42	0.11005749E-03	0.13889844E-03
33	50	0.11642541E-03	0.14672322E-03
33	58	0.12270290E-03	0.15422986E-03
33	66	0.12856489E-03	0.16105951E-03

TIME	DIST	YY	XX
41	2	0.67866436E-04	0.84317493E-04
41	10	0.71679678E-04	0.92970425E-04
41	18	0.81123667E-04	0.10657479E-03
41	26	0.92150483E-04	0.11886841E-03
41	34	0.10089485E-03	0.12800579E-03
41	42	0.10762675E-03	0.13583490E-03
41	50	0.11390646E-03	0.14362232E-03
41	58	0.12022069E-03	0.15125498E-03
41	66	0.12624782E-03	0.15835222E-03

TIME	DIST	YY	XX
49	2	0.67808679E-04	0.83719714E-04
49	10	0.70155030E-04	0.89575070E-04
49	18	0.77419157E-04	0.10121845E-03
49	26	0.87790918E-04	0.11398699E-03
49	34	0.97416341E-04	0.12437419E-03
49	42	0.10494661E-03	0.13273594E-03
49	50	0.11141946E-03	0.14053792E-03
49	58	0.11772070E-03	0.14823236E-03
49	66	0.12386180E-03	0.15554161E-03

TIME	DIST	YY	XX
57	2	0.67781351E-04	0.83426159E-04
57	10	0.69200759E-04	0.87255335E-04
57	18	0.74556635E-04	0.96636242E-04
57	26	0.83702296E-04	0.10893530E-03
57	34	0.93599272E-04	0.12024865E-03
57	42	0.10195519E-03	0.12941926E-03
57	50	0.10885274E-03	0.13744924E-03
57	58	0.11522525E-03	0.14518536E-03
57	66	0.12143014E-03	0.15264736E-03

TIME	DIST	YY	XX
65	2	0.67768603E-04	0.83280901E-04
65	10	0.68614914E-04	0.85721636E-04
65	18	0.72435097E-04	0.92937800E-04
65	26	0.80097044E-04	0.10407883E-03
65	34	0.89684210E-04	0.11576324E-03
65	42	0.98638847E-04	0.12577946E-03
65	50	0.10611679E-03	0.13426751E-03
65	58	0.11270112E-03	0.14212242E-03
65	66	0.11897302E-03	0.14969257E-03

YTP1 0.11409E-03 YT2 0.10888E-03

TIME	DIST	YY	XX
1	2	0.10205766E-03	0.13061671E-03
1	10	0.94259943E-04	0.12121935E-03
1	18	0.86007494E-04	0.11101626E-03
1	26	0.78275966E-04	0.10091212E-03
1	34	0.72332521E-04	0.92496673E-04
1	42	0.68852721E-04	0.87040214E-04
1	50	0.67432236E-04	0.84516374E-04
1	58	0.67087574E-04	0.83799459E-04
1	66	0.67054075E-04	0.83712424E-04

TIME	DIST	YY	XX
9	2	0.10781037E-03	0.13769932E-03
9	10	0.94805131E-04	0.12683225E-03
9	18	0.87532505E-04	0.11619159E-03
9	26	0.79856613E-04	0.10563582E-03
9	34	0.72694339E-04	0.96809540E-04
9	42	0.67221044E-04	0.91044916E-04
9	50	0.64039675E-04	0.88342916E-04
9	58	0.62753766E-04	0.87552863E-04
9	66	0.62446561E-04	0.87448017E-04

TIME	DIST	YY	XX
17	2	0.10791607E-03	0.14415404E-03
17	10	0.10005494E-03	0.13278266E-03
17	18	0.88566026E-04	0.12108970E-03
17	26	0.81613150E-04	0.11021624E-03
17	34	0.74442359E-04	0.10091477E-03
17	42	0.67960339E-04	0.94586925E-04
17	50	0.63171843E-04	0.91395922E-04
17	58	0.60479796E-04	0.90312460E-04
17	66	0.59424914E-04	0.90096771E-04
TIME	DIST	YY	XX
25	2	0.10801110E-03	0.14997918E-03
25	10	0.10083141E-03	0.13833777E-03
25	18	0.93317124E-04	0.12631823E-03
25	26	0.82961210E-04	0.11463027E-03
25	34	0.76317941E-04	0.10496183E-03
25	42	0.69766145E-04	0.98032949E-04
25	50	0.64115345E-04	0.94166825E-04
25	58	0.60106031E-04	0.92553833E-04
25	66	0.57917481E-04	0.92056186E-04
TIME	DIST	YY	XX
33	2	0.10809673E-03	0.15523653E-03
33	10	0.10154935E-03	0.14347456E-03
33	18	0.94533970E-04	0.13129832E-03
33	26	0.87253050E-04	0.11934867E-03
33	34	0.77859120E-04	0.10892506E-03
33	42	0.71668982E-04	0.10149188E-03
33	50	0.65887856E-04	0.96930554E-04
33	58	0.61124243E-04	0.94643371E-04
33	66	0.57847326E-04	0.93675291E-04
TIME	DIST	YY	XX
41	2	0.10817389E-03	0.15998144E-03
41	10	0.10218541E-03	0.14822277E-03
41	18	0.95657451E-04	0.13599817E-03
41	26	0.88758722E-04	0.12391616E-03
41	34	0.81735997E-04	0.11316942E-03
41	42	0.73304952E-04	0.10493732E-03
41	50	0.67740678E-04	0.99765398E-04
41	58	0.62793886E-04	0.96787844E-04
41	66	0.58852994E-04	0.95229537E-04
TIME	DIST	YY	XX
49	2	0.10824340E-03	0.16426379E-03
49	10	0.10277491E-03	0.15261030E-03
49	18	0.96694973E-04	0.14042911E-03
49	26	0.90164787E-04	0.12829856E-03
49	34	0.83421415E-04	0.11733707E-03
49	42	0.76799085E-04	0.10865161E-03
49	50	0.69386936E-04	0.10264556E-03
49	58	0.64536885E-04	0.99044191E-04
49	66	0.60376725E-04	0.96875010E-04
TIME	DIST	YY	XX
57	2	0.10830605E-03	0.16812864E-03
57	10	0.10331281E-03	0.15666320E-03
57	18	0.97652911E-04	0.14460257E-03
57	26	0.91477675E-04	0.13249635E-03
57	34	0.85012041E-04	0.12139407E-03
57	42	0.78574696E-04	0.11235299E-03
57	50	0.72517053E-04	0.10578900E-03
57	58	0.66126391E-04	0.10138810E-03
57	66	0.61972328E-04	0.98653516E-04
TIME	DIST	YY	XX
65	2	0.10836251E-03	0.17161669E-03
65	10	0.10380356E-03	0.16040578E-03
65	18	0.98537188E-04	0.14853002E-03
65	26	0.92703077E-04	0.13651109E-03
65	34	0.86512489E-04	0.12533415E-03
65	42	0.80267345E-04	0.11600865E-03
65	50	0.74305324E-04	0.10897359E-03
65	58	0.68906418E-04	0.10398826E-03
65	66	0.63459781E-04	0.10054404E-03

M S YTP2 0.11410E-03 YAP2 0.65782E-0

EXHIBIT D

M	YTP2	YBP2
1	0.10000E-03	0.82006E-04
2	0.11095E-03	0.74664E-04
3	0.11449E-03	0.70446E-04
4	0.11478E-03	0.67707E-04
5	0.11410E-03	0.65782E-04
6	0.11325E-03	0.64368E-04
7	0.11248E-03	0.63304E-04
8	0.11185E-03	0.62496E-04
9	0.11135E-03	0.61877E-04
10	0.11096E-03	0.61404E-04
11	0.11065E-03	0.61040E-04
12	0.11042E-03	0.60761E-04
13	0.11024E-03	0.60546E-04
14	0.11011E-03	0.60382E-04
15	0.11000E-03	0.60259E-04
16	0.10992E-03	0.60158E-04
17	0.10986E-03	0.60083E-04
18	0.10981E-03	0.60026E-04
19	0.10977E-03	0.59982E-04
20	0.10975E-03	0.59948E-04
21	0.10972E-03	0.59922E-04
22	0.10971E-03	0.59902E-04
23	0.10969E-03	0.59887E-04
24	0.10968E-03	0.59875E-04
25	0.10968E-03	0.59866E-04

APPENDIX II

THE EQUILIBRIUM THEORY MODEL

In liquid-solid systems characterized by relatively rapid mass transfer rates the approximation is made that the fluid and solid phases respond to temperature changes in the system such that local fluid solid equilibrium is instantaneously attained everywhere in the adsorbing column. Under these conditions solute moves axially within the column in sharply defined wave fronts. An equation predicting the solute concentration along these fronts is obtained in a relatively simple analytical fashion for systems with linear isotherms. The method is presented in detail elsewhere.[2,5] In summary fashion, however, the method is as follows.

The equation of continuity for the liquid-solid adsorbant system is given by (15) with same conditions holding as in the previous treatment i.e.,

$$\varepsilon v \frac{\partial y}{\partial z} + \varepsilon \frac{\partial y}{\partial t} + (1-\varepsilon) \rho_s \frac{\partial x}{\partial t} = 0. \qquad (15)$$

the assumption of local fluid-solid equilibrium means that (17) is always true, or

$$y = \frac{x}{M}, \qquad (A-1)$$

where M is a function of temperature, which is, in turn, a function of time. Equation (A-1) is solved for x, differentiated with respect to time and substituted into (15) to yield

$$(1+m)\frac{\partial y}{\partial t} + v\frac{\partial y}{\partial z} + \frac{\partial m}{\partial T}\frac{\partial T}{\partial t}\, y = 0 \qquad \text{(A-2)}$$

where

$$m = \frac{(1-\varepsilon)\,\rho_s}{\varepsilon}\, M. \qquad \text{(A-3)}$$

The time dependent parameters in (A-2) are given as square wave functions (sq), i.e.,

$$T = T_o + \tau sq\ (\omega t) \qquad \text{(A-5)}$$

$$M = M_o - asq\ (\omega t) \qquad \text{(A-6)}$$

$$v = v_o - v_o \phi_B sq\ (\omega t) \qquad \text{(A-7)}$$

where for $(n-1)\ \pi/\omega < t \leq n\pi/\omega$, $sq(\omega t)=1$, and for $n\pi/\omega < ts\ (n+1)\ \pi/\omega$, $sq(\omega t)= -1$ for all integers $n>0$. Characteristic lines in the z-t plane are chosen such that, for upflow,

$$\frac{dz}{dt} = \frac{V_o(1-\phi_B),}{(1+m_o)\ (1-b)} \qquad \text{(A-8)}$$

and, for downflow,

$$\frac{dz}{dt} = \frac{V_o(1+\phi_B)}{(1+m_o)\ (1+b)} \qquad \text{(A-9)}$$

where

$$b = \frac{a}{1+m_o} \quad . \qquad \text{(A-10}$$

Along these characteristics, then, (A-2) becomes

$$\frac{dy}{y} = \frac{d\,[1-bsq\ (\omega t)]}{1-b\ sq\ (\omega t)} \qquad A-11)$$

or, upon integration

$$y\,[1-b\ sq\ (\omega t)] = C \qquad (A-12)$$

C being the constant of integration. For the hot half-cycle to cold half-cycle transition, then, along any concentration front whose position is defined by (A-9),

$$\frac{y_{2,n}}{y_{1,n}} = \frac{1-b}{1+b} \qquad (A-13)$$

and, for the cold half-cycle to hot half-cycle transition, along fronts whose position is defined by (A-8),

$$\frac{y_{1,n+1}}{y_{2,n}} = \frac{1+b}{1-b} \qquad (A-14)$$

For a half-cycle of duration τ, the position of the concentration wave fronts are given by integrating (A-8) and (A-9) to obtain

$$L_1 = \frac{v_o\ (1-\phi_B)\tau}{(1-b)\ (1+m_o)} \qquad (A-15)$$

$$L_2 = \frac{v_o\ (1+\phi_B)\tau}{(1+b)\ (1+m_o)}\ , \qquad (A-16)$$

for upflow and downflow, respectively.

Chen and Hill[2] have shown that there are three possible regions for operation of the continuous parametric pump based on the relative

lengths of axial concentration front traversal and column length. These regions are pictured on Figure A-1 and are defined by

a. Region I, $L_2 \leq L_1$, $L_1 \leq h$ (A-17)

b. Region II, $L_1 < L_2$, $L_1 \leq h$ (A-18)

c. Region III, $L_1 > h$ $L_2 > h$. (A-19)

It has also been shown that a different set of equations predict parametric pump performance in each of the three regions. These equations, which combine (A-13) and (A-14) with the external mass balance equations, (8) - (12), are given elsewhere,[2,5] and yield the typical performance curves shown in Figure A-2.

Figure contains a semi-logarithmic plot of cold half-cycle bottom product concentration versus number of cycles and a linear plot of cold half-cycle top oroduct concentrations with cycle number. Of primary interest are the bottom product concentration curves since their characteristic shape changes most drastically from region to region. In Region I the bottom product concentration is a monotonically decreasing function of cycle number. In fact, for linear isotherms and equilibrium operation in Region I,

$$\lim_{n \to \infty} \frac{y_{BP2\ n}}{y_o} = 0 \qquad \text{(A-20)}$$

i.e., "perfect separation," or complete removal of solute from the lean product stream is possible. Region III separations are severely limited when compared to Region I and the characteristic shape of

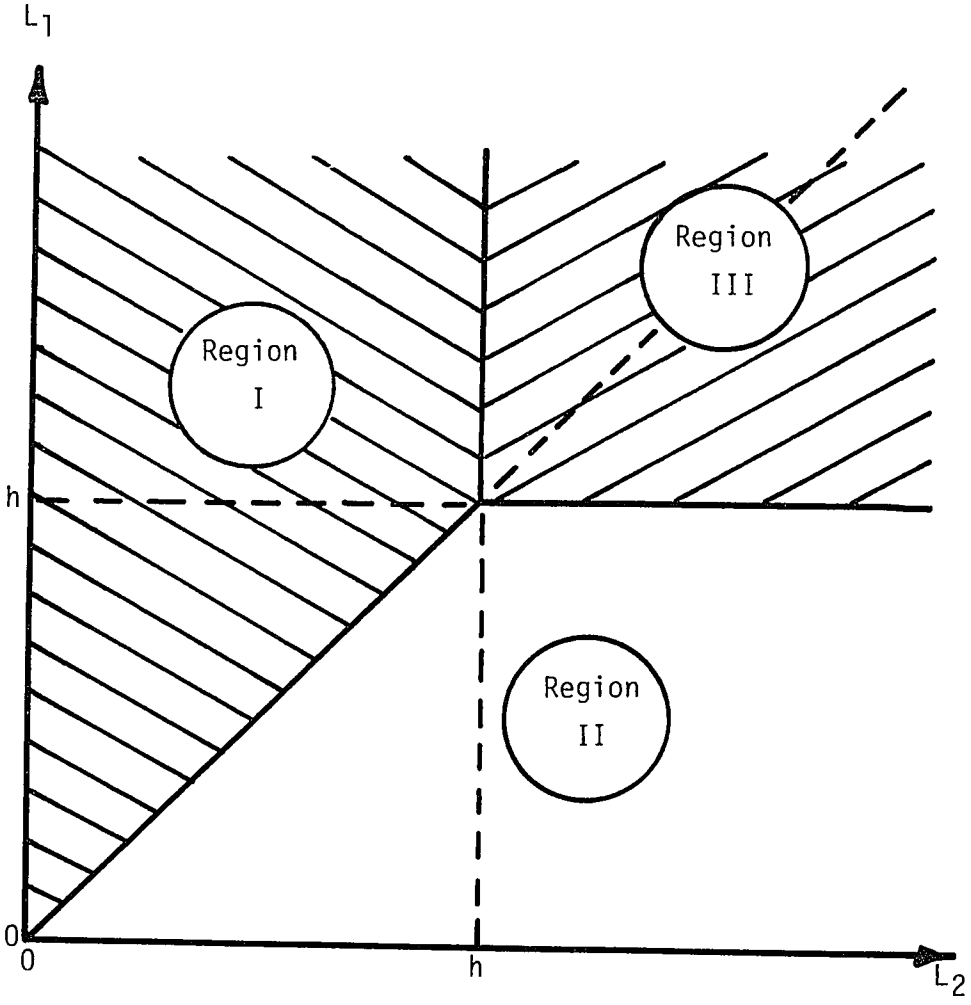

FIGURE A-1 - REGIONS OF OPERATION FOR THE CONTINUOUS PARAMETRIC PUMP

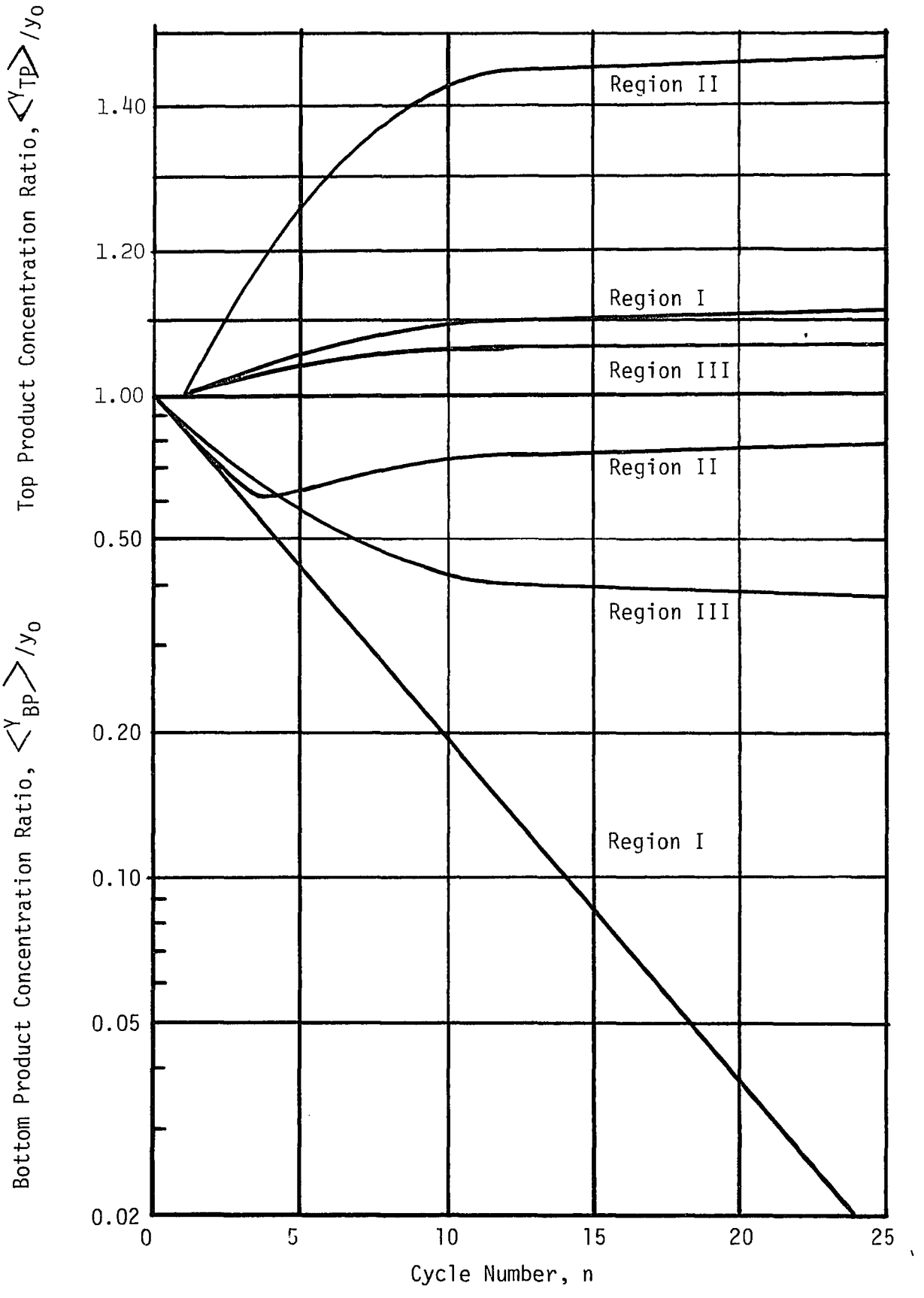

FIGURE A-2 - TYPICAL EQUILIBRIUM PARAMETRIC PUMP PERFORMANCE CURVES

the curve is a function that decreases quickly to a nearly constant separation after a few cycles of operation. For Region II, however, a distinct minimum in bottom product concentration appears at a theoretically predictable point. The appearance of this minimum is directly related to concentration front penetration length in the following manner.

Regardless of region of operation, the liquid phase concentration adjustments taking place within the adsorbant bed during any complete cycle of operation are given by (A-13) and (A-14). The solution of the internal equations makes no assumption about mode of operation of the parametric pump. It merely quantifies the individual adsorptive capacity of the solid particles, and for any temperature change within the solid bed, the change in adsorptive capacity is rendered by the parameter, b, which is a measure of the difference between the two temperature dependent equilibrium states.

The adsorptive capacity of the entire solid bed is given by the penetration length. When compared with column height, h, the penetration length is a direct measure of the extent to which the solid bed is saturated with solute at the given temperature. If the extent of saturation on the adsorptive cold half-cycle (L_2) is exceeded by the extent of saturation on the desorptive hot half-cycle (L_1), there is a net minus accumulation of solute in the bed and a net movement of solute towards the concentrated end of the column (Region I). If, however, the reverse is true; the extent of saturation

on the cold cycle (L_2) exceeds the extent of saturation on the hot half-cycle (L_1), a net positive accumulation of solute in the bed results and there is a net movement of solute towards the lean end of the column (Region II).

More simply stated, in Region I solute loading of the adsorptive bed during the cold half-cycle is exceeded by column regeneration capacity during the hot half-cycle. In Region II, solute loading during the cold half-cycle exceeds column regenerative capacity in the hot half-cycle.

For a given temperature difference between the cold and hot half-cycles, then, the column loading during the cold half-cycle is increased by increasing the rate of bottom product withdrawal. Here L_1 decreases and L_2 increases via (A-15) and (A-16). When $\phi_B > b$, $L_2 > L_1$ and the transition from Region I to Region II is reached. Increasing ϕ_B to the point where $\phi_B > b$ has increased column loading beyond the column's regenerative capacity.

When column length is reduced to the point where the entire column is saturated with solute on the cold half-cycle, break through of solute from one end of the column to the other has been achieved. At this point, regardless of regenerative capacity in the hot half-cycle, separation of solute to the opposite ends of the column has been disrupted and limited separation result. This describes operation in Region III.

APPENDIX III

DETERMINATION OF MASS TRANSFER COEFFICIENTS

A. Theory

The equation of continuity for a column of solid adsorbant in contact with a solution containing one adsorbable solute in an inert solvent is given by (15),

$$v \frac{\partial y}{\partial z} + \frac{\partial y}{\partial t} + \frac{1-\varepsilon}{\varepsilon} \rho_s \frac{\partial x}{\partial t} = 0 \qquad (15)$$

Some appropriate initial and boundary conditions that apply to the experiments described in this Appendix are:

a. At 5°C, at $t=0$, $z>0$, $y=y_o = 0$

at $t=0$, $z>0$, $x=x_o = 0$

at $t>0$, $z=0$, $y=y_F$

b. At 70°C, at $t=0$, $z>0$, $y=y_o = y_F$

at $t=0$, $z>0$, $x=x_o = y_F/M_2$

at $t>0$, $z=0$, $y=y_F$.

If, at some time, t, breakthrough of the solute is achieved at the discharge end of the adsorbant column (axial distance h), a continuous axial concentration gradient is established, which changes with time. For sufficiently short columns at times not near the initial

breakthrough or final saturation of the column, this gradient is approximately linear and is given by

$$\frac{\partial y}{\partial z} \approx \frac{\Delta y}{\Delta} = \frac{y_h - y_F}{h} \tag{A-21}$$

The breakthrough curve during either an adsorption process or desorption process having the initial conditions described above has the general appearance shown in Figure A-3. A time t, shown on Figure A-3, the shape of the breakthrough curve can be approximated by an appropriate numerical method, in our case a five-point formula

$$\frac{\partial y}{\partial t} \approx \frac{\Delta y}{\Delta t} \tag{A-22}$$

So, combining (A-22) and (A-21 with (15) gives an expression for the rate of interphase mass transfer at time t and axial distance h where the expressions on the right-hand side of the equation may be obtained from experimental data of Y_h vs. t, to wit,

$$\frac{\partial x}{\partial t} = \frac{-v \frac{\Delta y}{\Delta z} - \frac{\Delta y}{\Delta t}}{\left(\frac{1-\varepsilon}{\varepsilon}\right) \rho_s} \tag{A-23}$$

Now, the equation relading the rate of interphase mass transfer to resistance, λ, and a driving force, is given by (19) for linear adsorption isotherms

$$\frac{\partial x}{\partial t} = \lambda \left(y - \frac{x}{M}\right) \tag{19}$$

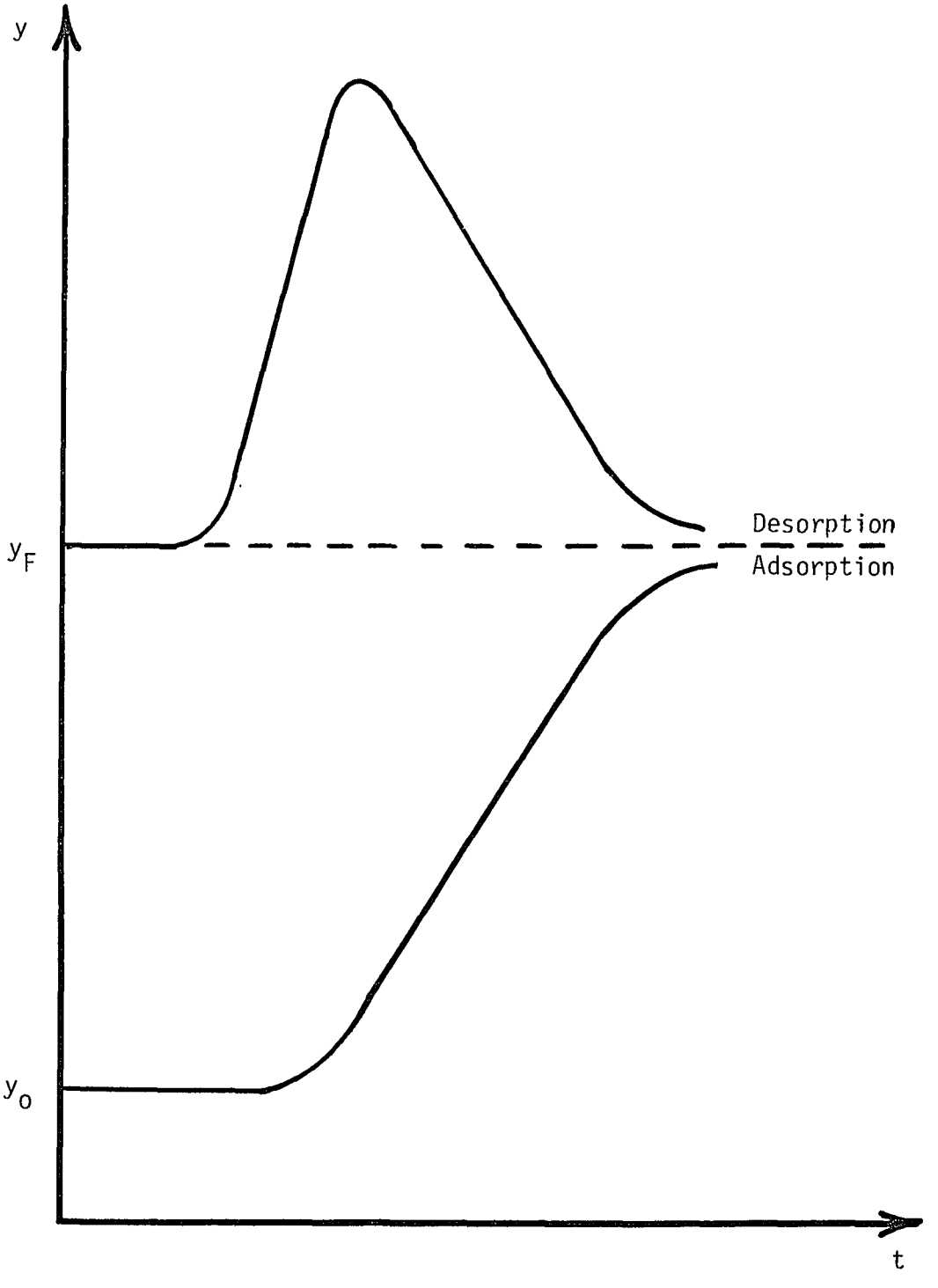

FIGURE A-3 - TYPICAL BREAKTHROUGH CURVES FOR ADSORPTION EXPERIMENTS.

Knowing, $\frac{\partial x}{\partial t}$ at axial distance h vs. time allows as to calculate x at any time by numerical integration, i.e.

$$x \approx x_o + \int \left(\frac{\partial x}{\partial t}\right) \tag{A-24}$$

where the symbol I indicates a Simpson's rule integration. Combining (A-24) and (A-23) with (19) gives

$$\lambda = \frac{-v \frac{\Delta y}{\Delta z} - \frac{\Delta y}{\Delta t}}{\left(\frac{1-\varepsilon}{\varepsilon}\right) \rho_s \left[y - \left(xo + \int \left(\frac{\partial x}{\partial t}\right) \right) \Big/ M \right]} \tag{A-25}$$

where all the terms on the right-hand side of the equality are available from experimental data.

B. Experimental Method and Results

A 1.0 cm diameter by 10.0 cm long column of BioRad AG11A8 ion retardation resin at the initial conditions given above was fed with 0.1M aqueous MaCl solution at a given constant flow rate. Column temperature was maintained by the jacket fluid. Effluent solution was collected in 1.0 cm^3 fractions and analyzed by electrical conductivity for NaCl content to yield breakthrough curves similar to Figure A-3.

The experimental data are given on Tables A-1 and A-2. Two experiments were conducted, one at 5°C and the other at 70°C. Gregory[12] reports an exponent of 0.3 for the velocity dependence.

Numerically extrapolating the calculated λ to the logarithmic intercept, using a slope of 0.30 gives values for β, as illustrated on Figure A-4, so that

at 5°C, $$\lambda_2 = 0.0736\ v_2^{0.30} \quad , \qquad \text{(A-26)}$$

and, at 70°C, $$\lambda_1 = 0.3280\ v_1^{0.30} \qquad \text{(A-27)}$$

TABLE A-2

BREAKTHROUGH DATA AT 5°C

$y_o = 0$ $y_F = 0.10$ mole/l $x_o = 0$ t in min., y in mole/l.

v = 2.00 ft/sec. h = 11.70 cm

Volume Displaced (cm^3)	Time, t (min.)	Concentration, y (mole/l)
1.00	1.67	.0680
2.00	3.25	.0157
3.00	4.83	.0081
4.00	6.68	.0048
5.00	8.26	.0022
6.00	10.01	.0070
7.00	11.68	.0190
8.00	13.35	.0294
9.00	15.10	.0376
10.00	16.68	.0478
11.00	18.26	.0624
12.00	20.01	.0616
13.00	21.84	.0676
14.00	23.42	.0584
15.00	25.17	.0680
16.00	26.92	.0688

TABLE A-3

BREAKTHROUGH DATA AT 70°C

$y_F = y_o = 0.100$ mole/l $x_o = 0.054$ mole/gm t in min., y in mole/l

v = 2.15 ft/sec. h = 10.0 cm

Volume Displaced (cm^3)	Time, t (min.)	Concentration, y (mole/l)
1.00	1.50	.070
2.00	2.98	.086
3.00	4.49	.098
4.00	5.95	.101
5.00	7.43	.104
6.00	8.97	.121
7.00	10.49	.137
8.00	12.00	.153
9.00	13.50	.159
10.00	15.06	.159
11.00	16.57	.155
12.00	18.10	.153

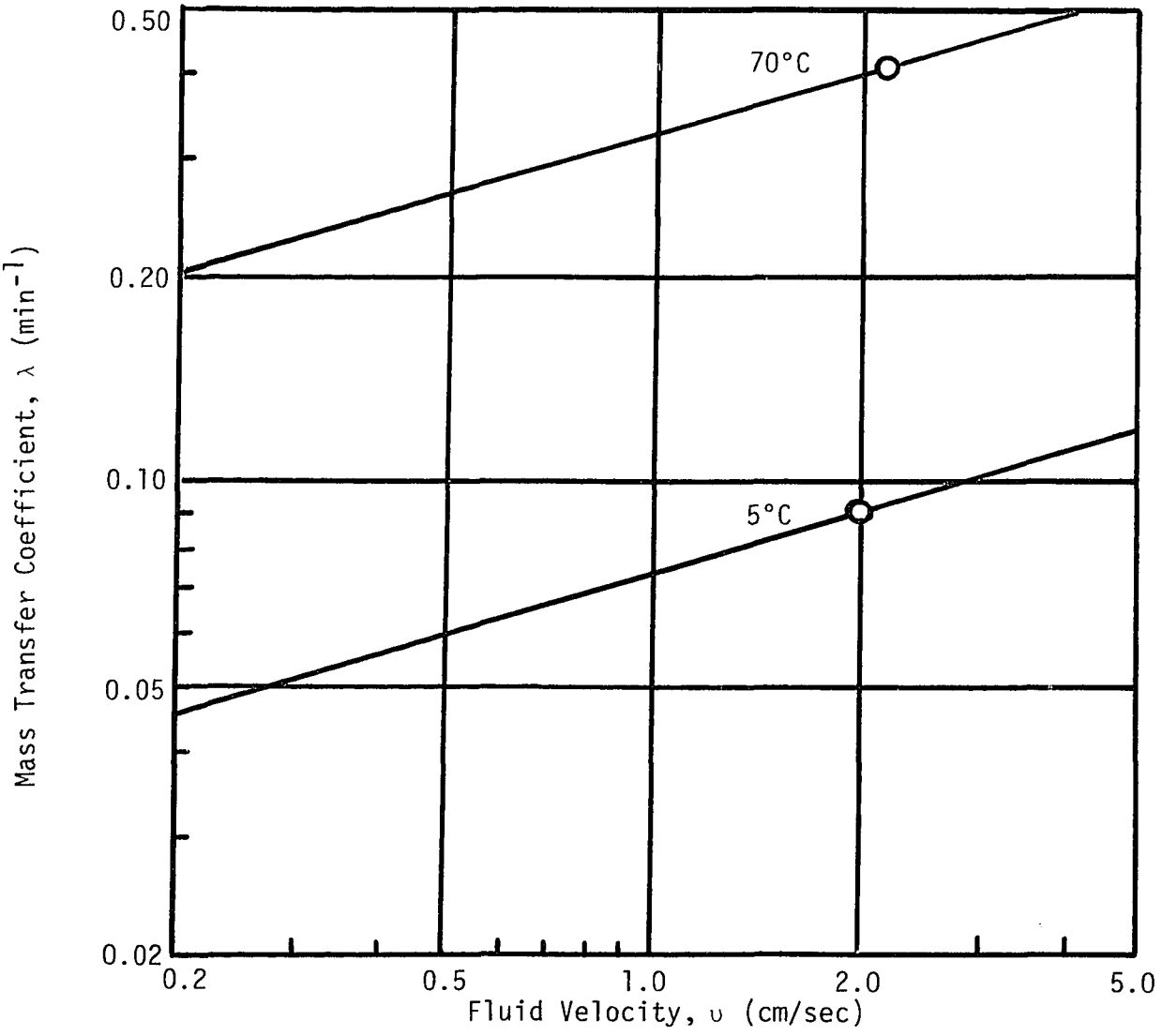

FIGURE A-4 - DEPENDENCE OF λ ON TEMPERATURE AND FLUID VELOCITY.

APPENDIX IV

ASPECTS OF PRELIMINARY DESIGN AND ECONOMICS

A. Preliminary Design of A Desalination Unit

The principal application of continuous parametric pumping for the experimental system studied here is desalination of brackish water for human consumption. From the data reported earlier, it is clear that near-equilibrium conditions are required to obtain separations sufficient to reduce the NaCl content of brackish water (p.1-0.3M NaCl) to potable water (0.0001M NaCl), a separation factor of 1000-3000. Non-equilibrium operation of the type studied here yields separation factors of 2-4, well below the required separation. Accordingly, the following aspects of preliminary process design and economic analysis will be based on equilibrium operation.

The basis for the design must, of course, be the capacity of the desalination unit, W_{BP}, in gal./day. Of particular interest are the uncontrolled variables, brackish water concentration (Y_o, molarity) and temperature, (T_o,°C). Controlled variables that depend on the specific physical characteristics of the liquid solid system are operating temperatures and half-cycle time.

Experimental determination of the parameters b and m_o for the liquid-solid system, which depend on the slopes of the adsorption isotherms of the operating temperatures, is required. These

temperatures are limited by the stability of the adsorbant. The contact time required for approach to equilibrium must also be determined and this is a strong function of the cold half-cycle temperature, where the rate of interphase mass transfer is slowest. These parameters provide the basis for preliminary process design and are manipulated as shown below.

The principles of the design and economic analysis will be treated in general but will be applied to a specific case during the treatment for purposes of illustration. Single desalination units yielding 100,000 gal./day or more of fresh water are typical. Assume a brackish water feed 0.30M in NaCl is available for treatment. The temperatures cited in this study, namely, 5°C and 70°C, for which b = 0.137 and m_o = 1.9375, will be used. The data on Figure 11 indicate that a four-hour half-cycle will insure a fairly close approach to equilibrium conditions.

For operation in equilibrium Region I, where complete removal of NaCl from the brackish water is possible, we require that $\phi_B < b$ from equations (77) - (79). A "safe" value of ϕ_B is chosen, e.g., ϕ_B = 0.125 vs. b = 0.137, and design may proceed.

Sizing major items of process equipment is accomplished in the following manner. Using flows in gal./hr., neglecting density effects, the reservoir rate is determined by

$$Q = \frac{W_{BP}}{\phi_B} \qquad \text{(A-28)}$$

For our example

$$Q = \frac{4167 \text{ gal./hr.}}{0.125} = 33{,}376 \text{ gal./hr.}$$

The reservoirs must be capable of holding the flow for an entire half-cycle plus the dead volume. Thus, if V_R is the reservoir volume,

$$V_R = (1+C_B)\frac{W_{BP}}{\phi_B}\tau \qquad \text{(A-29)}$$

For our example, we assume a 5% dead volume, and

$$V_R = \frac{(1.05)\ (4167)\ (4)}{(0.12)} = 145{,}833 \text{ gal.}$$

To further insure that Region I operation obtains, from equation (A-17), $L_1 \leq h$, or

$$h = \frac{v_o(1-\phi_B)\tau}{(1-b)\ (1+m_o)} \qquad \text{(A-30)}$$

Multiplying through by the cross-sectional area for reservoir flow, A, the colume volume, V_{COL}, is given by

$$V_{COL} = Ah = \frac{A_{vo}(1-\phi_B)\tau}{(1-b)\ (1+m_o)} \qquad \text{(A-31)}$$

or,

$$V_{COL} = \frac{Q(1-\phi_B)\tau}{\varepsilon(1-b)\ (1+m_o)} \qquad \text{(A-32)}$$

For our example,

$$V_{COL} = \frac{(33376)\ (1-0.125)\ (4)}{(0.38)\ (1-0.137)\ (1+1.9375}$$

$$= 120{,}704 \text{ gal.} = 16{,}113 \text{ ft}^3 .$$

Now, the particular configuration of the adsorbant bed becomes important. Fluid flow in the bed is laminar, limiting heat transfer rates for inter-half-cycle heating and cooling. Clearly, a jacketed bed of the type treated in the experimental section of this work is inappropriate, assuming relatively large bed diameters will be required. The bed must then be confined to relatively small tubes encased in a shell to contain the heating and cooling media, much like a shell and tube fixed bed reactor. The tubes must be of a diameter and length such that

a. The bed volume is V_{COL}

b. The heat transfer area is sufficient to provide inter-half-cycle heating and cooling in a small fraction of the half-cycle time, τ.

c. The heat transfer area is sufficient to provide the appropriate amount of heating or cooling during the remainder of the half-cycle.

d. The configuration of the unit is optimum, or, for preliminary design, is at least reasonable.

Satisfying criteria b and c, above, requires energy balances and, hence, some consideration of energy efficiency. The inter-half-cycle energy requirement is that the entire contents of the adsorbent bed (liquid plus solid) undergo temperature change $\pm (T_1-T_2)$. Clearly, we have at our disposal a large heat source/sink in the body of brackish water at To from which we draw our feed to the unit. We can, therefore, approach To in the column from either T_1 or T_2 during the beginning of each half-cycle by using the brackish water as the auxiliary fluid. Then, continued heating or cooling is provided by combustion or refrigeration, respectively, in hot and cold auxiliary fluid reservoirs. Figures A-5 and A-6 show the process flows during the various phases of operating for both hot and cold half-cycles, respectively.

The tube size is determined by heat transfer requirements during the initial heating or cooling phases of a given half-cycle. For laminar flow inside the tubes,

$$\frac{hD}{k} = 1.62 \left(\frac{4wCp}{\Pi kL}\right)^{1/3}$$

or, rearranging

$$h = 1.62\left(\frac{4wCp}{\Pi kL}\right)^{1/3} \frac{K}{D} . \qquad \text{(A-33)}$$

The energy requirement during any phase of operation is given by

$$q = h(\Pi DL)\Delta T_{\ell m} \qquad \text{(A-34)}$$

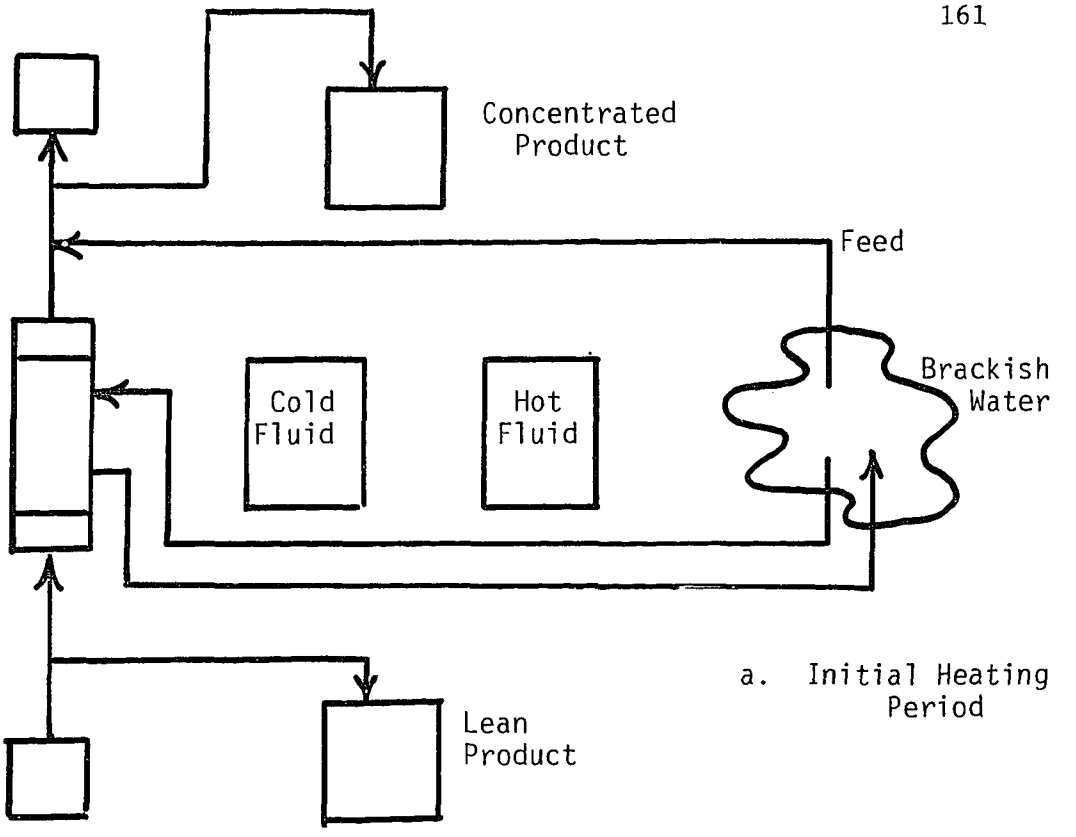

a. Initial Heating Period

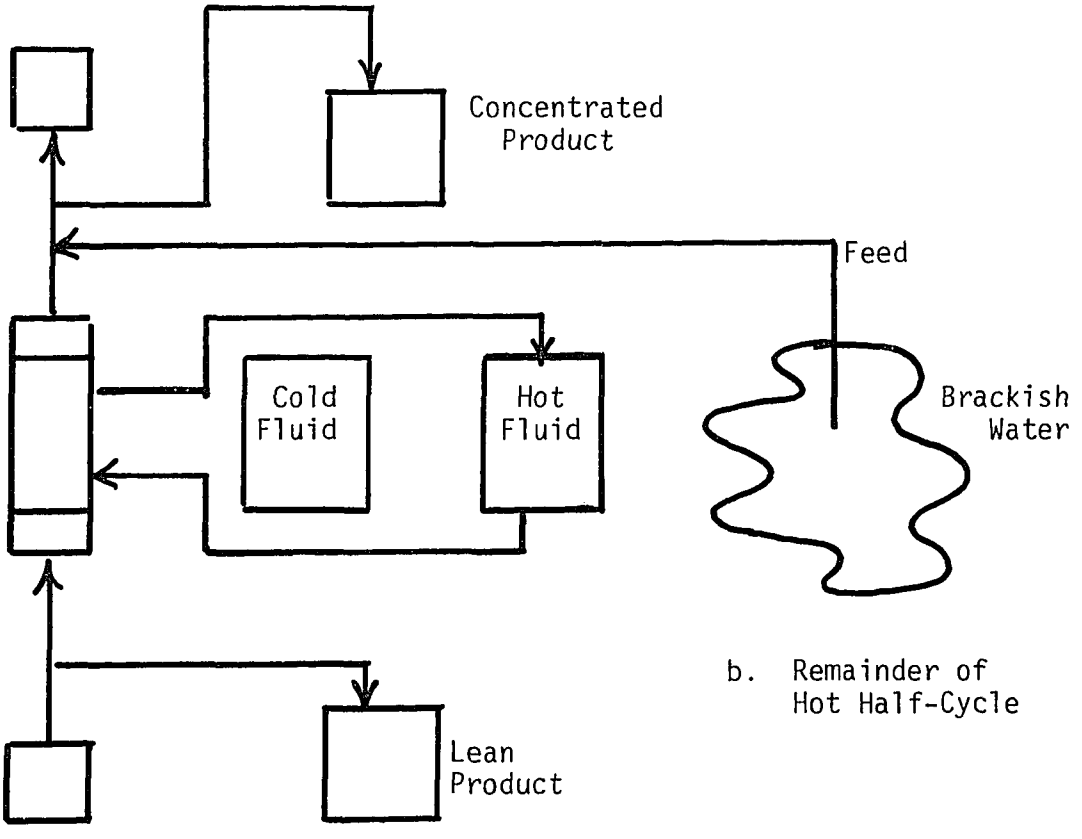

b. Remainder of Hot Half-Cycle

FIGURE A-5 - PROCESS FLOWS, HOT HALF-CYCLE

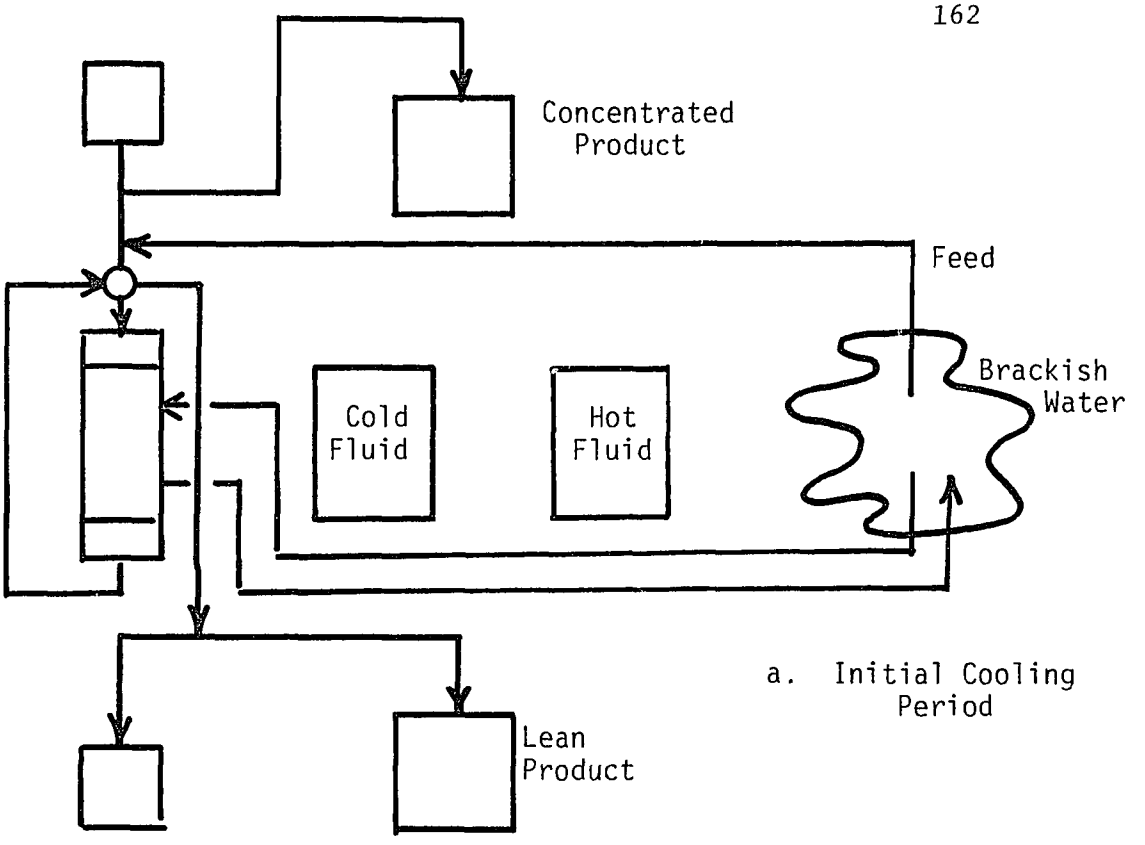

a. Initial Cooling Period

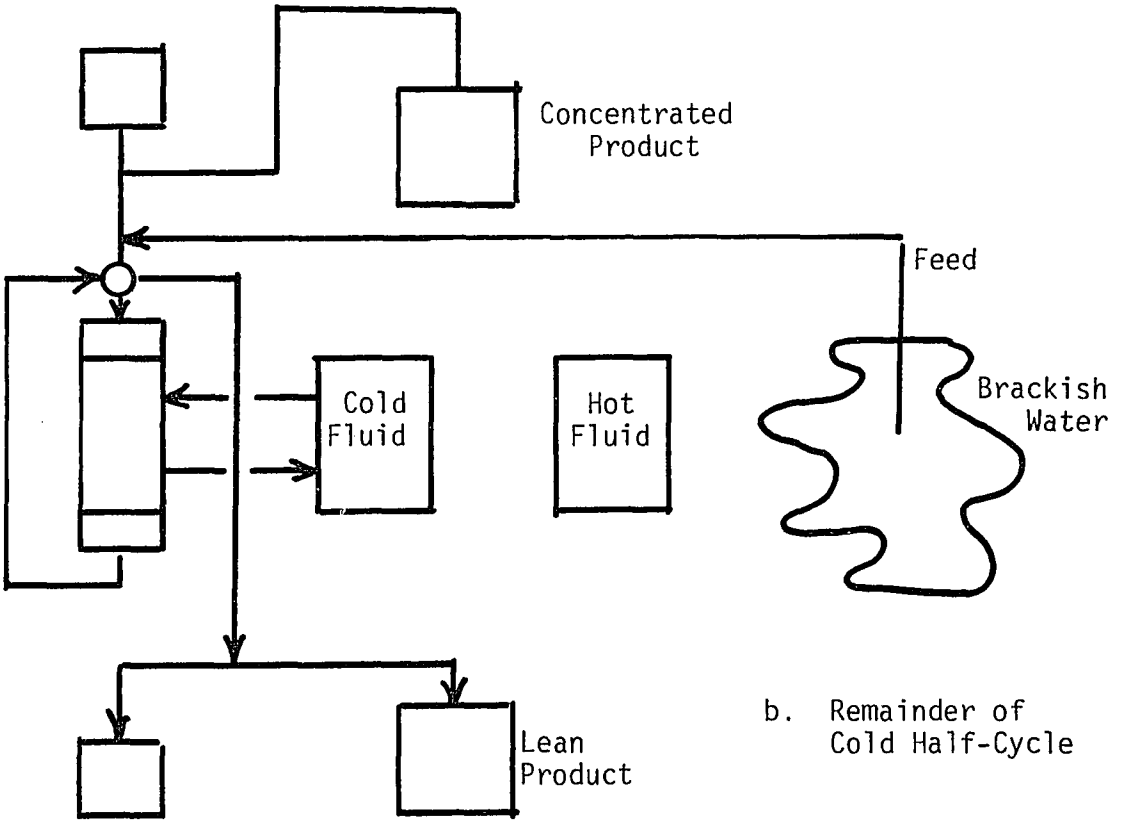

b. Remainder of Cold Half-Cycle

FIGURE A-6 - PROCESS FLOWS, COLD HALF-CYCLE

where the tube-side resistance to heat transfer is assumed to be controlling. Combining (A-33) and (A-34) and eliminating D, we obtain

$$L^{2/3} = \frac{q}{1.62\Pi k \Delta T_{\ell m}} \left(\frac{4wCp}{\Pi k}\right)^{-1/3} \qquad \text{(A-35)}$$

Considering the flowing fluid, the energy requirement is given by

$$q = \rho V_{COL} Cp \frac{\Delta T}{t} \qquad \text{(A-36)}$$

where t is an appropriately small fraction of the total half-cycle time and ΔT is the temperature difference experienced by the column contents. Using (A-35) and (A-36), L and D are calculated for each of the phases of operation, giving the required heat transfer area for each phase of operation. The L and D combination yielding the largest area is chosen for preliminary column design.

Table A-4 illustrates this calculation where, for our example, we choose t=15 minutes and assume hot fluid available at 90°C and cold fluid available at -10°C. We have also assumed a 5°C approach to To of the column contents before changing auxiliary fluid to heated or refrigerated brackish water and that the flow of auxiliary fluid is large enough that its temperature change is small. The required heat transfer area is 527, 497 ft^2 at D=1.466 inches. Letting D=1.5 inches, L=1,343,260 ft.

TABLE A-4

CALCULATION OF TUBE LENGTH AND DIAMETER

BASED ON HEAT TRANSFER REQUIREMENTS

Initial Column Temp. (°C)	Final Column Temp. (°C)	Heat Required (Btu/Hr.)	Temp. of Auxiliary Fluid (°C)	ΔT_{lm}	W (Lb/Hr.)	L (Ft)	D (In.)	Heat Transfer Area (Ft^2)
5	25	40,540,322	30	22.37	243,269	1,060,677	1.67	463,733
25	70	111,485,886	90	68.72	243,269	898,378	1.81	425,703
70	70	6,842,999	90	36.00	243,269	10,042	17.15	45,087
70	35	70,945,564	30	30.29	312,775	1,374.44	1.466	527,497 ←
35	5	60,810,483	-10	49.16	312,775	527,510	2.37	327,301
5	5	2,932,714	-10	27.00	312,775	52,836	7.48	103,467

Selection of shell diameter and column height is a problem in cost optimization. A large number of small-diameter tubes must be arranged and supported in a relatively large diameter shell, so that material and fabrication costs are both important. For the purposes of preliminary design, a trial and error procedure is employed to arrive at a "most reasonable" adsorbant bed configuration

a. For various column lengths, the number of tubes, N_T, is determined by dividing the tube length requirement, L, by the column length, h_{COL}

$$N_T = L/h_{COL} \tag{A-37}$$

b. The flow cross-section for the adsorbant bed is calculated by

$$Acs = \frac{N_T \Pi D^2}{4} \tag{A-38}$$

c. Assuming the tubes take 90% of the column cross-section, leaving about 10% for the thin tube walls and flow of heat transfer fluid in the shell, the total column diameter is given by

$$D_{COL} = \sqrt{N_T D^2 / 0.9} \tag{A-39}$$

For our example, Table A-5 is prepared, giving column diameters for various column lengths, indicating a considerable latitude in choice of column configuration.

It is apparent, however, that shorter column lengths require a very large number of tubes. Longer columns require less tubes but supporting tubes of the lengths suggested in Table A-5 in a column-type arrangement is difficult. Although the laboratory column was oriented vertically, there is no reason to assume that this must be the case in a commercial-size device. Therefore, longer columns oriented horizontally are to be favored, and the 200-foot long column on Table A-5 seems to be an appropriate compromise choice for preliminary process design.

As an additional energy conservation measure, assuming the cost of refrigeration cooling is greater than steam or combustion heating, the thermal energy accumulated in the hot top reservoir will be dissipated by exchange with the cold bottom stream in the manner illustrated on Figure A-6, which is a flow diagram for the process on the cold half-cycle. An energy balance at the feed point during the hot half-cycle yields

$$(1-\phi_T)\ (T_1-T) = (\phi_T+\phi_B)\ (T-To) \qquad (A-40)$$

and for downflow gives

$$(1+\phi_B)\ (T-T') = (\phi_T+\phi_B)\ (T'-To). \qquad (A-41)$$

At the heat exchanger, using an approach temperature difference of ΔT,

$$T'' = T' + \Delta T \qquad (A-42)$$

TABLE A-5

ESTIMATION OF REQUIRED COLUMN DIAMETER

FOR GIVEN COLUMN LENGTHS

Column Length (Ft)	Number of Tubes	Tube Flour Cross-Section (Ft^2)	Column Diameter (Ft)
30	44,775	549.5	27.9
50	26,865	329.7	21.6
80	16,791	206.1	12.1
100	13,433	164.9	15.3
120	11,194	137.4	13.9
150	8,955	109.9	12.5
200	6,717	82.4	10.8
250	5,373	65.9	9.7
300	4,478	55.0	8.8

For our example T = 70°C, To = 30°C, and T will be assumed to be 5°C.

We calculate ϕ_T by a steady state overall material balance on the system, assuming $y_{BP} = 0$ and y_T is fixed.

$$\phi_T = \phi_B \left(\frac{yo}{y_T - yo}\right) \tag{A-43}$$

Assuming $y_T/yo = 1.5$, we have

$$\phi_T = (0.125)\left[\frac{1}{1.5-1}\right] = 0.25$$

so that

$$T = 56.7$$

$$T' = 50.0$$

$$T'' = 55.0$$

During downflow, the energy requirement during the cold half-cycle is

$$q_2 = \rho Q(1+\phi_B)C_p \Delta T_2, \tag{A-44}$$

where, because the tube-side and shell-side flows are equal, ΔT_2 is identical to the temperature difference across the heat exhcanger. For our example,

$q_2 = (8.33)\ (34,772)\ (1+0.125)\ (1.0)\ (5)\ (1.8) = 2,932,714$ btu/hr.

where the 1.8 factor converts °C to °F.

During upflow, the energy requirements for the hot half-cycle is given by

$$q_1 = \rho Q(1-\phi_B)C_p\Delta T \qquad \text{(A-45)}$$

where

$$\Delta T_1 = T_1 - T'' \qquad \text{(A-46)}$$

For our example,

$$q_1 = (8.33)\ (34{,}772)\ (1-0.125)\ (1.0)\ (70-55)\ (1.8) =$$

$$6{,}842{,}999 \text{ btu/hr.}$$

Clearly, from Table A-5, the available heat transfer area is more than enough to maintain adsorbant bed temperature during each half-cycle of operation.

The sum of the energy requirements for both the hot and cold half-cycles that are not provided by the brackish water heat source/sink are used to size the auxiliary fluid reservoirs. In sizing the units, it must be kept in mind that an entire full cycle of operation is available to generate the energy requirements in the auxiliary fluid reservoirs which, in turn, are discharged only over one half-cycle of operation. So that, for our example, the energy requirements H, are calculated from Table A-4 to be,

$$H_2 = 2{,}266{,}917 \text{ btu/hr.}$$

$$H_1 = 6{,}905{,}433 \text{ btu/hr.}$$

Therefore, the refrigeration unit for the cold auxiliary fluid reservoir is sized at 200 tons and the combustion heater for the hot auxiliary fluid reservoir is sized at 7 million btu/hr.

Finally, the heat exchanger at the column top is sized using the energy transfer taking place, a reasonable overall heat-transfer coefficient for that service and a 5°C temperature difference for the driving force, i.e.,

$$A = Q(1+\phi_B)Cp\Delta T_2 / U\Delta T_{lm} \qquad \text{(A-47)}$$

For our example, we assume U = 200 btu/hr-ft^2-°F, and

$$A = \frac{(8.33)\ (34{,}772)\ (1.125)\ (1.0)\ (70-10)\ (1.8)}{(200)\ (5)\ (1.8)}$$

$$= 19{,}551\ ft^2$$

Table A-6 summarizes the preliminary design figures derived for the desalination unit, giving sizes for the major items of equipment.

The above design represents a convenient "unit cell" for parametric pumping desalination design. Larger liquid storage tanks and adsorbant columns are not desirable, so that multiples of the 100,000 gal/day unit described here would be applied to desalination plants into the 1,000,000 gallons/day class.

B. Economic Comparison with Evaporative Desalination

The current method of choice for desalination of brackish water is evaporative desalination, usually in multiple effects. Desalination plants in the 100,000 - 2,000,000 gallons/day range are common. The principal item of cost in evaporative desalination is, of course, energy costs associated with steam consumption for the evaporation. Of primary interest, then, in cost consideration for these plants is the "steam economy" expressed as lb. water evaporated per lb. of purchased steam feed to the highest-temperature evaporator in the multiple-effect system. Energy costs for the evaporation on a dollar per gallon basis are given by

$$C_E = \frac{8.33 c_3 \lambda}{S}$$

On the other hand, for the parametric pumping unit, using the same cost basis, energy costs are given by

$$Cpp = \frac{c_2 H_2 + c_1 H_1}{2 W_{BP}}$$

For this analysis we assign a unit cost to combustion energy, i.e., assume combustion using fuel oil costs one unit per btu. Then other costs are given by

c_1 = combustion costs = 1.0 unit/btu

c_2 = refrigeration costs = 3.0 units/btu

c_3 = steam costs = 1.25 units/btu.

TABLE A-6

ESTIMATE OF EQUIPMENT SIZES FOR 100,000 GAL/DAY

PARAMETRIC PUMPING DESALINATION UNIT

Item	Quantity	Description	Size
1	2	Storage Tanks, Fresh Water or Brine	150,000 gal.
2	1	Adsorbant Bed, Shell and Tube	10.8 ft. ID by 200 ft. long with 6750 1.5" tubes
3	2	Reservoir Pumps, Centrifugal	80 gpm
4	3	Auxiliary Fluid Pumps, Centrifugal	500 gpm
5	1	Feed Pump, Centrifugal	30 gpm
6	1	Shell and Tube Heat Exhcanger	19,500 $ft.^2$
7	1	Combustion Unit for Heating Water at 90°C	7 MM Btu/Hr.
8	1	Refrigeration Unit for Cooling Brine at -10°C	200 ton

At the break-even point, where energy costs per unit product are the same for both evaporative and parametric pumping desalination, the steam economy is given by

$$S = \frac{8.33c_3\lambda}{\frac{c_2H_2+c_1H_1}{2W_{BP}}}$$

For our example,

$$S = \frac{(8.33)\ (1.25)\ (860)}{\frac{(3.0)\ (2,266,917) + (1.0)\ (6,905,433)}{(2)\ (4,167)}} = 5.44$$

Therefore, where steam economy in a multiple-effect evaporator plant is less than 5.44 (probably at less than seven effects) desalination by parametric pumping is more economical, on an energy cost basis, than by evaporation. An evaporation plant containing less than seven effects is, most probably, a plant in the lower capacity range, say 100,000 - 500,000 gallons/day, where one to five parametric pumping "unit cells" have an equivalent capacity.

This suggests that desalination by parametric pumping is competitive with evaporation for smaller size plants. For 1,000,000-2,000,000 gallons/day capacity, where ten to twenty parametric pumping "unit cells" are required, an evaporation plant of seven or more effects is certainly more attractive from an equipment size point of view. For example, at 1,500,000 gallons/day, eight 12,000-ft^2 evaporators in series are surely preferable to fifteen 200-feet long

adsorption columns and thirty 150,000 gallon reservoir tanks. However, at 300,000 gallons/day, three 200-feet long adsorption columns and six 150,000 gallons reservoir tanks compare favorably with eight 3,000-ft^2 evaporators with their associated auxiliary equipment.

REFERENCES

1. Acrivos, A., "Method of Characteristics Technique--Application to Heat and Mass Transfer Problems," Industrial and Engineering Chemistry, Vol. 48, No. 4, April 1956, pp. 703-710.

2. Aris, R., "Equilibrium Theory of the Parametric Pump," Industrial and Engineering Chemistry Fundamentals, Vol. 8, No. 2, May 1969, pp. 603-604.

3. Busbice, M.E., and Wankat, P.C., "pH Cycling Zone Separation of Sugars," Journal of Chromotography, Vol. 114, 1975, pp. 369-381.

4. Chen, H.T., and Hill, F.B., "Characteristics of Batch Semicontinuous, and Continuous Equilibrium Parametric Pumps," Separation Science, Vol. 6, No. 3, June 1971, pp. 411-434.

5. Chen, H.T., Rak, J.L., Stokes, J.D., and Hill, F.B., "Separations via Continuous Parametric Pumping," AIChE Journal, Vol. 18, No. 2, March 1972, pp. 356-361.

6. Chen, H.T., Jaferi, J., and Stokes, J.D., Paper 93 presented at 73d. National Meeting of the American Institute of Chemical Engineers, Minneapolis, Minn., August 28, 1972.

7. Chen, H.T., Reiss, E.H., Stokes, J.D., and Hill, F.B., "Separations vis Semicontinuous Parametric Pumping," AIChE Journal, Vol. 19, No. 3, May 1973, pp. 589-595.

8. Chen, H.T., Stokes, J.D., and Lin, W.W., Paper 7f presented at 4th Joint Meeting of the American Institute of Chemical Engineers--Canadian Society of Chemical Engineers, AIChE, ESCE, Vancouver, British Columbia, September 12, 1973.

9. Chen, H.T., Park, J.A., and Rak, J.L., "Equilibrium Parametric Pumps," Separation Science, Vol. 9, No. 1, 1974, pp. 35-45.

10. Chen, H.T., Lin, W.W., Stokes, J.D., and Fabisiak, W.R., "Separation of Multicomponent Mixtures via Thermal Parametric Pumping," AIChE Journal, Vol. 20, No. 2, March 1974, pp. 306-310.

11. Chen, H.T., Rastogi, A.K., Kim, C.Y., and Rak, J.L., "Nonequilibrium Parametric Pumps," Separation Science, Vol. 11, No. 4, 1976 pp. 335-346.

12. Chen, H.T., Hsieh, T.K., Lee, H.C., and Hill, F.B., "Separation of Protiens via Semicontinuous pH Parametric Pumping," AIChE Journal, Vol. 23, No. 5, September, 1977 pp. 695-701.

13. Dore, J.D., and Wankat, P.C., "Multicomponent Cycling Zone Adsorption," Chemical Engineering Science, Vol. 31, 1976, pp. 921-927.

14. Gregory, R.A., Jr., "Parametric Pumping: Study of Direct Thermal Open Systems," Doctoral Dissertation, Princeton University, Princeton, N.J.,

15. Gupta, R., and Sweed, N.H., "Modeling of Nonequilibrium Effects in Parametric Pumping," Industrial and Engineering Chemistry Fundamentals, Vol. 12, No. 3, 1973, pp. 335-341.

16. Jenczewski, T.J., and Myers, A.L., "Separation of Gas Mixtures by Pulsed Adsorption," Industrial and Engineering Chemistry Fundamentals, Vol. 9, No. 2, 1970, pp. 216-221.

17. Patrick, R.R., Schrodt, J.T1, and Kermode, R.I., "Thermal Parametric Pumping of Air-SO_2," Separation Science, Vol. 7, N9. 4, 1972, pp. 331-343.

18. Pigford, R.L., Baker, B., and Blum, D.E., "An Equilibrium Theory of the Parametric Pump," Industrial and Engineering Chemistry Fundamentals, Vol. 8, No. 1, February 1969, pp. 143-149.

19. Pigford, R.L., Baker, B., and Blum, D.E., "Cycling Zone Adsorption, A New Separation Process," Industrial and Engineering Chemistry Fundamentals, Vol. 8, No. 4, November 1969, pp. 848-851.

20. Rak, J.L., An Experimental Study of Continuous Parametric Pumping, Master's Thesis, Newark College of Engineering, Newark, N.J., 1972.

21. Rice, A.W., "Some Aspects of Separation by Parametric Pumping," Doctoral Dissertation, Princeton University, Princeton, N.J., May 1966.

22. Rolke, R.W., "Recuperative Parametric Pumping: Model Development, Evaluation, and Use for Study of Separation Capabilities," Doctoral Dissertation, Princeton University, Princeton, N.J., October 1967.

23. Rolke, R.W., and Wilhelm, R.H., "Recuperative Parametric Pumping," Industrial and Engineering Chemistry Fundamentals, Vol., 8, No. 2, May 1969, pp. 235-246.

24. Sabadell, J.E., and Sweed, N.H., "Parametric Pumping with pH," Separation Science, Vol. 5, No. 3, June 1970, pp. 171-181.

25. Shaffer, A.G., and Hammin, C.E., "Enzyme Separation by Parametric Pumping" AIChE Journal, Vol. 21, No. 4, July 1975, pp. 782-786.

26. Shendalman, L.H., and Mitchel, J.E., "A Study of Heatless Adsorption in the Model System CO_2 in He," Chemical Engineering Science, Vol. 27, 1972, pp. 1449-1458.

27. Sweed, N.H., "Parametric Pumping: Separations via Direct Thermal Mode," Doctoral Dissertation, Princeton University, Princeton, N.J., October 1968.

28. Sweed, N.H., and Gregory, R.A., "Parametric Pumping: Modeling Direct Thermal Separations of Sodium Chloride-Water in Open and Closed Systems," AIChE Journal, Vol. 17, No. 1, January 1971, pp. 171-176.

29. Turncock, P.H., and Kadlec, R.H., "Separation of Nitrogen and Methane via Periodic Adsorption," AIChE Journal, Vol. 17, No. 2, March 1971, pp. 335-342.

30. Wankat, P.C., "Liquid-Liquid Extraction Parametric Pumping," Industrial and Engineering Chemistry Fundamentals, Vol. 12, No. 3, 1973, pp. 372-381.

31. Wankat, P.C., "Thermal Wave Cycling Zone Adsorption," Journal of Chromotography, Vol. 88, 1974, pp. 211-228.

32. Wilhelm, R.H., Rice, A.W., and Bendelious, A.R., "Parametric Pumping: A Dynamic Principle for Separating Fluid Mixtures," Industrial and Engineering Chemistry Fundamentals, Vol. 5, No. 1, February 1966, pp. 141-144.

33. Wilhelm, R.H., and Sweed, N.H., "Parametric Pumping: Separation of Mixture of Toluene and n-Heptane," Science, Vol. 159, January 1968, pp. 522-524.

34. Wilhelm, R.H., Rice, A.W., Rolke, R.W., and Sweek, N.H., "Parametric Pumping: A Dynamic Principle for Separating Fluid Mixtures," Industrial and Engineering Chemistry Fundamentals, Vol. 7, No. 3, August 1968, pp. 337-349.

Other References:

Butts, T.J., Gupta, R., and Sweed, N.H., "Parametric Pumping Separations of Multicomponent Mixtures," Chemical Engineering Science, Vol. 27, 1972, pp. 855-866.

Butts, T.J., Sweed, N.H., and Camero, A.A., "Batch Fractionation of Ionic Mixtures by Parametric Pumping, "Industrial and Engineering Chemistry Fundamentals, Vol. 12, No., 1973, pp. 467.

Camero, A.A., and Sweed, N.H., "Separation of Nonlinearly Sorbing Solutes by Parametric Pumping," AIChE Journal, Vol. 22, No. 2, March 1976, pp. 369-376.

Chen, H.T., and Maraganaro, J.A., "Optimal Performance of Equilibrium Parametric Pumps," AIChE Journal, Vol. 20, No. 5, September 1974, pp. 1020-1022.

Chen, H.T. and D'Emidio, V.J., "Separation of Isomers vis Thermal Parametric Pumping," AIChE Journal, Vol. 21, No. 4 July 1975, pp. 813-815.

Foo, S.C., and Rice, R.G., "On the Prediction of Ultimate Separation in Parametric Pumps," AIChE Journal, Vol. 21, No. 6, November, 1975, pp. 1149-1158.

Goto, S, and Matsubara, M., "Extraction Parametric Pumping with Reversible Reaction," Industrial and Engineering Chemistry Fundamentals, Vol. 16, No. 2, 1977, pp. 193-200.

Gregory, R.A., and Sweed, N.H., "Parametric Pumping: Behavior of Open Systems Part I: Analytical Solutions," Chemical Engineering Journal, Vol. 1, 1970, p. 207.

Gregory, R.A., and Sweed, N.H., "Parametric Pumping: Behavior of Open Systems, Part II: Experiment and Computation," Chemical Engineering Journal, Vol. 4, 1972, p. 139.

Gregory, R.A., "Comparison of Parametric Pumping with Conventional Adsorption," AIChE Journal, Vol. 20, No. 2, March, 1974, pp. 294-300.

Grevillot, G, and Tondeur, D., "Equilibrium Staged Parametric Pumping," AIChE Journal, Vol. 22, No. 6, November, 1976, pp. 1055-1063.

Rice, R.G., "Dispersion and Ultimate Separation in the Parametric Pump," Industrial and Engineering Chemistry Fundamentals, Vol. 12, No. 4, 1973, pp. 406-412.

Rice, R.G., and Foo, S.C., "Thermal Diffusion Effects and Optimum Frequencies in Parametric Pumps," Industrial and Engineering Chemistry Fundamentals, Vol. 13, No. 4, 1974, pp. 396-398.

Rice, R.G., "The Effect of Purely Sinussidal Potentials on the Performance of Equilibrium Parapumps," Industrial and Engineering Chemistry Fundamentals, Vol. 14, No. 4, 1975, pp. 362-365.

Wankat, P.C., "Review Cyclic Separation Processes," Separation Science, Vol. 9, No. 2, 1974, pp. 85-116.

VITA

I was born ,
where I attended elementary and secondary schools. I graduated in June of 1965 from Rutgers University, New Brunswick, N.J. with a B.S. in Chemical Engineering and an AB in Liberal Arts. During the summer of 1964 I spent three months as a Junior Engineer in process design and evaluation with Hercules, Inc. at Parlin, N.J. After four months (June-October, 1965) as a process development engineer at the Perth Amboy plant of E.I. duPont de Nemours and Co., I entered the U.S. Army as a Second Lieutenant and served as Officer in charge of the Maintenance and Operations Proceedures Branch of the Technical Support Directorate at Edgewood Arsenal, Maryland, being discharged as a First Lieutenant in November 1967.

From January 1968 to June 1972 I pursued an MS in Chemical Engineering at Newark College of Engineering, Newark, N.J., while working as a development engineer in the Technical Services Department at Merck and Co.'s Rahway plant. After receiving the MSChE in June 1972, I began work as a research engineer for FMC Corporation at their Carteret, N.J. facility while pursuing studies for the Doctor of Engineering Science at New Jersey Institute of Technology. During the period September 1973-June 1974 I was in residence at NJIT working under the auspices of a grant from E.I. duPont de Nemours and Co. Since November 1975 I have been doing research work at FMC Corporation's Princeton Research Center while continuing the studies described in this work.